NOVA SCHOOL OF SCIENCE & TECHNOLOGY

DEPARTMENT OF CHEMISTRY

JOÃO MIGUEL MOREIRA O'NEILL DE SOUSA

Bachelor degree in Chemical and Biochemical Engineering Sciences

OPTIMIZATION OF BIOREACTORS FOR PROLIFERATION OF MAMMALIAN CELLS IN CULTIVATED MEAT PRODUCTION

MASTER IN CHEMICAL AND BIOCHEMICAL ENGINEERING

NOVA University Lisbon
September, 2023

NOVA SCHOOL OF SCIENCE & TECHNOLOGY

DEPARTMENT OF CHEMISTRY

OPTIMIZATION OF BIOREACTORS FOR PROLIFERATION OF MAMMALIAN CELLS IN CULTIVATED MEAT PRODUCTION

JOÃO MIGUEL MOREIRA O'NEILL DE SOUSA

Bachelor degree in Chemical and Biochemical Engineering Sciences

Adviser: Katrin Neubauerová
Research Scientist, Bene Meat Technologies

Co-adviser: Maria Filomena Andrade de Freitas
Assistant Professor, NOVA University Lisbon

Examination Committee

Chair: Mário Fernando José Eusébio
Associate Professor, NOVA FCT

Rapporteur: Rui Manuel Freitas Oliveira
Associate Professor, Another NOVA FCT

Member: Maria Filomena Andrade de Freitas
Assistant Professor, NOVA FCT

MASTER IN CHEMICAL AND BIOCHEMICAL ENGINEERING

NOVA University Lisbon
September, 2023

Optimization of Bioreactors for Proliferation of Mammalian Cells in Cultivated Meat Production

Para o meu irmão.

Acknowledgements

I would like to offer my sincere gratitude to Jiří Janoušek and Roman Kříž for allowing me to do this study in a field I have been highly interested in.

A special and enormous thank you to Katrin Neubauerová who was my supervisor and has been my support and guidance through my stay at Bene Meat Technologies. She has been always ready to help, kind and inspiring throughout.

I want to thank Professor Maria Filomena Freitas, for being my co-supervisor who was always available for my doubts and allowed me to use school equipment to further develop my study. I would also like to thank Professors João Crespo and Rui Oliveira, for being available for my questions and showing the availability to meet with me for my questions.

And lastly, I want to thank my family and friends for their unconditional support and love, that allowed me to stay focused and motivated throughout the realisation of this study. Without you, not only this would have been much harder, but also my academic journey. You are always in my mind and heart.

”

“Shoot for the moon. Even if you miss, you’ll land among the stars.”

— Norman Vincent Peale, Somewhere in a book or speech
(Protestant clergyman, author)

Abstract

With the increasing volume of meat consumed in the world, and the consequent pollution problems that arise from farm animal cultivation, new ways to produce meat keep growing in research. The focus of this study is on the production of meat using cultivated mammalian cells, mainly the optimization of bioreactor systems and the conditions needed to achieve economically viable production of cells for human consumption.

The first part of the study is focused on the optimization of mass transfer coefficient in the aerated bioreactors. Several impeller geometries were tested, and in the case of a Toroidal geometry, the power number was estimated at 2.8, which is higher than the commonly used elephant ear impeller. The increase of stirring speed and aeration flow rate was shown to be linearly proportional to an increase in oxygen mass transfer rate. The experimental data failed to fit the empirical model studied, which showed the importance of specific models for each geometry and range of parameters. The impeller optimal position was shown in accordance to the literature, $\frac{1}{2}$ to $\frac{2}{3}$ of the vessel's diameter. Membrane aeration was tested, without reaching scalable results. The existence of baffles in the vessel was proven beneficial and the size of bubbles was proven hard to predict and of low importance for higher scale.

The second part studied the growth and viability of mammalian cells. The effect of shear stress was evaluated and proved the necessity of the addition of a shear protectant. The use of PEMF was tested against foaming, but no clear correlation was reached. A fed-batch cultivation was tested and the amino acid changes in the media was also evaluated and used to test the adaptation of a previously developed metabolic model. The error obtained was high, leading to the need of further optimization and cultivation data.

Keywords: Cultivated Meat, Bioreactor Optimization, Oxygen Mass Transfer, Shear Stress, Mammalian Cells, Metabolic Modelling

Resumo

Com o aumento do consumo mundial de carne e os consequentes problemas de poluição decorrentes da criação de animais para o mesmo, novas formas de produzir carne continuam a ser objeto de investigação. O foco deste estudo é a produção de carne utilizando células de mamíferos cultivadas, principalmente a otimização de sistemas de biorreatores e as condições necessárias para alcançar uma produção economicamente viável de carne para consumo humano.

A primeira parte do estudo centra-se na otimização do coeficiente de transferência de massa nos biorreatores com arejamento. Estudaram-se várias geometrias de agitadores e, no caso de uma geometria toroidal, o número de potência foi estimado em 2.8, o que é superior à geometria orelha de elefante comumente utilizada. O aumento da velocidade de agitação e do caudal de arejamento mostrou-se linearmente proporcional a um aumento do coeficiente de transferência de massa de oxigénio. Os dados experimentais não se ajustaram ao modelo empírico estudado, o que mostrou a importância de modelos específicos para cada geometria e gama de parâmetros. A posição óptima do agitador foi demonstrada em concordância com a literatura, estando no intervalo de $\frac{1}{2}$ a $\frac{2}{3}$ do diâmetro do biorreator. Foi testado o arejamento por membrana, sem atingir resultados escaláveis. A existência de chicanas no recipiente revelou-se benéfica e o tamanho das bolhas revelou-se difícil de prever e de pouca importância para uma maior escala.

A segunda parte estudou o crescimento e a viabilidade das células de mamíferos. O efeito do shear stress foi avaliado e comprovou a necessidade da adição de um protetor químico. A utilização de PEMF foi testada contra a formação de espuma, mas não se obteve uma correlação clara. Foi testada uma cultura em regime fed-batch e as alterações de aminoácidos no meio foram também avaliadas e utilizadas para testar a adaptação de um modelo metabólico previamente desenvolvido. O erro obtido foi elevado, levando à necessidade de mais otimização e dados de cultivo.

Palavras-chave: Carne Cultivada, Otimização de Biorreatores, Transferência de Massa de Oxigénio, Shear Stress, Células de Mamíferos, Modulação Metabólica

Contents

1 Motivation **1**

1.1 Contextualization . . . 1
1.2 Objectives . . . 1
1.3 Thesis Outline . . . 2

2 General Introduction **3**

2.1 Mammalian Cells for Food Production . . . 3
2.1.1 Main Setbacks in Cultured Meat . . . 4
2.1.2 State-of-the-art of Cultivated Meat Production . . . 6
2.2 Bioreactors in Biotechnology . . . 7
2.3 Oxygen Mass Transfer in Bioreactors . . . 9
2.3.1 Mass transfer dependence on bubble size . . . 10
2.3.2 Mass transfer dependence on mixing profile . . . 11
2.3.2.1 Impact of Eddies . . . 12
2.3.2.2 Reynold's Number . . . 13
2.3.2.3 Geometry of impeller . . . 14
2.3.3 Power input and mass transfer . . . 17
2.3.4 Mass transfer dependence on temperature and pressure . . . 18
2.3.5 Mass transfer dependence on medium properties . . . 18
2.3.6 Aeration types . . . 18
2.3.6.1 Perfusion Mode Aeration . . . 19
2.3.6.2 Internal Aeration . . . 20
2.3.6.3 Impact of Foaming in Aerated Bioreactors . . . 22
2.4 Metabolic Engineering . . . 23
2.4.1 Flux Balance Analysis (FBA) . . . 26

3 Materials and Methods **29**

3.1 Materials . . . 29
3.1.1 Equipment . . . 29

3.1.1.1 Custom Made Stirred Tank Bioreactor System (0.5 L to 1.5 L) . . . 30
3.1.1.2 Custom Made Vibromixer (0.5 L to 1.5 L) . . . 31
3.1.1.3 Custom Made Spinner Flask Bioreactor System (0.25 to 0.45L) . . . 32
3.1.1.4 Commercial Biostat B-Plus Bioreactor System by Sartorius (4-10 L) . . . 35
3.1.1.5 Control Equipment and Sensors . . . 35
3.1.1.6 Aeration Equipment . . . 35
3.1.1.7 External Stimulation Equipment . . . 36
3.1.2 Cells . . . 36
3.1.3 Media . . . 36
3.2 Methods . . . 37
3.2.1 Methods for O_2 kLa estimation (experimental and analytical) . . . 37
3.2.2 Experimental Setups for kLa optimization in Bioreactors . . . 38
3.2.2.1 Impact of Impeller Speed on kLa . . . 38
3.2.2.2 Impact of Impeller Geometry on kLa . . . 39
3.2.2.3 Impact of Impeller Position on kLa . . . 41
3.2.2.4 Impact of aeration flow rate on kLa . . . 41
3.2.2.5 Membrane Aeration and kLa . . . 42
3.2.2.6 Impact of Baffles on kLa . . . 43
3.2.2.7 Impact of Bubble size on kLa . . . 43
3.2.2.8 Impact of Additives on kLa . . . 44
3.2.3 Experimental Setups for Optimization of Bioreactors for Cell Viability . . . 44
3.2.3.1 Shear Stress Evaluation . . . 45
3.2.3.2 Antifoaming and Defoaming . . . 45
3.2.3.3 Fed-Batch Experiment . . . 46
3.2.4 Predictive python metabolic model estimations of nutrient consumption and growth . . . 47
3.2.5 Methods for analytical evaluation . . . 48
3.2.5.1 HPLC Concentration of Amino Acids Analysis Method 49
3.2.5.2 Cytometry Cell Density and Viability Analysis Method 49
Description of Cytometer Sample Measurement Method . . . 50

4 Results and Discussion **51**
4.1 Optimization of kLa in Bioreactors . . . 51
4.1.1 Impact of Impeller Speed on kLa . . . 52
4.1.1.1 Spinner Flask System Results . . . 52
4.1.1.2 Stirred Tank System Results . . . 53
4.1.1.3 Biostat System Results . . . 54

4.1.1.4 Discussion of Impact of Impeller speed on kLa 55
4.1.2 Impact of Impeller Geometry on kLa 57
4.1.2.1 Spinner Flask System Results 58
4.1.2.2 DIscussion of Results for Elephant Ear, Toroidal and Rushton Impellers 61
4.1.2.3 Power Number Estimation and Correlation 62
4.1.2.4 Vibromixer System Results 64
4.1.2.5 Discussion of Results for Vibromixer mixing with different plates 65
4.1.3 Impact of Impeller Position on kLa 66
4.1.3.1 Stirred Tank System Results 66
4.1.3.2 Discussion of Results for Stirred Tank System 67
4.1.3.3 Biostat System Results 69
4.1.3.4 Discussion of Results for Biostat System 70
4.1.3.5 Vibromixer System Results 71
4.1.3.6 Discussion of Results for Vibromixer System 72
4.1.4 Impact of aeration flow rate on kLa 73
4.1.4.1 Stirred Tank System Results 73
4.1.4.2 Vibromixer System Results 74
4.1.4.3 Spinner Flask System Results 75
4.1.4.4 Changes in kLa with increase of aeration rate in Spinner Flask system with stainless steel sintered spargers . . . 75
4.1.5 Membrane Aeration and kLa 77
4.1.5.1 Spinner Flask System Results 77
4.1.5.2 Discussion of Results for Spinner Flask System 77
4.1.6 Impact of Baffles on kLa 78
4.1.6.1 Spinner Flask System Results 78
4.1.6.2 Discussion of Results for Spinner Flask System 78
4.1.7 Impact of Bubble size on kLa 79
4.1.7.1 Spinner Flask System Results 79
4.1.7.2 Discussion of Results for Spinner Flask System 81
4.1.8 Impact of Additives on kLa 82
4.1.8.1 Spinner Flask System Results 83
4.1.8.2 Discussion of Results for Spinner Flask System 84
4.2 Optimization of Bioreactors for Cell Viability 85
4.2.1 Impact of different parameters on Cell Viability 85
4.2.1.1 Shear Stress Evaluation 85
Cell Line A Cultivation Results 86
Discussion for Cell Line A Cultivation Results 87
Cell Line B Cultivation Results 88
Discussion for Cell Line B Cultivation Results 89

Shear Stress Estimation 89
4.2.1.2 Antifoaming and Defoaming 90
PEMF Stimulation in Spinner Flask System Results 90
Discussion of PEMF Stimulation Effect 92
4.2.2 Experimental consumption of nutrients 92
4.2.2.1 Fed-Batch Experiment 92
Fed-Batch Cultivation in Stirred Tank System Results 93
Discussion of Results for Fed-Batch Cultivation in Stirred Tank System 94
4.2.3 Predictive python metabolic model estimations of nutrient consumption and growth 95

5 Conclusions **113**
5.1 Optimization of kLa in Bioreactors 113
5.1.1 Final Conclusions 115
5.2 Optimization of Bioreactors for Cell Viability 115
5.2.1 Final Conclusions 116

6 Future Directions **117**
6.1 Optimization of kLa in Bioreactors 117
6.2 Optimization of Bioreactors for Cell Viability 118

References **121**

List of Figures

2.1 Diagram of an example of a Stirred Tank Bioreactor [52] 8
2.2 Operating conditions and problems that rise from them in bioreactors . . . 12
2.3 Different stirring flow patterns, from left to right, axial, radial and tangential [84] 15
2.4 Different types of impellers used in bioreactors [86] 16
2.5 Modular Membrane Exchange aeration setup example [103] 19
2.6 Example of a Immersed Membrane Bioreactor [116] 21
2.7 Sintered metal sparger example [124] 22
2.8 Examples of different geometries for spargers [125] 22
2.9 Example of metabolic pathway, Glycolysis [141] 24
2.10 Schematic diagram of part of the metabolic network of Escherichia coli . . . 25
2.11 A simple example of a metabolic network 26
2.12 Metabolic reactions stoichiometry matrix S example 27

3.1 Stirred Tank bioreactor system during cell cultivation 31
3.2 Different Impellers used in Stirred Tank Bioreactor system 31
3.3 The two different plates used in the Vibromixer system 32
3.4 Spinner Flask Bioreactor system 33
3.5 Elephant Ear impeller used in Spinner Flask Bioreactor system 34
3.6 Toroidal Impeller used in this study 34
3.7 Biostat vessel on the left and control tower on the right 35
3.8 Metabolic model described in the model developed by Robitaille et al [188] 48

4.1 Change in kLa with increase of RPM on Spinner Flask system 53
4.2 Change in kLa with increase of RPM on Stirred Tank system 54
4.3 Change in kLa with increase of RPM on commercial Biostat 10L Bioreactor system 55
4.4 Change in kLa with increase of RPM on Spinner Flask system sparged, with Elephant Ear impeller 59

4.5 Change in kLa with increase of RPM on Spinner Flask system sparged, with Toroidal impeller, sparged and not sparged 60
4.6 Change in kLa with increase of RPM on Vibromixer system, comparing different plates 64
4.7 Changes in kLa with increase of RPM and change in distance between two 4 cm diameter elephant ear impellers on Stirred Tank system 67
4.8 Changes in kLa with increase of RPM and change in distance between two 7.5 cm diameter Rushton impellers on Biostat system 70
4.9 Changes in kLa with increase of aeration rate in Stirred Tank system 73
4.10 Changes in kLa with increase of aeration rate in Vibromixer system 74
4.11 Change in kLa with increase of RPM on commercial Biostat 10L Bioreactor system 75
4.12 Changes in kLa with increase of aeration rate and different pores sizes sintered spargers in Spinner Flask bioreactor system 80
4.13 Frame from video capture used to analyse bubble size distribution 80
4.14 Change in kLa with temperature for different concentrations of additives in Spinner Flask system 83
4.15 Viable cell growth over time of cultivation in 0.1% PEG medium and 900 RPM with Cell Line A in Stirred Tank bioreactor system 86
4.16 Viable cell growth over time of cultivation in medium without shear protectant, at 900 and 600 RPM with Cell Line A in Stirred Tank bioreactor system . . . 87
4.17 Viable cell growth over time of cultivation in medium with 0.01% PEG and slow increase to 650 RPM with Cell Line B in Stirred Tank bioreactor system 88
4.18 Results of one of the setups of PEMF treatment as antifoaming and defoaming technique. 90
4.19 Results of experiment with PEMF treatment, (1) the PEMF treated vessel surface and (2) the non-treated vessel surface 91
4.20 Results of experiment with PEMF treatment with induced foaming, (1) PEMF treated surface and (2) non-treated surface 91
4.21 Results from PEMF stimulation experiment with cells, (1) PEMF stimulated surface and (2) non-stimulated surface 92
4.22 Amino Acid, Glucose and Lactate concentration, as percentage of initial concentration, during fed-batch cultivation of Cell Line B 94
4.23 First part of the python code used, the required imports and loading and reading the metabolic matrix 95
4.24 Second part of the python code used, the function kinetics, used for computing the flux rates equations 96
4.25 Third part of the used python code, defining the ode function that used the kinetic equations from the previous function 97
4.26 Fourth and final part of the python code used for the model 98

4.27 Example of the python code used for optimization of the different kinetic constants in the metabolic mode 101
4.28 A snippet of the code used for the optimization of parameters for Cell Line B model using CMA-ES approach 108
4.29 Select Amino Acids concentrations over cultivation time with Cell Line A . 111
4.30 Select Amino Acids concentrations over cultivation time with Cell Line B . . 111

List of Tables

3.1 Parameters, characteristics and components of the Custom Made Stirred Tank and Vibromixer Bioreactor System used 30
3.2 Parameters, characteristics and components of the custom made Spinner Flask Bioreactor System used 33
3.3 Media and Additives used 36
3.4 Characteristics of the different setups for the study of Impeller Speed Impact on kLa 38
3.5 Characteristics of the different setups for the study of Impeller Geometry Impact on kLa 40
3.6 Characteristics of the different setups for the study of Impeller Position Impact on kLa 41
3.7 Characteristics of the different setups for the study of Aeration flow rate Impact on kLa 42
3.8 Characteristics of the different setups for the study of Membrane Aeration . 42
3.9 Characteristics of the different setups for the study of Baffles Impact on kLa 43
3.10 Characteristics of the different setups for the study of Bubble size Impact on kLa 43
3.11 Characteristics of the different setups for the study of Additives Impact on kLa 44
3.12 Characteristics of the different setups for the study of shear stress in Cell Lines A and B 45
3.13 Characteristics of the different setups for the study Antifoaming and Defoaming using PEMF 46
3.14 Characteristics of the setup for the Fed-Batch experiment 46
3.15 HPLC Method measurement conditions 49

4.1 Results for Impact of RPM on kLa on Spinner Flask system 52
4.2 Results for Impact of RPM on kLa in Stirred Tank system 53
4.3 Results for Impact of RPM on kLa on commercial Biostat 10L Bioreactor system 54
4.4 Increase of kLa per RPM in Spinner Flask, Stirred Tank and Biostat systems 56

4.5 Comparison of experimental data proportionality with literature proportionality . . . 57
4.6 Results for impact of Impeller Geometry with Elephant Ear impeller in the Sparged Spinner Flask system . . . 58
4.7 Results for impact of Impeller Geometry increase in kLa with RPM, Elephant Ear, not sparged in Spinner Flask system . . . 59
4.8 Results for impact of Impeller Geometry increase in kLa with RPM,Toroidal impeller, sparged and not sparged in Spinner Flask system . . . 60
4.9 Increase of kLa in percentage by RPM increase in different systems with different impeller geometries . . . 61
4.10 Results for impact of different mixing and different plate's geometry in Vibromixer system . . . 64
4.11 Increase of kLa in percentage by RPM increase in Vibromixer system with different plate geometries . . . 65
4.12 Results for impact on kLa of different impeller position, at different RPM values, for Stirred Tank system using 4 cm diameter elephant ear impellers . . . 66
4.13 Results for impact on kLa of different impeller position, at different RPM values, for Stirred Tank system and the kLa increase per RPM . . . 68
4.14 Results for impact on kLa of different impeller position, difference in kLa by distance for the same RPM . . . 68
4.15 Results for impact on kLa of different impeller position, at different RPM values, for Biostat system using 7.5 cm diameter Rushton impellers . . . 69
4.16 Results for impact on kLa of different impeller position, difference in kLa by distance for the same RPM . . . 70
4.17 Results for impact on kLa of different impeller position, difference in kLa by distance for the same RPM . . . 71
4.18 Results for impact on kLa of different plate position, at different RPM values, for Vibromixer system using trapdoor plates . . . 71
4.19 Results for impact on kLa of different distance between plates, difference in kLa by distance for the same RPM . . . 72
4.20 Results for impact on kLa of different distance between plates, difference in kLa by distance for the same RPM . . . 72
4.21 Results for impact on kLa of changing the aeration rate using Stirred Tank system . . . 73
4.22 Results for impact on kLa of changing the aeration rate using Vibromixer system . . . 74
4.23 Results for impact on kLa of changing the aeration rate using Spinner Flask system with stainless steel sintered spargers . . . 75
4.24 Results for increase in kLa with increase in aeration rate for Stirred Tank, Vibromixer and Spinner Flask systems . . . 76

4.25 Proportionality constant calculation between kLa and Vg for the studied systems . . . 76
4.26 Results of kLa calculations from the best membrane aeration setup, using the Spinner Flask system . . . 77
4.27 Results for impact of having baffles on kLa in Spinner Flask bioreactor system 78
4.28 Results for different pore size and different aeration flow rate in kLa on Spinner Flask system with sintered spargers . . . 79
4.29 Bubble number and size distribution in Spinner Flask system with different aeration rate and pore size spargers . . . 81
4.30 Change in bubble size, number of bubbles and kLa with VVM for different pore sizes . . . 82
4.31 Results of kLa calculations from different additives concentrations and different temperatures in the Spinner Flask system . . . 83
4.32 Impact of Temperature and Additives on the kLa in Spinner Flask system . 84
4.33 Results of cell viability and density over cultivation time in 0.1% PEG medium and 900 RPM with Cell Line A in Stirred Tank bioreactor system . . . 86
4.34 Results of cell viability and density over cultivation time in medium without shear protectant and 900 RPM with Cell Line A in Stirred Tank bioreactor system . . . 87
4.35 Results of cell viability and density over cultivation time in medium without shear protectant and 600 RPM with Cell Line A in Stirred Tank bioreactor system . . . 87
4.36 Results of cell viability and density over cultivation time in medium with 0.01% PEG and slow increase to 650 RPM with Cell Line B cells in Stirred Tank bioreactor system . . . 88
4.37 Results of cell viability and density over cultivation time in medium without shear protectant and slow increase from 150 RPM with Cell Line B in Stirred Tank bioreactor system . . . 89
4.38 Growth of cells and viability results in Fed-Batch experiment in Stirred Tank bioreactor system . . . 93
4.39 Concentration of amino acids, glucose and lactate over time in Fed-Batch experiment in Stirred Tank bioreactor system . . . 93
4.40 Experimental results from Cell Line A experiment for concentration of cells and amino acids over cultivation time . . . 99
4.41 Amino acids concentration and cell density over cultivation time from first simulation using the metabolic python model . . . 100
4.42 Summary table of the results and conclusions of the 2nd optimization of parameters and simulation . . . 102
4.43 Summary table of the results and conclusions of the 3rd optimization of parameters and simulation . . . 102

4.44 Summary table of the results and conclusions of the 4th optimization of parameters and simulation 103
4.45 Summary table of the results and conclusions of the 5th optimization of parameters and simulation 104
4.46 Summary table of the results and conclusions of the 6th optimization of parameters and simulation 105
4.47 Summary table of the results and conclusions of the 7th optimization of parameters and simulation 106
4.48 Summary table of the results and conclusions of the 1st optimization of parameters and simulation with Cell Line B cultivation data 107
4.49 Summary table of the results and conclusions of the 2nd optimization of parameters and simulation with Cell Line B cultivation data 109
4.50 Summary table of the results and conclusions of the best optimization of parameters and simulation with Cell Line B cultivation data 110

Acronyms

ATP	Adenosine Triphosphate
CFD	Computational Fluid Dynamics
CHO	Chinese Hamster Cells
CMC	Sodium Carboxymethyl Cellulose
DMEM	Dulbecco's Modified Eagle Medium
DO	Dissolved Oxygen
FBA	Flux Balance Analysis
FBS	Fetal Bovine Serum
FDA	Food and Drug Administration
FSC	Forward Scattering
HPLC	High Performance Liquid Chromatography
LC	Liquid Chromatography
MCA	Metabolic Control Analysis
MFA	Metabolic Flux Analysis
ODEs	Ordinary Differential Equations
OTR	Oxygen Transfer Rate
PEG	Polyethylene Glycol
PEMF	Pulsed Electromagnetic Field
PETG	Polyethylene Terephthalate Glycol
PI	Propidium Iodide fluorescence

RF Refractive Fluorescence detection
RID Refractive Index Detection
RPM Revolutions per Minute
RPS Revolutions per Second

SSC Side Scattering

VVM Volume of air per Volume of medium per Minute

Symbols

a	Interfacial Area for Mass Transfer (m^2)
α	Specific constant for mixing system for relatioship between k_La, power input, volume and superficial gas velocity
β	Specific constant for mixing system for relatioship between k_La, power input per unit of volume
C	Concentration of oxygen dissolved in liquid (mg/L)
χ	Specific constant for mixing system for relatioship between k_La and superficial gas velocity
C_{sat}	Saturation concentration of dissolved oxygen for a given system (mg/L)
D	Impeller Diameter (m)
d_b	Bubble diameter (mm)
$E(d_b)$	Effect of bubble diameter on bubble entrapment
ϵ	Rate of dissipation of viscous energy (W/m^3)
η	Size of dissipating eddies (μm)
H	Liquid height (m)
k_d	Cell death rate ($cell/s$)
k_L	Mass Transfer Coefficient (m/h)
k_La	Volumetric Mass Transfer Coefficient (h^{-1})
μ	Dynamic Viscosity of fluid ($Pa.s$) (also used to indicate the subdivision of units "micro"
N	Stirring speed (s^-1)

N_P	Dimensionless Power Number or Newton Number
P	Power input by mixing in an aerated vessel (W)
pC	Proportionality Constant between k_La and stirring speed
P_G	Power input from gas expansion of sparged air (W)
P_T	Total specific power input (W)
Re	Dimensionless Reynolds Number
ρ	Density of liquid phase (kg/m^3)
ρ_g	Density of gas phase (kg/m^3)
t	Time (s)
τ	Shear stress (Pa or N/m^2)
V	Volume of liquid (L)
v	Kinematic viscosity (m^2/s)
V_g	Superficial gas velocity (m/s)

1 Motivation

In this chapter the reasons behind this study will be explained as well as the objectives and the structure of the thesis itself. The real motivation and benefits of this field of study will be better understood in the General Introduction chapter.

1.1 Contextualization

In recent years the market for cultivated meat has been growing and consequently the number of companies and research has increased with it. The use of animal cells for large-scale production of biomass suitable for human consumption has many advantages over conventional animal breeding. In the General Introduction chapter, namely in the Mammalian Cells for Food Production subchapter, the state-of-the-art as well as the issues and advantages of this technology is explained in greater depth. In this field there is a great need for development and optimization in multiple techniques and technologies, namely in bioreactor systems, as will be further explained in the aforementioned chapter of General Introduction. Therefore, this study was made to focus on some of the factors and technologies that can be used and must be kept in mind in order to optimise the production of mammalian cells for the production of meat.

1.2 Objectives

The main objective of this study is to study the behaviour of different bioreactor systems, namely the different factors that influence the oxygen mass transfer and how to proceed in order to optimise a bioreactor system for mammalian cell production. Importance of choosing the ideal mixing properties and aeration is taken into account with shear stress, and total mass transfer. Multiple systems and vessels will be studied along with different equations and models.

Another focus of this study is the use of metabolic engineering models to aid in the optimization of the feeding and initial media composition for better growth rate and

behaviour of mammalian cells, namely the use of a previously developed model and the attempt to adapt it to a different comparable type of mammalian cells.

To achieve this main goals the following assignments were made:

- Theoretical study of different effects on oxygen mass transfer and technologies used
- Measuring oxygen content over time for different bioreactor systems changing mixing speed Revolutions per Minute (RPM), aeration rate Volume of air per Volume of medium per Minute (VVM) and other parameters that influence mass transfer
- Cultivation experiments with cells to estimate the limits of shear stress caused by different factors
- Cultivation experiments with cells to understand cell growth, metabolite production and amino acids consumption;
- Metabolic Model simulations and adaptation to different experimental data and mammalian cell lines

1.3 Thesis Outline

This thesis is divided into five main chapters. The first chapter (Motivation) is a short introduction to the objectives of this study as well as a short contextualization of the importance of this industry. Also including a short explanation of the organisation of the study done. Chapter 2 (General Introduction) explains the industry further, and gives a theoretical introduction to the main topics approached in this study. All the materials, equipment, cells and methods (experimental or analytical) are present in Chapter 3 (Materials and Methods). Chapter 4 (Results and Discussion), contains all experimental results and discussion of the same. The final chapter, chapter 5 (Conclusions) presents the conclusions drawn from each experimental topic studied, as well as future directions for the whole research.

2

General Introduction

The following chapter serves as an introduction to the most important theoretical concepts needed to grasp the full scope of the present thesis. The first section focuses on an overview of the general scientific research and development made over the last years to come closer to the main goal, namely the sustainable and affordable production of cultivated meat. There is also summarised the current State-of-the-art, including a superficial analysis of the main companies and countries doing this research and the research development over the last decade. The second section focuses on one of the most important parameters of bioreactors for mammalian cell cultivation, the mass transfer of oxygen and the optimization of the parameters that affect it. The third section focuses on another equally important topic for optimization, which is the media's composition. Mainly focusing on the development of analytical and predictive models to simulate the cell's metabolism, thus helping to reduce the time and financial costs behind countless optimization experiments.

2.1 Mammalian Cells for Food Production

FAO (Food and Agriculture Organisation of the United Nations) describes "Cell-based food production" as "the field of growing animal agricultural products directly from cell cultures" [1]. FAO and WHO (World Health Organisation) have collaborated and published a paper [1] entitled Food safety aspects of cell-based food, to give readers current technical knowledge on the multidisciplinary subject of cell-based food production, with a focus on food safety concerns. With such important organisations recognizing the importance of said technologies we can confirm that this field is developing rapidly.

Cell-based food production includes the in vitro development of animal cells or microbial cells for the creation of analogues of animal or plant products and have nutritional qualities that are similar to those of components made traditionally. This field of technology is evolving quickly, and several forms of large-scale cell-based food production facilities are in the works. In this study, there is a focus primarily on mammalian cells for food production, specifically different cell strains which will be mentioned as mammalian cell line A and B, throughout the rest of this study. The two mammalian lines used (A and B)

serve as a starting point for an in depth more detailed understanding of other mammalian cells needs in terms of economically viable industrial production.

2.1.1 Main Setbacks in Cultured Meat

After 10 years since the first public proof of this technology, questions about common product availability still remain. The main setbacks mentioned in 2013, by Professor Mark Post, were mainly the sustainability of the product, its quality and the acceptability of the consumers [2].

The first hamburger presented costs of thousands of euros to produce, and its quality as aforementioned was still far from perfectly mimicking a "real" hamburger. Even though it was shown to be possible, the scalability of this technology proves to be a big setback. A specialist team of patent experts have presented five main problems that need to be solved in order for it to be commonly available [3]. Another setback was due to the use of Fetal Bovine Serum (FBS).t This serum was the basis for the growth factors needed to develop the cells, and to obtain it, it is necessary to draw blood from a recently born calve. This goes against the goal of sustainability and slaughter free meat, presented by the idea at hand [4].

- **Consumer Acceptance:** Food production is becoming a bigger mystery to people as a whole. Many customers are more alienated from the food industry and meal preparation due to the prominence of highly processed convenience foods and a decline in culinary abilities. Consumers are used to the classic look, smell and most importantly the taste of the products they buy in the supermarket week after week. Other alternative protein sources, such as insects, have been slow to develop because they cannot replace the public acceptance of current meat products. For plant-based meat to gain acceptance, companies need to develop products that meet these characteristics. Instead of relying on animals that are easy to raise, producers can use only cell lines from animals with the best characteristics to produce products [5].

- **Price of Production:** Despite good progress over the past decade, cultured meat is still much more expensive to produce than traditionally raised meat. A study proved that a kilogram of beef cost about 5 euros to produce [6]. A kilogram of cultivated meat with current technology would cost around 40 euros minimum, which would easily be sold at retailers for 200 euros per kilogram [7]. This is mainly due to the small scale of the current production process and the high cost of culture raw materials (such as growth factors and their substitutes as well as other medium components [8]). We expect cultural media and conditions to be key areas in which companies in this space generate intellectual property. This situation can be improved if economies of scale are realised [3].

- **Environmental Impact:** Currently used technologies are very energy intensive. Nonetheless, as the processes grow towards a higher scale, the energy consumption per kilogram of product may decrease. It is undeniable that this technology of cultured meat has the potential to use less resources such as water, energy and feedstock, while reducing the emissions of greenhouse gases. Nevertheless it is still far from optimised at the current moment [3]. According to a study done at Oxford [9], depending on the type of meat, it is estimated that cultured meat would cause 78–96 fewer greenhouse gas emissions and require 7–45 less energy, can be up to almost 90 fewer acres of land needed, and 82–96 less water resources than currently produced European meat [10].

- **Product Regulation and Policy:** Singapore was the first country that has given regulatory approval to cultured meat products. Policymakers need to take a forward-looking stance on the issue if plant-based meat is to succeed. For example, in the United States, which is one of the largest consumer markets in the world, cultured meat products are jointly regulated by the United States Department of Agriculture and the Food and Drug Administration (FDA). In November 2022, FDA reviewed Upside Foods and its lab grown meat, as safe for consumers [7]. There is a certainty that things can get more complicated if the animal cells used for production are genetically modified. However, a recent report by the European Union and the World Health Organization suggests a desire to reduce the regulatory burden on producers of genetically modified foods [3, 11]. Another concern comes from a cultural standpoint and the change in meat production jobs, causing a loss of jobs in farming [12]. Said cultural and legislative changes have already been openly discussed in Italy, for example, that moved to ban lab-grown meat to protect food heritage in March 2023 [13].

- **Scale-up of Production Process:** The scale-up needed to achieve lower production costs will also present many challenges. Companies must develop scalable, optimised production facilities and ensure a robust supply chain. It will also require significant capital investment in production capacity to reach production levels that allow alternative meat to penetrate the consumer market in a meaningful way. A strong intellectual property position will be key to attracting this investment [3]. This factor is seen as the most important, due to the fact that by achieving higher production rates and lowering costs by using diverse optimization techniques the availability and price problems would be closer to being solved [14, 15]. In the present study, there is a focus on solving this problem, specifically the optimization of bioreactor parameters that could influence the reduction of production costs and result in higher product yields.

2.1.2 State-of-the-art of Cultivated Meat Production

The main focus of this study is the optimization of the production bioreactor for mammalian cells to produce meat, and it is important to refer to the current state-of-the-art in this recent industry and to do some summary of the important developments, growth and technologies. Good Food Institute [16], describes itself as "a nonprofit think tank working to make the global food system better for the planet, people, and animals. This organisation has presented complete state of industry reports on cultivated meat that have data about the growth and the main technology used.

The first cell-based beef burger was presented to the public in 2013, by Professor Mark Post, of Maastricht University in, Netherlands, who displayed it and had professional food critics taste the first cell based burger. The taste and general feel, as described by critics, was very close to a real regular hamburger, still far from perfect, but quite close [1, 17]. This hallmark was 10 years ago, and served as a proof to everyone that this could actually be done, and since then many companies have been born with hopes of becoming suppliers of cell-based meat and fish.

In a general economic overview, the main points to notice from the last year of 2022, are that FDA gave clearance to Upside Foods, for their cultivated chicken, which is not only a major breakthrough in the United States but also the world. Due to the magnitude of the American market, not only that but in the past month (June 2023) there has been official clearance from the U.S. department of agriculture for the sale of cultured meat by both Upside Foods and Good Meat [18]. Outside of the United States, Singapore has also approved the sale of cell-cultured meat. Another important development is the number of publicly announced cultivated meat companies has risen to more than 150, registered around the world in 26 different countries.

There are currently more than 20 operational industrial facilities worldwide dedicated to the production of cultivated meat, including the recent (June 2023) new facility from Mosa Meat [19, 20]. It is a pilot plant facility making the commercialization in Europe closer to reality. Related to prototypes development and product announcements over the last year, South Korea announced its first cultivated chicken fillets and nuggets, by Space F [21]. Germany-based company, Alife Foods revealed the world's first cultivated schnitzel (breaded cutlet) [22]. Mogale Meat and Mzansi Meat, both in South Africa have revealed first cultivated chicken breast and first cultivated beef burger, respectively [23, 24] and these are but a few examples of the growing economical and technological advancements in cultivated meat and seafood.

For the most important research developments in the last year related to the this study, we can also highlight the following:

- There has been development in bioreactor and bioprocessing such as the computially model for growth of cells in microcarriers [25]

- There have been published details on the pilot-scale processing, showing high cell

densities, the highest yet (100 million cells per millilitre) under perfusion conditions [26]

- The continuous development of optimised culture media [27], as well as the development of new mixing conditions, impellers that have reduced shear stress [28, 29], aeration techniques and other cultivation parameters have still been a possible bottleneck for upscaling and making the final products more commercially viable and competitive with animal grown meat, leading to multiple research on this front as well [30–32]

Other main developments over the last years can also be seen in the multiple topics that make up the development of sustainable lab grown meat [33–47]

2.2 Bioreactors in Biotechnology

The main way to cultivate microorganisms, and even mammalian cells (as in this study's case) is to use a bioreactor system. A bioreactor can be defined as a system developed and optimised for supporting biologically active systems [48, 49]. It can have multiple applications, as it is an indispensable part of any bioprocess. It can be used for cultivation of bacteria, fermentation processes and even for the production of cell biomass for food production [50].

A Bioreactor is mainly a fermentation vessel that should ensure the following parameters [51]:

- Agitation, for guaranteeing mixing of medium and cells, preventing sedimentation (in stirred suspension bioreactors, which will be the focus of this study) and also, as better explained below, improving gas mass transfer rate

- Aeration, in the case of aerobic fermentation cultures, which is the case of mammalian cells, specially for supply of oxygen

- Regulation of factors for the culture, such as pH level, pressure, aeration, nutrient feeding, temperature and liquid level

- Sterilisation, one of the most important factors in biotechnology is the sterility of the systems, specially in food and pharmaceutical industries Harvesting of cells/medium, the ability to remove the final product, being it a extracellular chemical or the biomass itself.

The main components of a bioreactor can be seen in the diagram shown in figure 2.1 below, as well as explained in greater detail in the sections below.

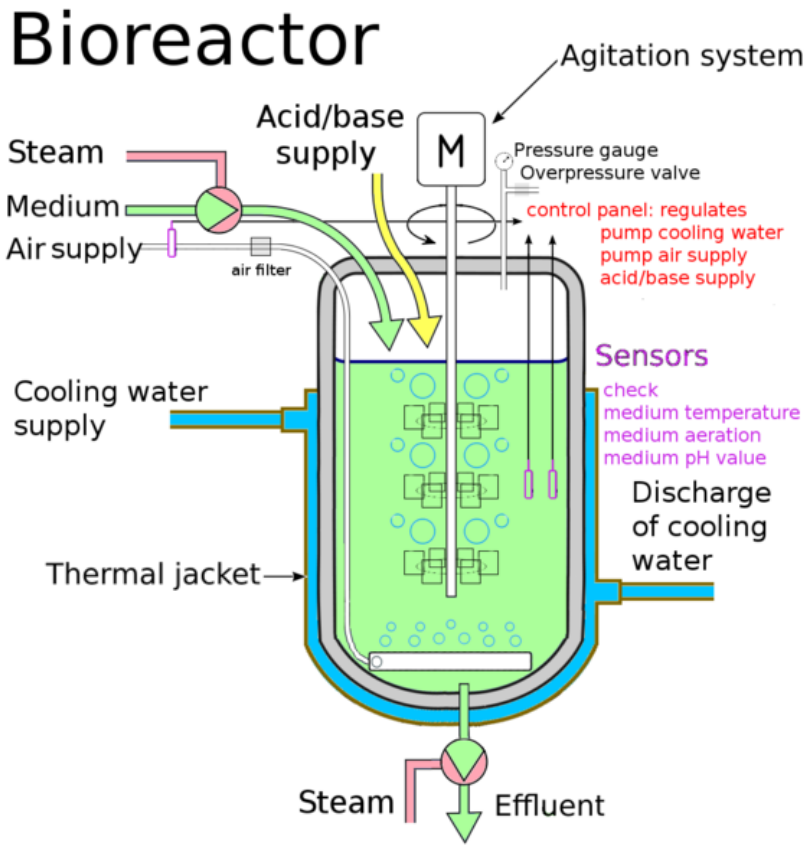

Figure 2.1: Diagram of an example of a Stirred Tank Bioreactor [52]

A complete bioreactor system must have some of the following parts: Fermenter Vessel; Heating and Cooling apparatus; Aeration System; Baffles; Impeller; Sparger; Feed Ports; Sampling Ports; Valves and Controlling Devices for environmental factors.

The existence of these compounds depend highly on the type of cultivation, and this can separate bioreactors into the following types [53]:

- Stirred tank fermentor [54] - Is the most common type of bioreactor in the industry, allows for continuous culture and has the existence of a shaft controlled by a motor that supports one or more impellers that in combination with the sparger allow for better distribution of gas and compounds in the vessel
- Airlift fermentor [55] - also known as tower reactor, it uses a two-zone system where only one zone is sparged directly with gas creating a downpour zone improving the oxygen transfer It is a simple design as it does not require moving parts and has lower cost than the continuous stirred tank reactor
- Bubble column fermentor [56] - mostly used for biological wastewater treatment and some fermentations. This system is similar to the above mentioned airlift fermentor,

the main difference being the distribution of the aeration and the sparging, the advantages are the same as the airlift system, being simple and having low operating cost

- Fluidized-bed fermentor [57] - this system constitutes packed beds with smaller particles, preventing clogging and high liquid pressure drop, in these bioreactors the cells are immobilised and move with the fluid. It is usually used when the use of catalysts is necessary and for immobilised enzymes or cells

- Photobioreactor [58] - These units are specialised for cultures where there is a need for direct sunlight or artificially illuminated, mostly for photosynthetic cultures such as microalgae and cyanobacteria

- Membrane bioreactor [59] - This system combines the common membrane filtration process with cultivation in bioreactors, resulting in removal of solids and well as removal of high nutrient levels to control the concentration gradients better, and even with the use of pure oxygen the benefits of this bioreactor are even bigger

From these different types, the main one this study will focus on is the continuous stirred tank reactor, which is the most commonly used in industrial scale. This type is in general preferred due to the existing industrial capacity, proven performance and easy scale-up, control and maintenance of homogenous conditions [60].

2.3 Oxygen Mass Transfer in Bioreactors

For the cultivation of mammalian cells, oxygen is one of the most important nutrients, especially because most cells have a low capacity to carry a large amount of it. Oxygen mass transfer is a difficult topic to optimise since it depends on multiple factors that influence the behaviour of the cells and the way the bioreactor functions. Without oxygen, mammalian cells like Chinese Hamster Cells (CHO), which is one of the most studied mammalian cell types for biotechnology applications, cannot properly proliferate or have stable metabolic activity, such as production of indispensable compounds and maintenance of the cell's metabolites [61, 62].

Cells consume Dissolved Oxygen (DO) and the amount available in water is restricted by the solubility of oxygen in water. This restriction causes limitations and even cell death if the conditions are not understood and optimised. For this reason it is imperative that the Oxygen Transfer Rate (OTR) is controlled and the value is enough for the needs. It is necessary to focus on two main parameters, namely a, the area that is available for mass transfer and the mass transfer coefficient, k_L [63]. These two parameters are usually described as Oxygen $k_L a$ or oxygen volumetric mass transfer rate, which is a compound parameter, between kL and a, which represents the aforementioned area of contact between liquid and gas available per unit of volume.

The process of generating DO is usually called aeration. There are multiple types of aeration systems that present multiple advantages and disadvantages. We can divide them according to the effect they have on kLa, the cells viability due to shear stress or economic viability and scalability to industrial processes. For a more detailed discussion on this topic, there is a need to study the effect of certain parameters on Oxygen kLa and the different techniques that exist nowadays for the aeration of bioreactors. In general, there is a good understanding of what maximises kLa when it comes to the parameters mentioned below. Nonetheless, the complexity comes from the effect said maximisation has on the viability of cells and economic viability of the production process as aforementioned.

2.3.1 Mass transfer dependence on bubble size

One of the most commonly used aeration methods in bioreactors is the use of bubble aeration, namely through the use of spargers. There are a number of factors that influence the way this is done as explained in more detail below. In bubble aeration the size of the bubbles impact the way they behave in the system. There have been multiple studies on this and the effect of bubble size on kLa and it is still a widely researched topic, evermore due to the increase in biotechnology advancements over the last years [64–66].

According to several research articles [67, 68] the behaviour of bubbles, the consequences of its size and effect on cells has been studied on multiple systems. Throughout the different studies there are some recurring conclusions that must be present when studying aeration. Namely, cell damage as a function of bubble size, bubble rise speed and mass transfer coefficient of oxygen and carbon dioxide based on bubble size [69].

As presented in the aforementioned studies, according to Laplace's equation, bubble size is related to the pressure inside of it and the difference with its environment. It is known that the smaller the bubble, the higher the pressure is inside when compared to the external pressure of the medium. During ascent in bioreactor, bubbles tend to get slightly larger due to reducing the pressure or by coalescence with other ones. Although the changing in shape and size is more commonly observed in larger bubbles, since smaller more pressurised bubbles tend to behave as solid particles. Another important factor to notice, which is related to the bubble size is that smaller bubbles have lower rising velocities due to a smaller buoyant force caused by a smaller volume of displaced fluid. The terminal velocity is reached when buoyant force and drag force are equal in intensity [70, 71]. Therefore they present longer residence time in the fluid which in terms allows for more time of contact between the gas-liquid boundary. This, in combination with the observed higher pressure and the increase in superficial area in relation to volume, are three main reasons why small bubbles have higher mass transfer rates of oxygen.

Nonetheless there are two other important factors to consider when it comes to aeration of bioreactors for cultivation of mammalian cells, namely the cell damage and the CO_2 absorption by the bubbles. When it comes to smaller bubbles we have seen really good advantages over larger sizes, when it comes to increasing kLa. As seen in Biotechnology

Volume 3, by H. J. Rehm and G. Reed [68], there is the occurrence of damage to the cells caused by bubbles. In the "Mechanisms of Bubble-Induced Damage" chapter of the aforementioned book, there is a clear pattern observed of increased cell death the smaller the bubble size. It is presented as a correlation between the rate of death of cells and the bubble diameter, as shown in equation 2.1.

$$k_d = \frac{\rho_g V_g}{\rho H} E(d_b) \tag{2.1}$$

Where k_d is the cell death rate, ρ_g and ρ are the densities of the gas and liquid phase, respectively, V_g is the gas superficial velocity and H is the liquid height. $E(d_b)$ is the effect of d_b bubble diameter on liquid entrapment.

Even though bigger bubbles cause less cell damage, as seen above, it also causes lower kLa due to lower residence time and lower surface area, which would result in higher sparging rate and higher mixing speeds. This antithetical relationship between "bubble size vs kLa" and "bubble size vs cell damage", lead to the conclusion that there must be two optimal bubble sizes that optimise these relationships, one small and one big. According to research [69], the bigger size should be close to 6mm while the smaller one, that should minimise cell damage and guarantee high kLa should be less than 1mm. In general, the most used sizes are small, since the high death cell damage is proven to be not as important as cell density grows, and the high kLa leads to less need for energy costs associated with increased mixing and gas feed rate [69]. However, this becomes more complex on a larger scale, as systems to produce smaller bubbles are harder to design, and the existence of longer bubble time residence due to higher water level height leads to the existence of coalescence. This specific problem will be better understood below, in the correlation between power input and kLa.

The last problem worth mentioning about smaller bubbles is the CO_2 scrubbing. As cell densities increase, not only does oxygen needs rise but also the need to dispose of the present dissolved C_2 that can be harmful to cells. The main difference between CO_2 and O_2 when it comes to the bioreactor with cells is that CO_2 has a much higher solubility than O_2 and the direction of transfer for these two compounds is contrary. This means that CO_2 moves from liquid to gas, while O_2 goes the other way. Due to much higher CO_2 solubility, the bubbles often reach the top of the bioreactor saturated with CO_2, while in contrast, they keep diffusing O_2 to the water during the whole rising process to the surface. Therefore, by not accounting for this effect, it is possible that the logical solution is to decrease the costs, by cutting the amount of air sparged and making sure the bubbles have as big as possible residence time. This leads to bubbles getting saturated with CO_2 too soon, and possibly not stripping all the CO_2 needed.

2.3.2 Mass transfer dependence on mixing profile

The second biggest parameter needed to account for in oxygen transfer, after the aeration, is the mixing profile. To ensure a homogeneous media content distribution, a commonly

used solution is stirring. Homogeneous distribution means that there are no concentration gradients or cell accumulation in dead zones as well as to break up the bubbles sparged into the reactor. Stirring depends on a lot of parameters, and the amount of equations that go into the creation of a working Computational Fluid Dynamics (CFD) model make it a complex subject. Though in this short section, we will go over the important parameters and research done in this field, namely on the importance of agitation for biotechnology fermentation and cell cultivation. A graph presented in Lilly, 1983 (Fig. 2.2), summarises well the operating boundaries for scale-up in bioreactors, that depend mainly on aeration and agitation and the important problems to minimise or prevent completely.

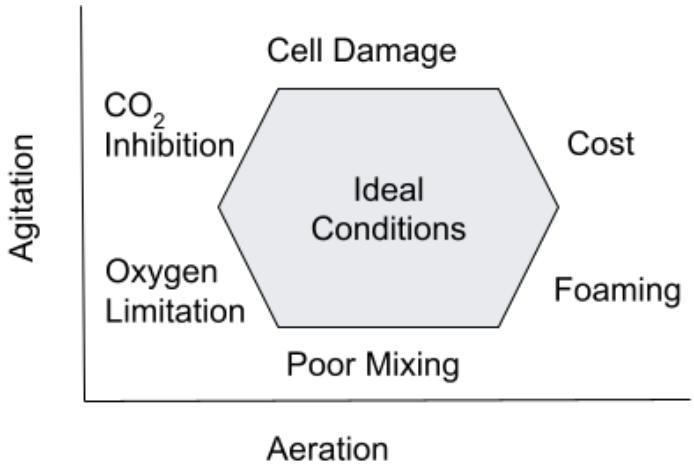

Figure 2.2: Operating conditions and problems that rise from them in bioreactors

Operating conditions and problems that rise from them in bioreactors.

It is standard practice to use agitation, in the form of stirring in cell suspension and microcarrier cultures to improve oxygen transport and provide a uniform environment for cell development. Microcarriers are usually small beads made from different materials such as gelatin or glucose, they provide attachment for cells and other advantages [72, 73]. Cell death and separation from microcarriers is observed when the stirring speeds are too high. In this study microcarrier culture was not further studied. Concerning cell suspension, due to fragility and relatively large size, mammalian cells are damaged by excessive agitation. Therefore, for bioreactor engineering and design, it is crucial to comprehend the hydrodynamics of agitated bioreactors and the mechanisms causing cell damage [74].

2.3.2.1 Impact of Eddies

One important concept to have in mind is the existence of eddies. In fluid dynamics, the definition of an eddy is that of the swirling of a fluid and the opposite moving current created when the fluid is in a turbulent flow regime [75]. The size of eddies depends on different characteristics of the system, another important consideration to have present is the concept of Kolmogorov microscales. Kolmogorov microscales, in fluid dynamics,

characterise the smallest scales in the turbulent flow regime of fluids. In this small scale, reaching the eddy size of cells, (which is within the size range that matters in biotechnology with mammalian cells) viscosity of the fluid dominates and the existing turbulence kinetic energy is transferred into the fluid as thermal energy. This concept is of extreme importance, specifically the Kolmogorov length scale, which describes the amount of distance at which the dissipation of the transfer of energy stops and defines a cut-off in the turbulence spectrum [76, 77]. This concept can be shown using the following equation 2.2.

$$\eta = -(\frac{v^3}{\epsilon})^{\frac{1}{4}} \tag{2.2}$$

Where η is the size of dissipating eddies, dependent on v and ϵ, which represent the viscosity of the medium and the rate of viscous energy dissipation by eddies per unit of fluid mass, respectively.

The aforementioned concept of the Kolmogorov length scale and the equation is used in computational fluid dynamics and for the giving case of agitated bioreactors, which are governed mostly by turbulent liquid flow, which leads to the existence of eddies. The largest observed eddies are found near the impeller region where the shear stress is the most intense [66]. The size of those eddies is similar to the impeller's blade width. These large eddies start a gradient of multiple smaller eddies through the dissipation region, which in turn reach the small scale described by the aforementioned equation 2.2. The rate of viscous energy dissipation, needed for the Kolmogorov length scale, can be calculated using the following equations 2.3 and 2.4 [78].

$$\epsilon = \frac{P}{\rho V} \tag{2.3}$$

$$P = N_P \rho N^3 D^5 \tag{2.4}$$

Where P is the mixing-power input, V is the liquid volume where the energy is dissipated, ρ is the fluid density, N_P is the dimensionless power number related to impeller geometry, N is the impeller rotation speed in Revolutions per Second (RPS) and D is the impeller diameter.

2.3.2.2 Reynold's Number

There is another fundamental concept to have in mind before diving more into the impact of the fluid dynamics caused by agitation and the impact on the oxygen mass transfer, and that is the Reynolds number. When characterizing the flow regime of a fluid, the Reynolds number is a must known parameter, that basically using the fluid's properties and calculates a dimensionless number that characterizes the flow regime in laminar,

turbulent or transition. Reynolds number corresponds to measuring the ratio between the inertial and viscous forces [79]. There are countless applications of this number and multiple scales and variations of the main equation but the following equation 2.5 [80] is most suitable for the work presented in this study. It is important to note that a stirred vessel system is fully turbulent for values of Re above 20000.

$$Re = \frac{\rho N D^3}{\mu} \tag{2.5}$$

Where ρ is the density of the fluid, μ is the dynamic viscosity, N is rotational speed (RPS) and D the diameter of the agitator.

According to the aforementioned equations, we can conclude that the higher the agitation speed the higher the power input, the higher the dissipation, and the smallest the eddy sizes, and because small eddies cause more damage to cells, it is important to minimize the needed rotation per unit of time of the impeller. According to past computational fluid dynamics studies [81], particles that are neutrally buoyant, meaning that have approximately the same density as the fluid (for example cells or microcarriers), tend to follow the motion of eddies larger than them. Therefore, smaller eddies or closer in size to aforementioned particles, collide with them and transfer the energy they carry onto said particle, causing the mentioned cell damage, or shear stress [74].

There have been multiple studies about the effect of different agitation rates in different bioreactors [82]. It was observed that in an agitated vessel, mammalian cell damage was only noticeable in the range of 160-200 RPM, where the bubbles in the aerated system break in the lower part of the vortex. Reduction of the vortex formation, by increasing the liquid level, allowed reaching cultivation without noticeable cell damage at 800 RPM.

2.3.2.3 Geometry of impeller

The geometry of the impeller used in stirred bioreactors defines the way the system is mixed and impacts substantially the flow dynamics. To classify impellers, usually, it is used the flow pattern they produce [83]. These flows can be described as:

- **Axial flow:** It produces a top to bottom motion in the tank, meaning that it is ideal for solid suspension and stratification, shear produced tends to be lower than that by radial flow impellers, nonetheless this depends on other factors as well
- **Radial flow:** The fluid is moved sideways and then it can either go up or down, creating two main circulations that go from the impeller to the top/bottom of the vessel and back to it. It is more suitable for high-shear applications, like liquid-gas dispersion (like the aeration of a bioreactor) and emulsification. Even though there is higher shear, there is less flow when compared to axial flow

- **Tangential flow:** In this last flow pattern, the fluid moves with the impeller in an horizontal way around the vessel, as with the movement of the paddle. This is usually used for mixing highly viscous materials, the shear is low and there is minimal vertical flow

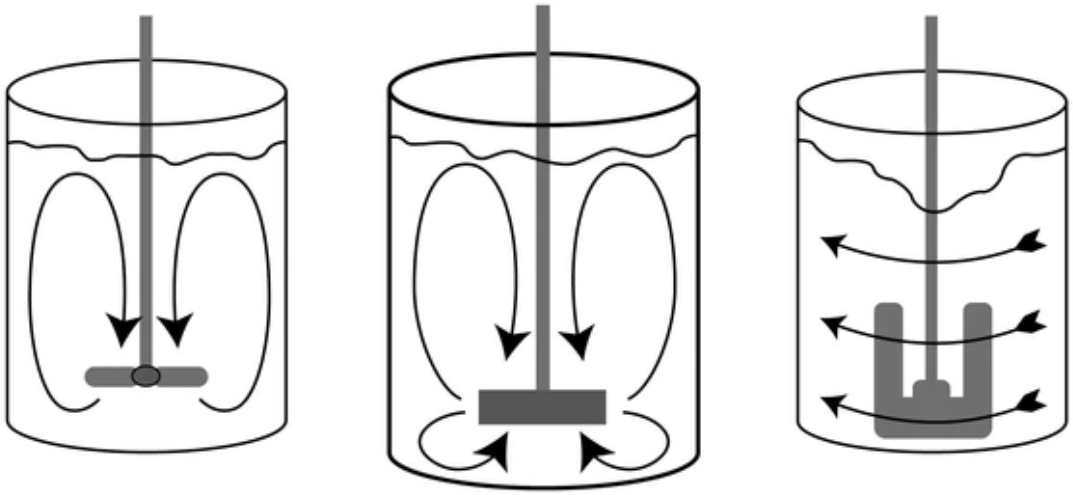

Figure 2.3: Different stirring flow patterns, from left to right, axial, radial and tangential [84]

According to each type of flow there has been an increasing amount of testing for the behaviour of bubbles in these different types of mixing regimes. The relationship between the shear stress, the power input into the system and the flow pattern that help reduce or increase the residence time of bubbles are all important considerations when creating an optimal system for a given application. Below we can see in figure 2.4 different types of impellers used.

There are hundreds of possible geometries for impellers, in this study only a few will be covered. Nonetheless there is another important parameter related to the impellers, and that is the size relationships and the position in the bioreactor. The relationship between diameter of the bioreactor and the impeller are directly correlated to the distribution of energy through the system and the formation of vortexes at higher or lower agitation speeds [85]. Also the specific ratio in impeller geometries, for example the height of the paddles to diameter of the impeller in Rushton impellers, or the number of blades/paddles and angle of the same, greatly influence the system. The height of the liquid level above the impeller also correlates to the formation of vortexes, that not only diminish the existence of vertical flows, but also create zones of higher shear stress for cells and make the gas-liquid transfer slower in some cases.

In the case of multiple impellers, it is also imperative that the distance between them is studied, as the flows can be confluent and create higher shear stress zones and impact the power number of the impeller system. For example, in a dual Rushton turbine system, the power drawn by the rotation of the shaft differs on the distance between both, which can be clearly observed by the flow patterns created [85].

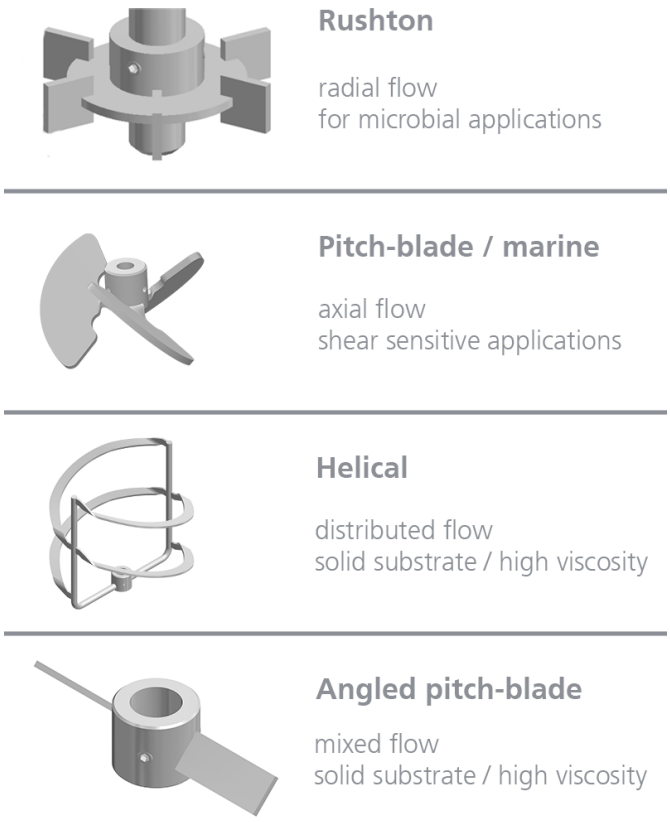

Figure 2.4: Different types of impellers used in bioreactors [86]

Correlated to this factor of mixing and vortexes, is also the existence of baffles. Most industrial and even lab scale systems present 4 or more baffles, these vertical elements, can be present in many shapes and sizes as well, but most commonly exist to prevent formation of vortexes and to improve the mixing of the vessel [87].

In conclusion the main important processes to keep in mind when optimising the mixing in bioreactors are as such:

- Breaking bubbles from sparger (in case of bubble aeration system)
- Eliminating dead zones (anaerobic zones)
- Guaranteed good mass transfer from air bubbles to cultivation broth
- Ensuring good mass transfer from cultivation broth to microorganisms/cells and fast distribution of components, by reducing existence of concentration gradients

- Getting good heat transfer between heating components and media

2.3.3 Power input and mass transfer

Power Input is an important way to correlate a system and the observed oxygen mass transfer rate. As mentioned above, one key parameter shown is the power input for mixing [87, 88]. Multiple attempts and correlations have been studied and made about the relationship between power input in a stirred bioreactor system and the observed oxygen mass transfer rate. In this study we will analyse the results given by existing equations and discuss them. For large systems, an example for a given range of parameters (such as specific range of viscosity, power input and aeration) can be seen in the following equation 2.6 [89].

$$k_L a = 0.027 \cdot P_T^{0.78} \cdot V_g^{0.44} \cdot \pm 35\% \tag{2.6}$$

Where $k_L a$ is the mass transfer coefficient of oxygen, P_T is the total specific power input dissipated into 1 m^3 of the liquid in the system, and V_g is the superficial velocity of the gas. This equation is empirical and the constants shown are specific to a limited range of vessel size, liquid properties and sparging air rate. Nonetheless it is important to know such empirical equations have been created for estimating and modelling conditions in bioreactors. For the main goal of optimization of the bioreactor the use and possible improvement of said empiric equations is necessary for evaluating conditions that would be too time consuming and expensive. The parameter P_T can be described as the sum of the power dissipated in the aerated vessel (P) and the power from the gas expansion of the sparged air (P_G). Which can be seen in equations 2.7, 2.8 and 2.9 [90].

$$P_G = g \cdot \rho \cdot V_g \tag{2.7}$$

$$P = 0.147 \cdot P_c^{0.94} \cdot V_g^{-0.36} \pm 30\% \tag{2.8}$$

$$P_C = \sum_{i=1}^{n} (P_i \cdot D^5) \cdot \frac{\rho_L \cdot N^3}{V} \tag{2.9}$$

The aforementioned equations are an example of the way to correlate power input into an aerated vessel and the volumetric gas mass transfer rate, in the discussion of the acquired data in this study these equations will be among the ones used to verify the results and to optimise the system.

2.3.4 Mass transfer dependence on temperature and pressure

Another important aspect of the bioreactor operating conditions are Temperature and Pressure.There have been multiple studies on the effect of these two conditions on the mass transfer coefficient, and the relationship is positively proportional. Meaning that by increasing temperature and pressure, the volumetric mass transfer coefficient of oxygen increases as well [91]. Due to the fragility of cells when it comes to temperature and pressure the ranges that can be used in this optimization are short, since the cells studied are mammalian and thrive at 37ºC.

Nonetheless it is important to understand also that the increase in temperature leads to decrease in viscosity, which in terms leads to the increase in kLa [92]. The decrease in surface tension caused by increased temperature is a beneficial impact. But, there is a disadvantage that ultimately can lead to smaller kLa value. So as the gas solubility of Oxygen decreases with increasing temperature, leads to the driving force being lower [93]. Pressure increase [94], leads to an overall increase in kLa, due to increasing the main driving force. Since the partial pressure difference between gas and liquid phases is responsible for creating the concentration gradient between both phases, by increasing pressure the partial pressure of gas in gas phase increases as well. Another direct implication is that the solubility of most gases increases with pressure, a contrary effect of temperature when referring to oxygen kLa.

2.3.5 Mass transfer dependence on medium properties

As seen above, the physical properties of the system greatly impact the effectiveness of mass transfer, and as aforementioned properties such as solubility, surface tension and viscosity greatly impact this complex process as well. For this reason it is important to take into consideration that the different additives that can ensure better cultivation conditions, also can affect the physical properties of the liquid-gas system, and affect mass transfer rate [95–97]. The main important factors to observe when adding different substances to the media are:

- **Viscosity -** higher viscosity leads to increased resistance to molecular diffusion
- **Surface Tension -** the increase in cohesive forces at the surface of the liquid can reduce the gas-liquid interfacial area, diminishing the mass transfer rate
- **Density -** the amount of solutes per unit of volume greatly impacts the other aforementioned properties, such as changing the way the fluid flows and the patterns for the distribution of oxygen within the liquid

2.3.6 Aeration types

The importance of oxygen mass transfer has been stated as well as the many of the complex parameters that influence it. Nonetheless regarding the operation conditions of

a bioreactor it is important to understand the different possibilities that exist for aeration. Aeration can be broken down into two main categories: External and internal [68, 98–100].

2.3.6.1 Perfusion Mode Aeration

Perfusion aeration (or external aeration), as the name suggests, involves the oxygenation of the bioreactor fluid through an outside loop. It means that the culture media is oxygenated outside of the bioreactor and pumped back in. This can be obtained mainly in two ways: Modular Membrane Exchangers [101–103] and Pressurised Tank Recirculation [104, 105].

Modular Membrane Exchangers work as membrane aeration systems that are connected to the main bioreactor. These types of systems use modular tubes that can be easily replaced and act as membrane diffusion units that allow for oxygen to diffuse through the membrane directly into the water without the need of bubbling. This type of system presents the normal advantages and disadvantages such as allowing for bubble free aeration and since the modules are outside of the bioreactor the circulating fluid is free of cells reducing fouling of the membrane. Also being outside of the system makes the maintenance of the system easier. But nonetheless to prevent fouling cells would need to be separated from the recirculated fluid and the speed of the diffusion of oxygen through the membrane is much slower than that from direct bubbling. In figure 2.5 we can see an example of this aeration setup.

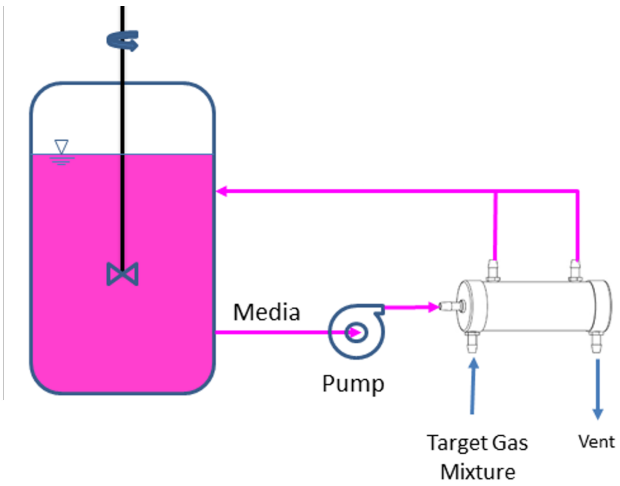

Figure 2.5: Modular Membrane Exchange aeration setup example [103]

Pressurised Tank Recirculation works similarly to the aforementioned modular membrane exchangers, in the way that as an external aeration method. The liquid has to be pumped free of cells into a separated tank, that is then pressured to increase solubility of oxygen and sparged without the concern for cell damage, and once again pumped back into the bioreactor. This system presents similar advantages to the one mentioned above, but it's mostly used for aquaculture and the increasing pressure process.It could be coupled with the recirculation increase the operating costs when compared to other internal aeration methods.

2.3.6.2 Internal Aeration

Internal aeration is the process by which oxygen gets into the bioreactor system by direct contact or transfer into the liquid inside of it. This process can be achieved mainly through surface contacting (bubbleless) or through sparging, which produces the above mentioned bubbles. The main ways used for internal aeration can be described as: Surface Aeration; Membrane Aeration or Immersion Aeration and Sparging. Each of the previously mentioned methods have a wide range of factors that impact their functionality and that will be explained shortly for the understanding of the systems.

Surface Aeration [106, 107] is the phenomena by which the surface of the liquid as it comes into contact with the gas surface diffusion of oxygen molecules happens according to the gradient of concentration and the available surface area. This type of aeration happens naturally and has to be accounted for when performing aeration of small vessels. As the volume grows the impact of the surface of the water becomes less accountable for the general mass transfer that happens for example in a sparged system. This process of surface aeration can also be enhanced or facilitated, as it is done in some aquaculture and ponds, by recirculation of water. The way this works is by pumping water from the bottom of the vessel or pond and sprinkling it on the surface. The impact of the water droplets create an increased surface area for oxygen transfer and the water from the bottom, in natural systems, is not heated by the light source, as it is in case of an open tank or pond. Thus the cold water that is sprinkled cools the surface water and since it's denser than the surface water. It also promotes recirculation of the system. These conditions can be optimised and simulated in vessels. Nonetheless as mentioned above, as the system grows to industrial volumes the impact of surface aeration diminishes. Thus rendering this aeration option not viable or at least not enough for mammalian cell cultivation, when by itself, it is important to note though the importance of it in smaller lab scale testing.

Membrane Aeration in Bioreactors [108–111] work in a similar way as the membrane exchangers mentioned previously. The main difference between both systems is that this one is inside the bioreactor and in direct contact with the growing culture. Membrane systems have a lot of complicated parameters to keep in mind. Nonetheless this has been developed and studied exponentially over the years, as the demand for low shear stress, bubble free, aeration technologies rises due to the growing market on cell cultures [112–114]. Of course said system is limited by the normal bottlenecks of membrane systems, namely the clogging and fouling with cells and cell debris. Disadvantage could be the higher degree of maintenance when compared to the more common sparging option and a more complex scale up, due to the fact that to achieve high kLa. It is necessary to reach high diffusion rates and for that reason high membrane area in the bioreactor. To implement this technology it is necessary to study the different materials that can be used as membranes for the system, meaning the thickness and the total contact area. There is also the need to study the geometry and the placement within the bioreactor, as a coil around the bioreactor circumference or central rotating with the shaft [115]. Also the mode

of operation such as the flowrate and pressure of the gas flowing through the membrane are important to optimise the system and to study its efficiency. In figure 2.6 we can see an example of a membrane bioreactor.

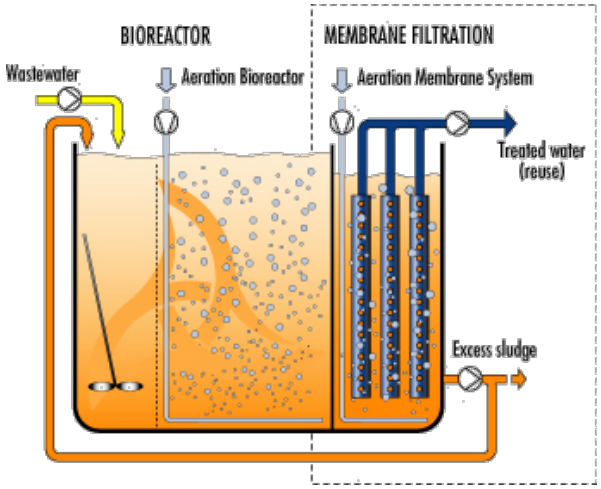

Figure 2.6: Example of a Immersed Membrane Bioreactor [116]

Lastly, the most studied and commonly used method of aeration is sparging. Sparging [117–120] is the direct release of bubbles into the system's liquid phase through the use of a sparger. The sparger can be as complex as a series of concentric circles with different sized holes drilled into them and separate gas supply or as simple as a silicone tube inside a reactor that releases the air that is being pumped inside it in the form of bubbles [121–123]. In this type of system it is important to study how many orifices the sparger has, how big are they and the distribution of the orifices. Since this greatly affects the distribution of the gas in the system, also as a common and widely used technique there are hundreds of different geometries studied and documented, such as perforated plates, tubes, disks, ladder distributors, tri-nozzle spargers, ring spargers and so on. One of the most common for high kLa is the sintered sparger, the sintered sparger, namely the stainless steel sintered sparger. It is basically a cylinder made of porous stainless steel of specific porous size that allows for the creation of multiple small bubbles at the same time, through each of the hundreds of orifices present.

The material used is also an important parameter to study according to the system needs, for our given bioreactor for mammalian cells, Stainless Steel 316L is the common one and resistant to corrosion and widely used for the sintered spargers. By using different hydrophobic or hydrophilic materials we can influence the process behaviour of sparger. Other important features of this technique are the operation parameters, such as flow rate, pressure and the placement of the sparger in terms of height and area (if it's centred or off centre). Even though this type of aeration produces bubbles which have been proven to cause damage to cells, it is still the most cost effective way to aerate bioreactors for this kind of application, so far, which might change as membrane aerated bioreactors develop more and new technologies. A sintered metal sparger producing small bubbles can be

seen in figure 2.7, as well as some different geometries that can be used in designing spargers in figure 2.8.

Figure 2.7: Sintered metal sparger example [124]

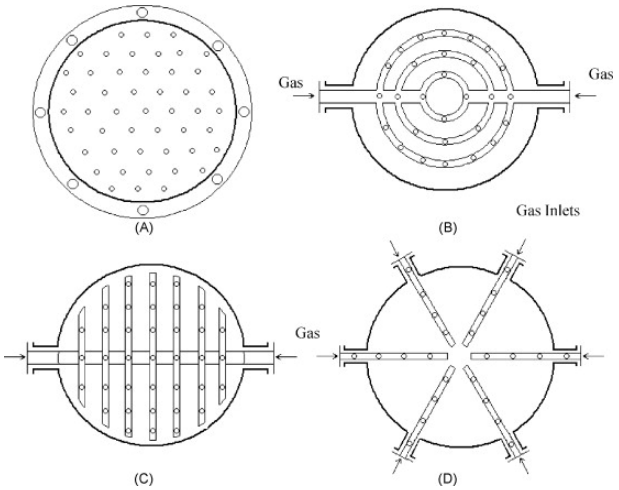

Figure 2.8: Examples of different geometries for spargers [125]

2.3.6.3 Impact of Foaming in Aerated Bioreactors

Foaming is one of the problems that many chemical processes face [126], for example biotechnology processes such as fermentation and in general cell cultivation.Especifically sparged cultivation, suffer this as well [127] mostly due to the fact that the cultivation broth has many foam active compounds, namely carbohydrates and some sugars and by products of cellular metabolism [128]. The main issues with foaming are the reduction of working volume, the trapping of cells and shear stress that leads to the death of the same. Foaming can also lead to blockage of outlets and even putting the sterility of the process in question [127]. With excessive foaming working volume is reduced, as the foaming occupies space used for reaction and gas permeation and can even clog or damage the equipment [129]. There are many ways to control foaming [130], namely the use of special

additives to cultivation media that change the physical properties, such as surface tension and viscosity which are the two main characteristics that influence foaming liquids.

Other forms of antifoaming (prevention of foam formation) and defoaming (active destruction of existing foam) include the use of physical structures like special impellers above liquid level [131] or a recently developed technique using micro engineered shapes that break foam bubbles when they come into contact with them [132]. The use of external simulation is also a well researched method of both defoaming and antifoaming, for example the use of ultrasound is already a common practice in industry [133–135]. Nonetheless there is not much known about the potential use of electromagnetic fields in defoaming or even as antifoaming treatment [136]. The use of magnetic fields and electro-magnetic fields have been known to change some physical properties of water [137], therefore the potential use of Pulsed Electromagnetic Field (PEMF) for defoaming is an interesting topic with potential applications.

2.4 Metabolic Engineering

Metabolic Engineering is the science of the modulation and definition of metabolic pathways in cells combining molecular biological techniques to enhance cellular behaviour. This has been a growing field of study over the years as biotech and pharmaceuticals evolve. Metabolic engineering allows complex mapping of metabolic networks that in turn allow for the better understanding of how everything is connected inside a cell. It could solve the questions as to how we can perceive the behaviour of cells and improve their efficiency, based on experimental, computational and modelling approaches of metabolic pathways. In the Fig. 2.9 we can observe a simple example of a metabolic network. There are a number of studies about typical approaches, namely to the media composition used for production of cell biomass, or various environmental parameters changing the behaviour of cells and even genetic modification [138, 139].

Metabolic pathways are sets of actions and interactions between different genes in cells and the products that result from the change in some component in said system, essential for the correct functioning of a biological system. In short terms, metabolic pathway is the sequence of reactions to take a feedstock compound to the end form product [140]. Well known examples of metabolic pathways that are crucial to cells are the production of immediate energy in the form of Adenosine Triphosphate (ATP) from Phosphocreatine, the production of short-term energy in anaerobic glycolysis and long-term energy in the form of oxidative production of ATP with oxygen [140].

Glycolysis is a metabolic pathway well studied that converts glucose into pyruvate, the free energy released is stored and used to generate energy in the form of ATP. In a cell there are dozens of metabolic pathways that together interact to form a metabolic network that

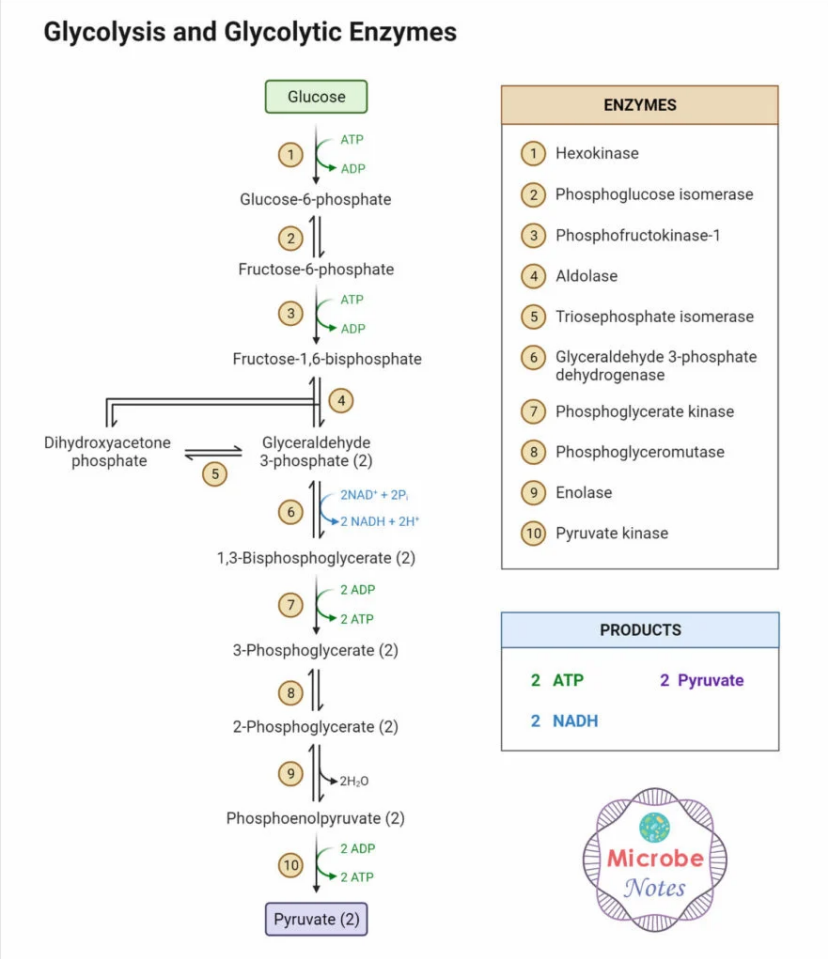

Figure 2.9: Example of metabolic pathway, Glycolysis [141]

dictates the behaviour cells, and one of the most important units of measurement related to metabolism is the flux. It is defined as the rate, quantity over time that metabolites are converted or transported between different pathways and compartments [142].

By studying and mapping this networks scientists can focus on changing specific reactions by gene manipulation or other above mentioned techniques and then share the findings and results, there are several public metabolic networks databases, ranging from organism specific ones such as EcoCyc [143], PseudoCyc [144] and general ones embracing all types of organisms such as KEGG [145] or BIGG [146].

The use of metabolic engineering for the analysis of the metabolic pathways and understanding the best conditions and optimising cells is often achieved through modelling, equations related to metabolic fluxes, the substrates and the kinetics of the reactions

involved.

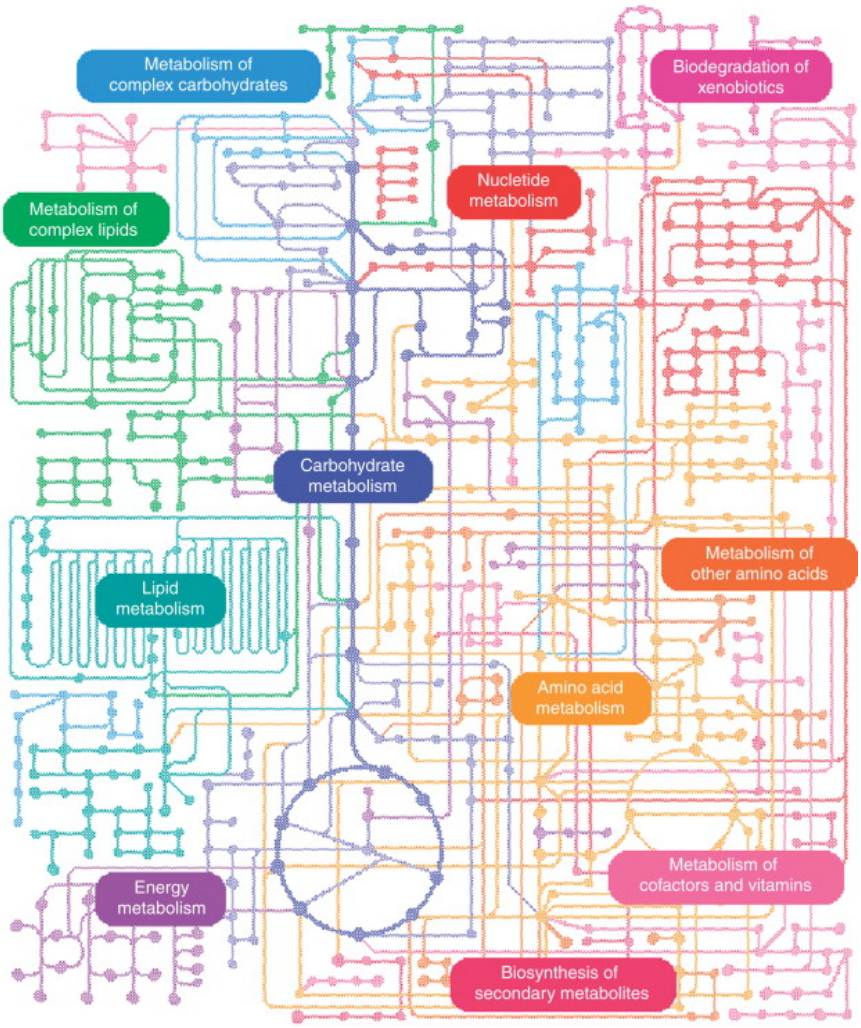

Figure 2.10: An example of a metabolic network, a schematic diagram of part of the metabolic network of Escherichia coli [142]

There are three main analysis modelling techniques used, which are: Metabolic Flux Analysis (MFA); Metabolic Control Analysis (MCA) and Flux Balance Analysis (FBA). The FBA will be explained in greater detail and used in this study to develop and demonstrate how to use programing and metabolic engineering analysis to optimise the conditions and media used for cells, as well as the potential use for gene manipulation mapping and simulation.

2.4.1 Flux Balance Analysis (FBA)

One of the main analysis techniques used in Metabolic Engineering is the Flux Balance Analysis [147, 148]. In this technique the metabolic fluxes are computed under the hypothesis of a main objective for the metabolism. The system created for this approach is still undetermined. It means that there won't be enough equations to compute all the given unknowns. Nevertheless that is not a problem, since FBA is used to compute under the assumption of a metabolic objective. It is important to note that the given solution may not coincide with reality because there is always the lack of constraints in a system, therefore the hypothetical solution reached to conclude the given objective can or not be a good indicator of the real behaviour of the system.

FBA is part of the metabolic engineering constraints-based metabolic modelling, meaning that the objective function of these tools is to predict the metabolic fluxes of a given network in steady-state conditions. As mentioned above, this is accomplished with an incomplete system of equations, resulting in solution "space" and not a single answer. With the use of different constraints we reduce the available space for solutions, getting the results closer to reality. Three commonly used constraints are: Metabolic reactions stoichiometry; Pseudo-steady state assumption and the Thermodynamics of the system [149, 150].

In these methods of analysis the main unit is the metabolic fluxes, and a metabolic network that can be explained as the system of interconnected metabolic reactions.

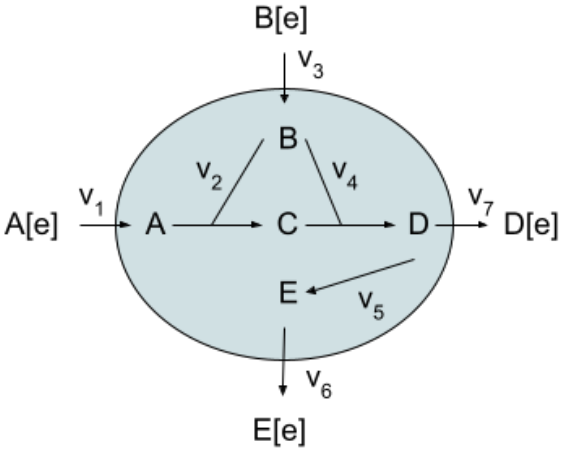

Figure 2.11: A simple example of a metabolic network

In figure 2.11 , we see 7 metabolic reactions, between 5 intracellular species (A,B,C,D and E) with given metabolic fluxes v (v1, v2, v3, v4, v5, v6 and v7). It can be seen that there are 4 reactions of exchange from the cell to the outside or vice-versa.

Metabolic fluxes are usually expressed in molar per unit of time per cell of substrate consumed in the given reaction. With this given example we can then create the metabolic reaction stoichiometry matrix, commonly called matrix S, which shows the relationship between reactions and metabolites. As can be seen below in Figure 2.12.

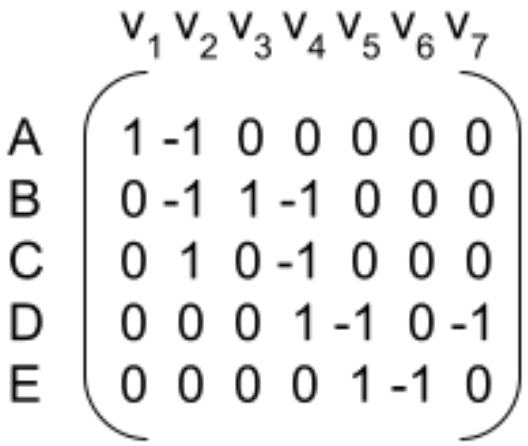

Figure 2.12: Metabolic reactions stoichiometry matrix S example

With this matrix by setting the constraint of pseudo-steady-state hypothesis, we are saying that the multiplication of S by the 1x7 matrix of fluxes (v) is equal to zero, therefore assuming that there is no accumulation of metabolites inside of the cells. Using these two in combination with other constraints and defining the metabolic objective allows us to reach an hypothetical solution. FBA is the common method of choice for most metabolic engineering studies. It can be used to design the composition of the culture medium (which will be the objective in this study), design gene modifications or even both. Some of the most common objective functions used in FBA are: Maximising ATP production, Maximising the rate of a given reaction for synthesis of a desired product, Minimising nutrient uptake and Maximising biomass or cell growth (which will be the objective set for the work in this study) [151, 152].

It is important to note that FBA models that are made using the mentioned constraints and linear optimization can be computed for example in python. It assumes that the cells behave optimally, which means that the reactions occur in a perfect way for maximisation of biomass or minimization of nutrient consumption for example. To implement FBA there are 4 main steps, such as: Defining the system, obtaining reaction stoichiometries, defining the biological constraints and objectives and finally optimising the model. In order to do the second step, there are countless databases with stoichiometric data for hundreds of organisms, as mentioned above in the introduction to metabolic engineering. The system is only as good as the complexity of it, given experimental data it is possible to make a model that approximates to the behaviour of the cells based on the data for given consumption of amino acids and other substrates over time. Of course basic models can be made using only the different kinetic parameters for each used metabolic pathway, but the

rigour of the model can be further increased by correlating the genes and corresponding enzymes involved in the catalysing reactions as well as the reversibility of them.

3

Materials and Methods

In this chapter, the equipment, cells, chemicals and methods used to reach the proposed goals and objectives will be described, as well as the characteristics of the systems used to conduct the experiments of this study.

3.1 Materials

3.1.1 Equipment

All the equipment and systems used to perform the experiments and gather the analytical data will be described below. For the purpose of this study, experiments were carried out in four different bioreactor systems which can be found explained in detail below.

In this study, multiple bioreactor setups, different parameters and even different aeration techniques were studied, as well as evaluated the impact in kLa. The four different bioreactor systems used were:

- **Custom Made Spinner Flask Bioreactor System -** used in most parameters studies due to its flexibility and availability of the system, as well as its low volume and easy setup. In the rest of the document, for simplicity, this system will be mentioned as Spinner Flask
- **Custom Made Stirred Tank Bioreactor System -** used in most cell experiments and for larger scale, different geometry and equipment evaluation. Due to the same reasons mentioned above, this system will from here on be mentioned as Stirred Tank
- **Custom Made Vibromixer Bioreactor System -** used in the experiments to evaluate the impact of different types of mixing; the system itself is identical to the Stirred Tank but with different mixing shafts, motors and plates. This system will be mentioned as Vibromixer

- **Sartorius Biostat B-Plus 10 L bioreactor (Sartorius, Germany) -** this commercial bioreactor was only available for a couple of measurements and experiments, and is the only commercial bioreactor system studied in this thesis. This system will be mentioned below as a Biostat

3.1.1.1 Custom Made Stirred Tank Bioreactor System (0.5 L to 1.5 L)

This bioreactor system (Figure 3.1) was used in most of the experiments and is composed of a glass vessel split into three parts. The top part which has the central opening for the shaft is connected to the motor and the impeller. Six different ports are placed on the top of the lid, mentioned for feeding, sampling and probes that could be connected. The two different bottom parts allow for either up to 0.5 L or 1.5 L working volume,respectively. The dimensions of the system and further specifications can be found in table 3.1 below.

Table 3.1: Parameters, characteristics and components of the Custom Made Stirred Tank and Vibromixer Bioreactor System used

Custom Made Stirred Tank Bioreactor System (0.5L-1.5L)				
Working volume (L)	**Diameter (cm)**	**Height (cm)**	**Bottom Shape**	**Motor**
Up to 0.5 / 1.5*	12	25 / 36*	Round	Stepper motor SX17-1005LQCEF [153]
Control	**Heating**	**Impeller**	**Shaft**	**Aeration**
Separate custom made control box able to connect pH, DO, CO_2 probes and control RPM up to 900 RPM.	1 / 2* Heating Belts controlled by custom control box with Ascon Tecnologic KR1 [154]	Elephant Ear Impeller with 3, 4 and 5 cm diameter and Rushton Impeller with 3.5 cm diameter and six 1 cm high paddles	Stainless Steel, hollow shaft with screwable extensions	Through shaft exiting at the bottom of the impeller or through handmade sparging capillary from stainless steel

*Depends on the bottom part used.

The Stirred Tank bioreactor system can be seen below as well as the impellers used and equipment in figures 3.1 and 3.2.

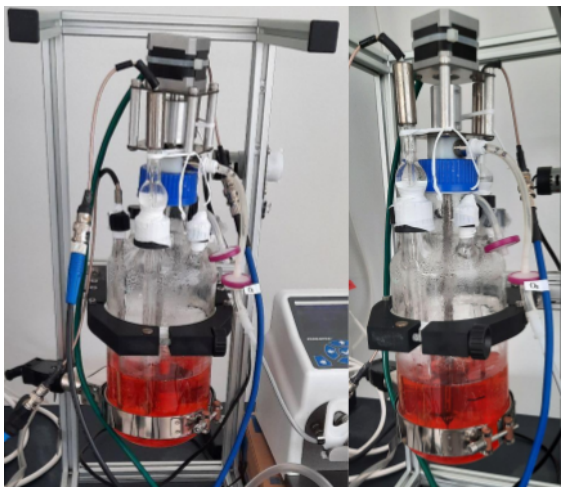

Figure 3.1: Stirred Tank bioreactor system during cell cultivation

Figure 3.2: Different Impellers used in Stirred Tank Bioreactor system, from right to left, stainless steel elephant ear impeller, bottom marine impeller and middle marine impeller

3.1.1.2 Custom Made Vibromixer (0.5 L to 1.5 L)

The above described glass bioreactor system could be converted into a Vibromixer system [155]. It is the same as that explained in table 3.1, except for the motor and the mixing. This system works differently from the other stirred systems.This type of mixing consists in the vertical movement of the shaft with one or more 3D printed plates attached to it.

The mixing plates in this system are of two different shapes, both with 5 cm diameter, and 0.5 cm opening. The difference being the number and shape of the holes, as shown below in figure 3.3.

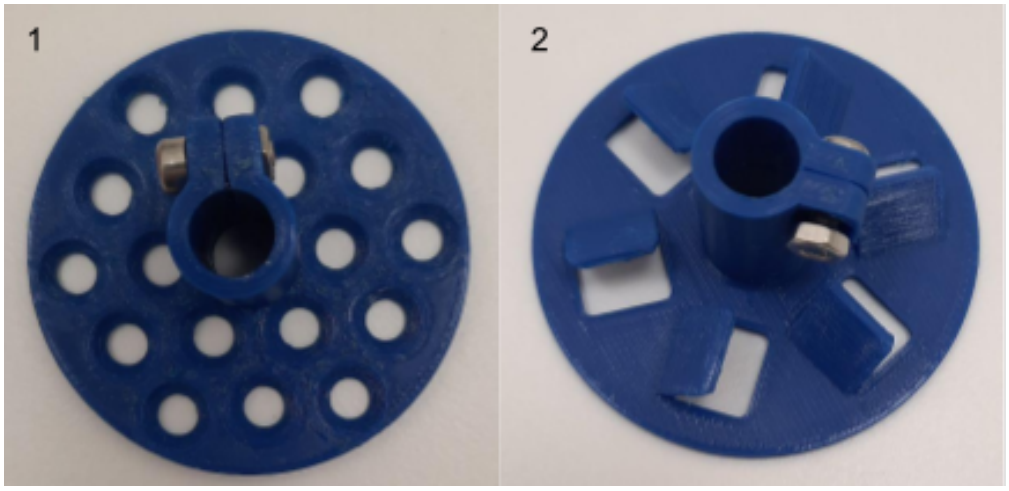

Figure 3.3: The two different plates used in the Vibromixer system, number 1 - Perforated Plate and 2 - Trapdoor Plate

3.1.1.3 Custom Made Spinner Flask Bioreactor System (0.25 to 0.45L)

For smaller scale experiments and measurements in this study, a custom made Spinner Flask Bioreactor system was used. Bioreactor system composed of commercially available glass bottles with custom made glass sampling port and sparger at the bottom. Different types of impellers were connected through the shaft with a stirring engine that was attached to the lid; the detailed characteristics can be seen below in table 3.2.

Table 3.2: Parameters, characteristics and components of the custom made Spinner Flask Bioreactor System used

Custom Made Spinner Flask Bioreactor System				
Working volume (L)	**Diameter (cm)**	**Height (cm)**	**Bottom Shape**	**Motor**
0.25-0.45	9.2	11	Flat	2 Phase Hybrid Stepper Motor 17HS3401 [156]
Control	**Heating**	**Impeller**	**Shaft**	**Aeration**
Custom made arduino control box for RPM up to 350 RPM.	No specific heating system used - Placed inside Incubator or with Heating Plate.	3D printed Polyethylene Terephthalate Glycol (PETG) filament different diameter Elephant Ear impellers and one custom-made Toroidal Impeller*	3D printed PETG filament of different length*	Through a sparging port in the bottom of the glass vessel

*Shaft and Impellers are printed as one piece together and screwed in a connector to the motor.

The Spinner Flask Bioreactor system and its components can be seen below in figures 3.4 and 3.5.

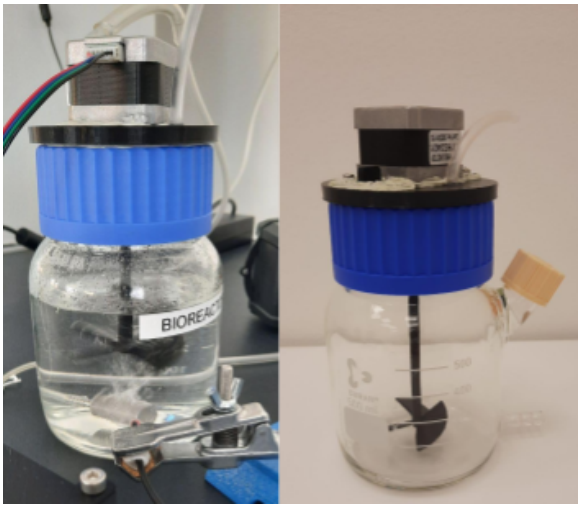

Figure 3.4: Spinner Flask Bioreactor system without sparging port on the left and with sampling port on the right

Figure 3.5: 3D printed PETG filament Elephant Ear impeller used in Spinner Flask Bioreactor system

The Toroidal Impeller is a recent development, used mostly in drones and as boat propellers [157, 158], and can be seen in figure 3.6 below.

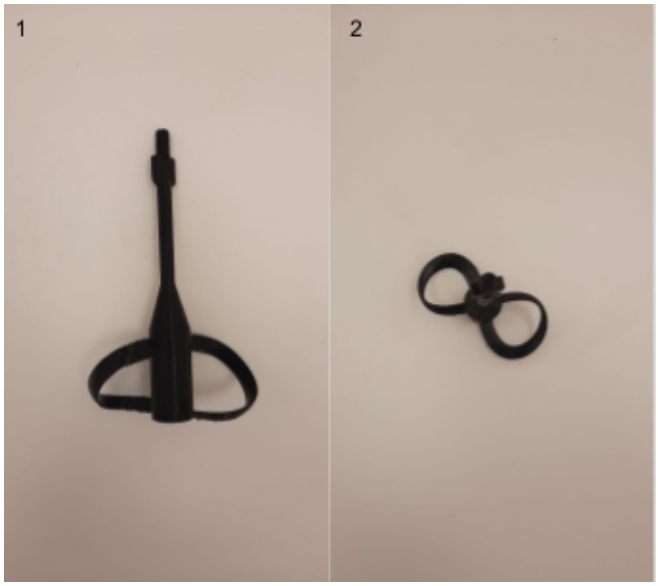

Figure 3.6: 3D printed PETG Toroidal Impeller geometry with 6 cm diameter and two blades used in this study. Side view in picture number 1 and top view in picture number 2

3.1.1.4 Commercial Biostat B-Plus Bioreactor System by Sartorius (4-10 L)

And lastly, for this study, a commercial 10 L Bioreactor Biostat B-Plus system from Sartorius [159] was used. The bioreactor system comprised a control tower and a heating circulator, Julabo 200F [160] to heat the vessel using water through the heating jacket. This system was equipped with 2 stainless steel rushton impellers, 6 blades, with 2 cm height each one and 7.5 cm diameter. The bioreactor setup can be seen below in figure 3.7. This reactor was rented, which limited the amount of experimental data gathered and changes that could be made to the system. The vessel has 22 cm of diameter and 40 cm of height.

Figure 3.7: Biostat vessel on the left and control tower on the right

3.1.1.5 Control Equipment and Sensors

All the probes used for experimental work were commercial autoclavable probes made by Theta [161].

In order to calculate the oxygen mass transfer rate, the Dissolved oxygen (DO) concentration was measured with a Presens Compact Fiber Optic Oxygen Meter OXY-1 SMA [162]. This device uses pulses of light to measure the DO in a solution where an Oxygen Sensor Spot SP-PSt3-NAU [163] is placed.

3.1.1.6 Aeration Equipment

Three different pump were used for the aeration of the bioreactor systems : A membrane pump EHEIM air200 [164] with two air outlets with a maximum flow rate 1 L/min each one; a four channel peristaltic pump ISMATEC REGLO ICC ISM4406 [165], with each channel being able to produce a flow rate of up to around 40 mL/ming; and a single channel peristaltic pump Kamoer FX-STP [166] with a maximum flow rate of 140 mL/min.

Nonetheless an important equipment used and studied were Porous Sintered Steel Spargers, from HENGKO [167], of different pore sizes that will be as well specified according to the experimental set-up.

3.1.1.7 External Stimulation Equipment

The study of the effect of external stimulation on foaming and defoaming, was done on equipment using Pulsed Electro-Magnetic Field (PEMF), namely, BTL EMSCULPT [168]. This machine produces a PEMF that is used for physiotherapeutic treatment. Due to the fact that this device is for human health application the parameters used are of low intensity, since it ensures the safety for human use. The potential impact of PEMF technology for antifoaming and defoaming was recorded and tested in 5 different experimental setups.

3.1.2 Cells

Two different mammalian cell lines were used, which as aforementioned will be referred to as A and B. The main difference between the A and B lines used, is that B was adapted to the conditions relevant for future work, allowing for different metabolic behaviour, more details are not available due to corporate intellectual property reasons.

3.1.3 Media

The main compounds in the media used for the experiments can be seen below in table 3.3.

Table 3.3: Media and Additives used

Media and Additives	
Name / Source	**Description**
HyClone Dulbecco's Modified Eagle Medium (DMEM) F12 [169]	Classical Cell Culture Media
Phenol Red Solution [170]	Common pH indicator for the culture medium, namely in DMEM F12
Polyethylene Glycol (PEG) [171]	Non-ionic hydrophilic polymer used as a shear protectant
Sodium Carboxymethyl Cellulose (CMC) [172]	Anionic linear structured cellulose used as a shear protectant
Non-commercial Soy Hydrolysate	Culture media component
Gibco™ Penicillin-Streptomycin [173]	Culture media component used as antibiotic

3.2 Methods

All the main methods used to gather data as well as to understand the primary results will be explained in this section. Further description of the individual differences between experiments and the analysis of said results is available in the Results and Discussion chapter.

3.2.1 Methods for O_2 kLa estimation (experimental and analytical)

For obtaining the data necessary for the calculation of the mass transfer coefficient, the following procedure was used:

1. Bioreactor filled with distilled water and heated to desired temperature
2. Nitrogen sparged into the bioreactor until the value shown by the oxygen meter was at 5% of oxygen saturation
3. Sparging of atmospheric air until the percentage of oxygen measured was 50% of saturation or higher

The number of measurement points differed in each setup, nonetheless for most experiments the measurement interval was a 5-15 seconds The oxygen volumetric mass transfer rate was calculated as shown below, with equation 3.1 [174].

$$OTR = \frac{dC}{dt} = k_L a(C_{sat} - C) \tag{3.1}$$

Where OTR is the Oxygen Transfer rate, equal to the change in concentration, C, in the liquid over a period of time, t. $k_L a$ is the oxygen mass transfer rate coefficient, and C_{sat} is the saturation concentration for the given temperature, pressure and medium properties.

The dataset for each experiment was analysed in six different ways, showing 6 different kLa values, obtained the following way:

- **Method 1:** By graph analysis to find the highest slope, representing the highest Oxygen Transfer Rate (OTR) and then using that OTR and the equivalent of 50% saturation of Oxygen at the given temperature, to calculate kLa
- **Method 2:** Using the data from the interval between 35% and 50% saturation of oxygen in the liquid to calculate the OTR and then use the 50% saturation at the given temperature to calculate kLa
- **Method 3:** Integrating each time point and the variation of concentration to calculate the kLa between each measurement and use all of the positive values of kLa to calculate the average kLa for the experiment

- **Method 4:** The same procedure as above but for only the concentration interval from 35% to 50% of oxygen saturation in the liquid at the given temperature
- **Method 5:** Integration as well, but this time instead of using each time point, an interval of 1 minute or half a minute was used depending on the observed OTR rate
- **Method 6:** The same procedure as above but using the standard saturation interval of 35% to 50%

These methods will be mentioned throughout the study as method 1 through 6.

3.2.2 Experimental Setups for kLa optimization in Bioreactors

For the study of kLa optimization, a number of experiments and parameters have been approached using the four aforementioned bioreactor systems. Below we can see the description for the different setups used. Throughout the study only two different temperatures were used, 25°C and 37°C. The different temperatures were taken into account to compare the results, and were done mainly due to technical implications (in which the use of ambient temperature was suitable) and in the case of 37°C, it was used to better estimate values for the experimental cultivations.

3.2.2.1 Impact of Impeller Speed on kLa

Below in table 3.4 it is presented all the main characteristics of the setups used in the different bioreactor systems. In this study all systems except for the Vibromixer were studied.This is because the stirring speed of the Vibromixer is not correlated the same way, as the mixing mechanism is different.

Table 3.4: Characteristics of the different setups for the study of Impeller Speed Impact on kLa

Bioreactor System	Tempera -ture (°C)	Volume of liquid (L)	Type of Impeller	N (RPM)	Aeration rate (VVM)
Spinner Flask	25	0.4	Elephant Ear 4 cm	100 - 350	0.01
Stirred Tank	37	0.5	Elephant Ear 4 cm	150 - 500	0.16
Biostat	37	10	2x Rushton 7.5 cm diameter, 2 cm height of blades	50 - 350	0.05

In order to evaluate the results obtained from the study of impeller speed impact on kLa some literature equations were used. Some coefficients were also calculated to better understand the relationship between values obtained.

A commonly found equation that correlates overall KLa [175] with power input and gas velocity is equation 3.2 found below.

$$K_L a = \alpha(\frac{P}{V})^{\beta}(V_g)^{\chi} \tag{3.2}$$

Where $K_L a$ is the total volumetric mass transfer coefficient (s^{-1}), P is the mixing power input in gassed vessel (W), V is the liquid volume (m^3) and V_g is the gas superficial velocity (m/s).

The constants α, β and χ are related to the system's conditions. Nonetheless a simpler correlation for upscaling processes mentioned in some studies [176] can be seen below in equation 3.3.

$$k_L a \propto (N^3 D^2)^{0.74}(V_g)^{0.28} \tag{3.3}$$

In the study for determination of impact of impeller speed, two indicators were calculated to measure the different increase to better visualise the data. The first indicator was kLa increase by 1 RPM, which was calculated as the ratio between the increase in kLa between two consecutive data points and the RPM increase between said data points. This shows how the growth changes per RPM. The second indicator was overall increase in kLa which shows how much the kLa increased between two consecutive data points.

Using the above mentioned equations, the proportionality constants were also estimated using equation 3.4. The value of pC corresponds to proportionality constants between kla_1 and kla_2 , which are the values of kla for data point 1 and 2 and the same for N_2 and N_1, for stirring speed. This proportionality constant can be averaged from all data points for a given system. The averaged pC was then compared to an example from literature.

$$pC = \frac{ln(\frac{k_L a_2}{k_L a_1})}{ln(\frac{N_2}{N_1})} \tag{3.4}$$

The error, or percentual difference between both was also calculated to observe and discuss the values.

3.2.2.2 Impact of Impeller Geometry on kLa

In table 3.5 we have the important characteristics that were used in the experimental setups. For this purpose only two systems were used, namely the Spinner Flask and the Vibromixer. Biostat and Stirred Tank systems were not used in this part because there was not the possibility of changing the impeller geometry.

Table 3.5: Characteristics of the different setups for the study of Impeller Geometry Impact on kLa

Bioreactor System	**Temperature (°C)**	**Volume of liquid (L)**	**Type of Impeller / Mixing Plate**	**Aeration rate (VVM)**
Spinner Flask	25	0.5	Elephant Ear 4 cm,	0 - 0.01
Vibromixer	25	0.5	Trapdoor and Perforated plates	0.05

In order to better understand the mixing and the impact of impeller geometries it is necessary to understand the power number correlation to it. In a lot of studies the simple power number calculation can be done with equation 3.5, seen below [177–179].

$$N_P = \frac{P}{\rho D^5 N^3} [178] \tag{3.5}$$

Using the above equation, the estimations of power number to compare mixing profiles were discussed. Where N_P is the Power Number, intrinsic characteristic of a given impeller geometry; P is the power drawn into the system, in Watts; ρ is the density of the liquid, in kg/m^3; D is the diameter of the impeller in m and N is the stirring speed in RPS (revolutions per second).

3.2.2.3 Impact of Impeller Position on kLa

In this study the effect of impeller position on mixing properties was studied. All systems were studied, with the exception of the Spinner Flask, due to the lack of precise changes in the impeller position, and the smaller scale of the system itself. In table 3.6 we can see all the important characteristics of the systems used. All values used for distance between impellers were done so in correlation to the possible changes that could be done and the relationship with the vessel's diameter, as will be further discussed in the Results chapter. The impeller distance from the bottom was kept the same, except for the Stirred Tank system, where the difference in distance between impellers could only be obtained by changing the lower impeller increasing the distance from the bottom of the vessel.

Table 3.6: Characteristics of the different setups for the study of Impeller Position Impact on kLa

Bioreactor System	**Temperature (°C)**	**Volume of liquid (L)**	**Type of Impeller / Mixing Plate**	**Aeration rate (VVM)**	**Distance between Impellers (cm)**
Stirred Tank	37	1.5	2x Elephant Ear 4 cm	0.09	11.5 - 15.5
Biostat	37	10	2x Rushton 7.5 cm	0.05	10 - 20
Vibromixer	25	0.5	2x Trapdoor plates	0.09	3 - 7

3.2.2.4 Impact of aeration flow rate on kLa

In this experimental part, potential beneficial effects of aeration were evaluated. Biostat wasnt examined due to the inability of producing lower values in the commercial aeration system. In the table 3.7 below we can see all the main characteristics of the systems studied. All the systems show a different type of aeration in order to understand how the oxygen content changed with the aeration rate in all the different setups.

The agitation used was different in each system according to the limitations of the mixing motor and the creation of vortices due to high RPM. The values were high in order to achieve a higher kLa number.

Table 3.7: Characteristics of the different setups for the study of Aeration flow rate Impact on kLa

Bioreactor System	**Temperature (°C)**	**Volume of liquid (L)**	**Type of Impeller / Mixing Plate**	**Aeration rate (VVM)**	**N (RPM)**
Stirred Tank	37	0.5	Elephant Ear 4 cm	0.08 - 0.28	500
Spinner Flask	25	0.5	Elephant Ear 4 cm	0.08 - 0.32	250
Vibromixer	25	0.5	Perforated plate	0.02 - 0.08	350

In this study the calculation of the proportionality constant was also done in the same way as the above mentioned equations 3.3 and 3.4.

3.2.2.5 Membrane Aeration and kLa

For this study the use of the Spinner Flask system was also due to the flexibility and ease of use. Silicone is known to be highly permeable to oxygen [180]. For this study the objective was to use silicone tubing around the interior of the Spinner Flask bioreactor vessel and use wire to hold the tubing coil in place. After deoxygenation of the liquid in the bioreactor by pumping of N_2, air started to flow through tubing and the value of DO increased. There were three different setups done, and there was a control measurement made to compare the kLa without any sparging or membrane transfer, just superficial air transfer.This was used to compare the different setups and see if the membrane aeration actually worked and how much of an increase it was. This is also important due to the fact that, as mentioned, in smaller volumes the impact of superficial oxygen transfer is not negligible. After multiple setups, an optimised setup with increased pressure was reached. In his optimised setup the submerged part of the tube, measured close to 80 cm, with 6 mm external diameter, 4 mm internal diameter and 1 mm wall thickness. The total area submerged for oxygen transfer roughly translates to 152 cm^2. The pressure was increased slightly to increase diffusion through tube walls.

Table 3.8: Characteristics of the different setups for the study of Membrane Aeration

Bioreactor System	**Temperature (°C)**	**Volume of liquid (L)**	**Type of Impeller**	**Aeration rate (VVM)**	**N (RPM)**
Spinner Flask	25	0.5	Elephant Ear 4 cm	0.08	250

3.2.2.6 Impact of Baffles on kLa

The most common type of baffles used in mammalian cell culture are vertical rectangles made out of stainless steel that are connected to the inner side of the bioreactor and act as a flow breaker [181]. There are multiple ways to place them and multiple shapes that can be used and studied, but in this study we only focus on the kLa effect of having baffles. For this, and due to the existence of previous experimental data, there were only two experimental setups made, both in the Spinner Flask system. For this study, the only system used was the Spinner Flask, due to the inability of changing the number of baffles in the other vessels at the time the study was conducted. In the table 3.9 below it is presented all the important characteristics of the setups used. The Toroidal impeller was used; as well as high RPM; due to previous results obtained, concluding that it creates a vortex, for which the baffles are used to prevent.

Table 3.9: Characteristics of the different setups for the study of Baffles Impact on kLa

Bioreactor System	**Temperature (°C)**	**Volume of liquid (L)**	**Type of Impeller**	**Aeration rate (VVM)**	**N (RPM)**	**Baffles details**
Spinner Flask	25	0.5	Toroidal 6 cm	0.01	300	0-2 rectangular vertical

3.2.2.7 Impact of Bubble size on kLa

The study of how a single bubble behaves in different conditions is still a continuously researched topic presently [182, 183], and the difficulty of making a reliable computational fluid dynamics (CFD) model simulation of bubbles in a bioreactor is also quite high [184]. For this study the use of sintered spargers was necessary, to evaluate how the pore size impacted the bubble size and by correlation the kLa. The only system that allowed for simple utilisation of these spargers was the Spinner Flask. Below the main characteristics of the system can be seen.

Table 3.10: Characteristics of the different setups for the study of Bubble size Impact on kLa

Bioreactor System	**Temperature (°C)**	**Volume of liquid (L)**	**Type of Impeller**	**Aeration rate (VVM)**	**N (RPM)**	**Sintered Spargers' Pore size (μm)**
Spinner Flask	25	0.5	Elephant Ear 4 cm	0.08 - 0.32	250	0.5 - 30

In this study, once again the calculation of change percentage was done, similarly to how it was previously explained for the change in kLa per increase of N. In this case the

changes were related to the number of bubbles, size and kLa per increase aeration rate; VVM.

3.2.2.8 Impact of Additives on kLa

The composition of the culture media used for the cultivation of cells has a lot of different components that change the active behaviour of the system in terms of physicochemical properties, some compounds usually called additives are added to the media to allow cells higher viability for different conditions, an example of this are shear protectants. Shear protectants are chemicals that are used to protect cells from shear stress of the mixing and aeration conditions, the way that these compounds work changes a lot from one to another and most of the times there isn't a great understanding about the nature of their functionality. The cells used in this study, like most mammalian cells, are quite susceptible to shear stress, therefore the use of shear protectants is common. Therefore there were studies done to understand the impact on the oxygen transfer rate by using two of these compounds. In this study, the system itself was not important, therefore due to the flexibility of the system all additives were tested in a spinner flask.All the important characteristics of the setup can be seen below in table 3.11. The three different fluids tested were pure distilled water, 0.04% w/w CMC in distilled water and 0.1% w/w PEG in distilled water, according to the ideal concentrations studied beforehand [185, 186].

Table 3.11: Characteristics of the different setups for the study of Additives Impact on kLa

Bioreactor System	**Temperature (°C)**	**Volume of liquid (L)**	**Type of Impeller**	**Aeration rate (VVM)**	**N (RPM)**	**Additives used**
Spinner Flask	25 or 37	0.4	Elephant Ear 4 cm	0.1	250	CMC and PEG

3.2.3 Experimental Setups for Optimization of Bioreactors for Cell Viability

For the study of cell cultivation, and parameters that affect the cell viability in bioreactors, different experimental setups were used in Stirred Tank and Spinner Flask Bioreactor systems, which can be seen below. In order to achieve the maximum productivity possible it is necessary to keep cell density as high as possible and doubling time as short as possible without sacrificing other parameters or making the process too expensive. This is specifically true when speaking about lab grown meat, since the product is the cells themselves and the process must be as cheap as possible to be able to be an affordable and competitive product with regular farm grown meat. Therefore in this chapter three main topics will be discussed and studied:

- The impact of two main parameters on cell viability, namely foaming and shear stress

- The experimental evaluation of nutrient consumption and cell growth using a fed-batch experiment
- A possible way to implement linear programing with metabolic engineering is to use or create a metabolic model to mimic the cell culture behaviour and possibly use these models to optimise the conditions needed, without resorting to hundreds of experiments

3.2.3.1 Shear Stress Evaluation

For this study two cell lines were studied, Cell Line A and B. In both of them the use of shear protectants was tested to estimate and try to measure the limit conditions of shear stress. In table 3.12 we can see the main important characteristics of the used setups. The value of 900 RPM was used due to being the safe upper level of agitation for the stirrer motor. The system used was the Stirred Tank due to the higher degree of control factors in this system and higher RPM values.

Table 3.12: Characteristics of the different setups for the study of shear stress in Cell Lines A and B

Bioreactor System	**Temperature (°C)**	**Volume of liquid (L)**	**Type of Impeller**	**Aeration rate (VVM)**	**N (RPM)**	**Additives used (% w/w)**
Stirred Tank	37	0.5	Elephant Ear 4 cm	0.06	250-900	0 - 0.1 PEG

To discuss the shear stress caused, and to estimate it the use of literature equations was employed. As described in literature [187] an approximation of the shear stress can be made using equations 2.2, 3.6 and 3.7.

$$\tau = \frac{\epsilon}{v}^{0.5} \cdot \mu \tag{3.6}$$

$$\epsilon = N_P \cdot N^3 \cdot D^2 \tag{3.7}$$

Where τ represents shear stress in N/m^2, μ is viscosity in kg/m.s, ϵ represents the energy dissipated by the impeller mixing in m^2/s^3 and v the kinematic viscosity of the fluid.

3.2.3.2 Antifoaming and Defoaming

In this study the Spinner Flak system was once again the system of choice due to its scale. The BTL EMSCULPT PEMF therapy machine was used. The main conditions of the setups can be seen in table 3.13 below. In all setups two spinners were always used, to have a

control system for comparison of the results. The aeration is ensured by using EHEIM air200 membrane pump. After 2 hours of bubbling ,pictures were taken to compare foaming. The treatment was done using one of the applicators from the PEMF device. In all experimental setups the intensity was the maximum allowed, 75hz frequency, at 50% intensity of field and during 1 hour. The applicator was placed under the bioreactor and the efficient height of the PEMF treatment was enough to reach at least half of the medium level. Below in table 3.13 we can see the characteristics of the system used.

Table 3.13: Characteristics of the different setups for the study Antifoaming and Defoaming using PEMF

Bioreactor System	**Temperature (°C)**	**Volume of liquid (L)**	**Type of Impeller**	**Aeration rate (VVM)**	**N (RPM)**	**Additives used (% w/w)**
Stirred Tank	37	0.35	Elephant Ear 4 cm	0.1 and 4.5	250-900	1.25 PEG

3.2.3.3 Fed-Batch Experiment

For the Fed-Batch experiment Cell Line B was used in the Stirred Tank system, which allowed the greatest monitoring and control. The main characteristics of the setup can be seen below in table 3.14.

Table 3.14: Characteristics of the setup for the Fed-Batch experiment

Bioreactor System	**Temperature (°C)**	**Volume of liquid (L)**	**Type of Impeller**	**Aeration rate (VVM)**	**N (RPM)**	**Additives used (% w/w)**
Stirred Tank	37	0.5	Elephant Ear 4 cm	0.06	250	0.1 PEG

The first step to cultivation was done in batch mode, which means that the bioreactor was filled with prepared and sterilised cultivation media and then seeded with the necessary amount of cells to ensure that they grow well over the maximum time they can. The amount of biomass, the time required to achieve it and also the density possible to reach in batch cultivations is not as high as in continuous or semi-continous cultivation mode. This is because after cells exhaust the nutrients or the amount of waste metabolites they produce reach an inhibitory level they stop growing and start dying.

Based on the previous experiments the feeding solution was optimised and the feeding was done at the third day of the cultivation. The feeding solution was 50 mL of distilled water with 750 mg of Glucose, 8 mg of Aspartic Acid, 14.5 mg of Glutamic Acid, 16.5 mg of Asparagine, 14.5 mg of Serine and 13.5 mg of Glutamine dissolved in it.

3.2.4 Predictive python metabolic model estimations of nutrient consumption and growth

As seen by all the above mentioned experiments, there are a lot of parameters that need to be optimised in order to get the highest productivity in cell culture. In order to achieve the best results an enormous amount of experimental data is required, which takes a lot of time and money to acquire doing multiple experiments. In order to cut short the amount of data required there is an important topic to have always in mind when making experiments for optimization, and that is statics. It is important to make sure that the experimental procedures and data gathering is done in a statistically correct way to acquire statistically relevant data. Using this type of data gathering and treatment the relationship between parameters can be better accessed, this includes making more than one reactor at the "same" parameters, taking multiple samples at the same time and measuring more than once the same sample. By doing duplicates or triplicates the variability can be understood and the average can be used to get better results of relationships between different changes done.

Another way to decrease time and money spent and to properly evaluate the next steps in optimization is the use of linear programming modelling, namely metabolic engineering techniques in order to simulate the behaviour of cells, as explained in the general introduction section. In this section of the results and discussion a previously developed model by Robitaille et al [188] was used. This model is a dynamic metabolic model that could describe monoclonal antibodies (mAb) producing CHO cell lines in batch and fed-batch cultivation. This model allows for the optimization of culture media in order to achieve a certain objective for these specific types of CHO cell lines. The objective of this study is to use linear programming in python to simulate batch cultivation using the model developed by Robitaille et al, starting by adapting said model to experimental data from our Cell Line B, which could be compared to the CHO line for which the model was developed.

The metabolic network described in this model can be seen below in figure 3.8. The kinetic equations described in this model are based on biologically relevant mechanistic formulations, where the rates use Michaelis-Menten kinetics. The linear programming model used was based on a previous one. The adapted model can be split into four main parts that will be shown below:

1. Importing the relevant python packages and reading the metabolic matrix from Robitaille's model, which can be seen in figure 3.8

2. Computing the kinetics and rates of reactions based on the constraints and Michaelis-Menten equations that Robitaille's model describes

3. Computing the system of ordinary differential equations (ODEs) that depend on time, and taking the kinetics defined by the previous function

4. Computing the solution for the system of Ordinary Differential Equations (ODEs) using defined starting conditions for concentrations of compounds inside cells and the cultivation media, plotting the results over time and saving the data inside a csv excel file for further analysis

The complete used code had multiple changes overtime, from which the most important ones are the presented ones in the Results and discussion session.

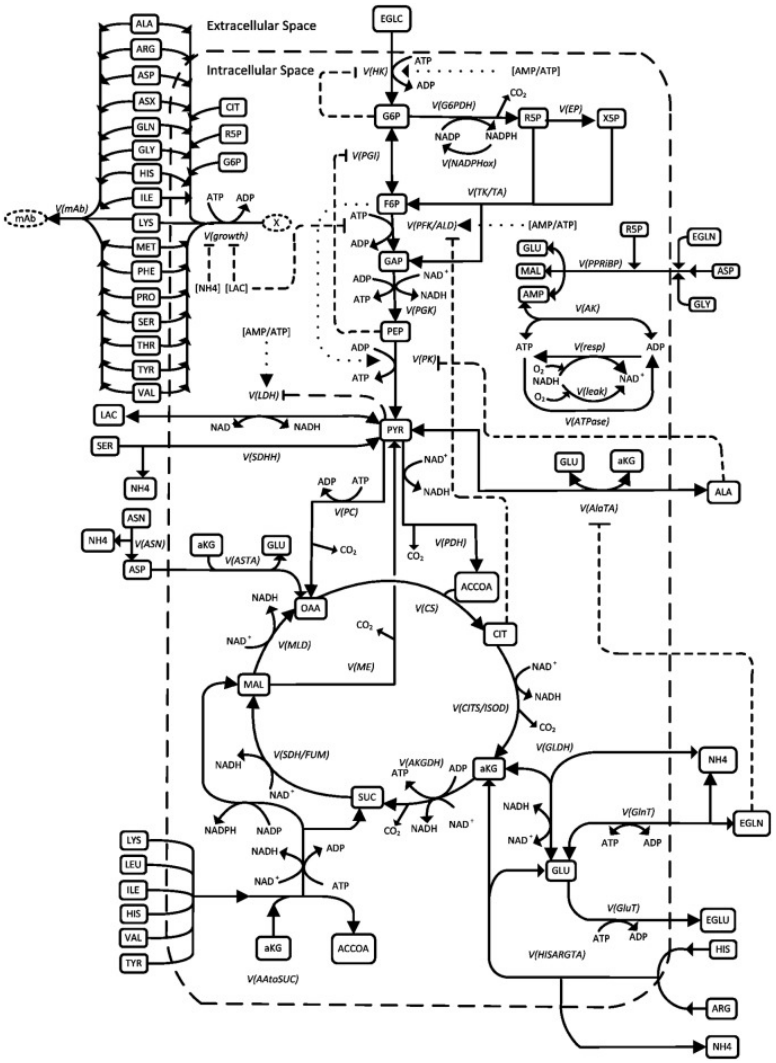

Figure 3.8: Metabolic model described in the model developed by Robitaille et al [188]

3.2.5 Methods for analytical evaluation

For analysis of nutrient consumption and production, and to evaluate the cell density and viability of each experiment done with cells two main techniques were used. Namely a High Performance Liquid Chromatography (HPLC), was used for analysing the concentration of amino acids and other important compounds. Flow Cytometry was used for gathering data about the viability and number of total cells per unit of volume. Certain

measurements and concentrations, such as osmolality measurements were in certain experiments, also analysed by a third party to evaluate the efficiency of HPLC methods and to confirm results.

3.2.5.1 HPLC Concentration of Amino Acids Analysis Method

The samples containing different composition and concentration of amino acids, glucose and lactic acid were analysed by liquid chromatography (LC) and applying different detection techniques (Refractive Fluorescence detection (RF) and Refractive Index Detection (RID)). All measurements were performed on one Liquid Chromatography (LC) instrument, Nexera XS [189], equipped with LPGE and above-mentioned detectors. Measurement conditions are summarised in Table 3.15.

Table 3.15: HPLC Method measurement conditions

Substance	Conditions of Equipment
Amino acids	**Column:** Shim-pack XR-ODS II (100 × 3.0 mm, 2.2 μm); **Solvent:** phosphate buffer; **Method:** gradient elution, pre-column derivatization of amino acids
Glucose	**Column:** Shim-pack SCR-101N (300 × 7.9 mm, 10 μm); **Solvent:** pure water, **Method:** isocratic elution
Lactic acid	**Column:** Shim-pack GIST C18-AQ HP (250 × 3.0 mm, 3 μm); **Solvent:** phosphate buffer; **Method:** isocratic elution

3.2.5.2 Cytometry Cell Density and Viability Analysis Method

The second equipment used for analysis of results in cell experiments was Mindray Flow Cytometer BriCyte E6 [190]. This analytical method is based on detection of fluorescence emitted by propidium iodide staining, that is absorbed by dead cells through the disrupted cell wall. Specifically targeted staining allows to easily distinguish live and dead cells [191, 192]. Measurement conditions were:

- Voltages of 40 V, 220 V and 400 V for Forward Scattering (FSC), Side Scattering (SSC) and Propidium Iodide fluorescence (PI), respectively
- Flow rate of analysis of 10 μL/min
- Volume of sample 10 μL

These settings, mainly the voltages, are specific for the particular equipment mentioned above. The measurements and relationship between FSC, SSC and PI was used to evaluate cell density and viability.

Description of Cytometer Sample Measurement Method

1. Take two samples from a bioreactor/vessel, each sample should be 200 μL, both of them filtered through a 100 μm filter to prevent cytometer blockage

2. Add 400 μL of trypsin [193] to one of them, the trypsinized sample will be placed in an incubator for 10 minutes. The trypsin will destroy the binding proteins in the cell membrane making them unable to stick to each other and to the walls of the measuring tube

3. Add Propidium Iodide (PI) solution to both samples, 0.2 μL for both samples. Measure samples in a cytometer and use the value of live cells from the trypsinized sample and the dead cells from the non-trypsinized sample.Trypsin peels off living cells, but also completely destroys dead cells, so the number of living cells correspond to the reality, but the value of dead cells is lower. Thus, for the proper evaluation, the value of live cells was taken from the trypsinized sample and the number of the dead cells from the non-trypsinized sample

From several cytometry measurements the evaluation of the doubling time can be made, this is a critical parameter to evaluate how well a culture is growing.

4

Results and Discussion

In this chapter, the results of the experimental work will be presented, followed by discussion of obtained data.

The first and most prominent part in this study is the optimization of Oxygen kLa in Bioreactors. There were a total of four different main bioreactor systems studied, where the change of kLa was compared to the change of multiple parameters to obtain enough data. Empirical correlations were observed and compared to the literature. In this part, the experiments were performed without the presence of cells, for most part.

The second and one of the most important parts when it comes to biotechnology, specifically for meat production, is the optimization of Bioreactors for Cell Viability. This subchapter shows different experiments to evaluate the potential threats to cell growth and also a practical study of cultivation of mammalian cells in one of the aforementioned bioreactor systems. Optimization of cell medium culture by adapting an existing Metabolic Model for Chinese Ovary Hamster (CHO) cell line was tested, through the use of linear programing optimization and Metabolic Engineering techniques.

4.1 Optimization of kLa in Bioreactors

As mentioned above, this subchapter will explain and discuss the results of kLa evaluation and the impact of different parameters. The main procedure common to all calculations is explained in the Material and Methods section, Details on the different bioreactor systems used can also be found in that section, in the Equipment subchapter.

4.1.1 Impact of Impeller Speed on kLa

The first parameter and the most studied one, is the impact of Impeller Speed, or Rotations per Minute (RPM). All of the measurements were performed in wide range RPM values in order to compare properly the impact and corresponding data and can be seen in table 4.1 below .

4.1.1.1 Spinner Flask System Results

Table 4.1: Results for Impact of RPM on kLa on Spinner Flask system

N (RPM)	kLa (h-1) Method 1	kLa (h-1) Method 2	kLa (h-1) Method 3	kLa (h-1) Method 4	kLa (h-1) Method 5	kLa (h-1) Method 6
100	0.96	0.87	0.60	0.75	0.60	0.75
150	1.11	1.02	0.69	0.90	0.69	0.89
200	1.13	1.10	0.78	0.96	0.76	0.97
250	1.21	1.12	0.79	0.98	0.80	0.97
300	1.29	1.20	0.85	1.05	0.85	1.03
350	1.17	1.20	1.02	1.06	0.99	1.06

The first two methods were highly unreliable due to the fact that the driving force of oxygen transfer, which is the difference between oxygen saturation and oxygen level in the liquid, was standardised across the whole measurement. Therefore, the use of integration of each measurement interval improved the precision of the value. We can clearly see that Method 1 and 2 show higher values, due to the aforementioned reason and the latter four methods show similar results to each other (in the given example above).

Nonetheless, all the methods were used and studied in all experimental setups, which allowed for a clearer understanding that the bigger time interval used in methods 5 and 6 was able to remove “errors”. The “errors” are caused by uncertainties in the measuring probe and the possible variation of the values due to a non optimal setup, which caused for some bad consecutive measurements; negative variation of oxygen concentration for example; which led to the implementation of wider time intervals for the integration of the OTR to calculate the given kLa. Using 1 minute intervals (in methods 5 and 6), instead of 5 second ones (in methods 3 and 4). The use of the standardised interval of 35% to 50% (methods 2, 4 and 6) oxygen saturation in the liquid, allowed a clearer and more accurate comparison between different setups and systems across all methods.

This allowed the conclusion of method 6 being the most accurate, shown in the rest of the study, presented with the highest difference percentage based on the other methods.

As expected for most methods the kLa value increases with the increase in RPM, which can be explained by the increase in power input into the system, below in figure 4.1 we can see a graph made with the kLa methods against RPM, and the relationship between both.

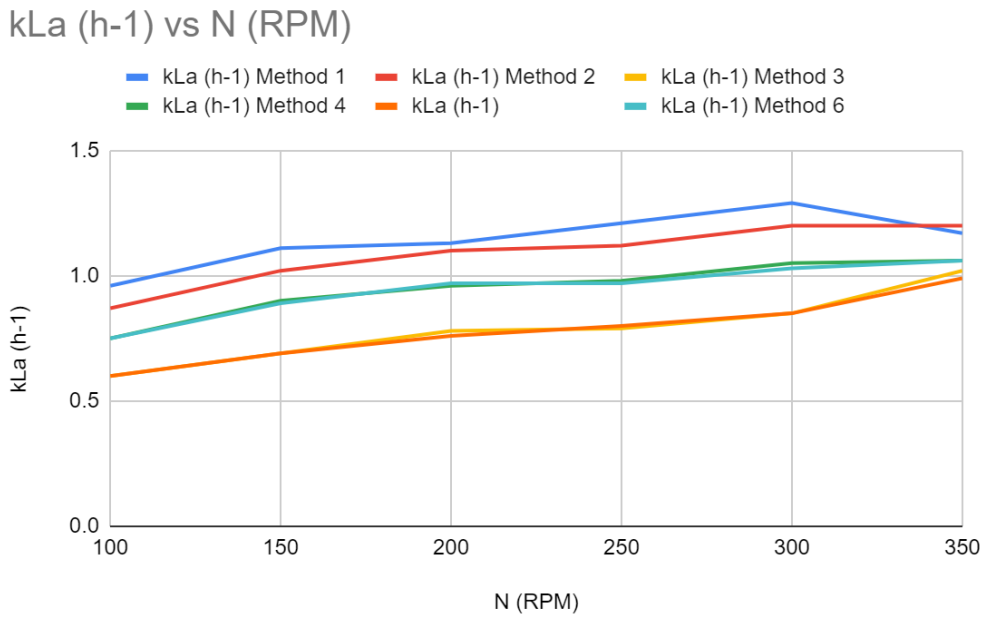

Figure 4.1: Change in kLa with increase of RPM on Spinner Flask system

4.1.1.2 Stirred Tank System Results

Table 4.2: Results for Impact of RPM on kLa in Stirred Tank system

N (RPM)	kLa (h-1) Method 6	Uncertainty of kLa when compared to all methods' average (%)
150	2.49	14
250	2.93	13
350	3.99	14
500	6.96	11

In figure 4.2 and table 4.2 it can be seen that the N values used are different due to the possibility of higher RPM values in this system. The uncertainty percentage shown, which is present in all kLa measurements below, corresponds to the difference between the average of the 6 methods and the chosen method 6 value. Due to the nature of the described methods 1 and 2, the average will always be bigger than the chosen value.

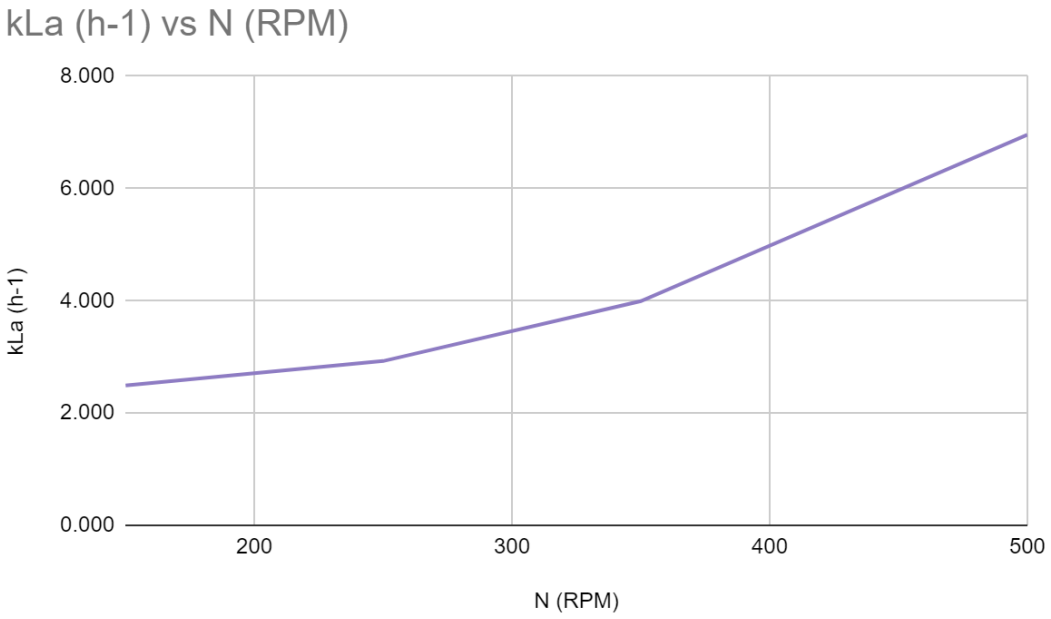

Figure 4.2: Change in kLa with increase of RPM on Stirred Tank system

4.1.1.3 Biostat System Results

In the Biostat system, the stirring speed values, N, were also different from the rest due to the larger size of the vessel and impellers and the objective was to try to stay in the same ranges of tip speed as well as get higher kLa values.

Table 4.3: Results for Impact of RPM on kLa on commercial Biostat 10L Bioreactor system

N (RPM)	**kLa (h-1) Method 6**	**Uncertainty of kLa when compared to all methods' average (%)**
50	8.32	12
150	10.40	16
250	18.84	24
350	32.97	23

The results shown in table and figure 4.3 show an exponential increase of kLa with RPM. The values used were similar to the ones in other systems, except for the first value, which was used to study the kLa on this different system, given the different impellers geometry and volume of the vessel.

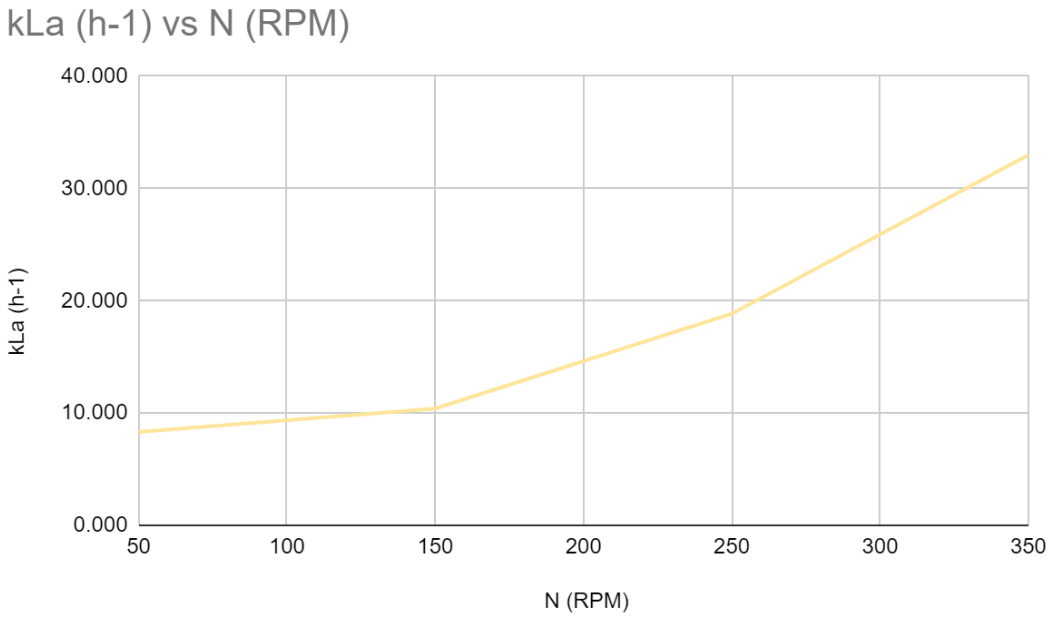

Figure 4.3: Change in kLa with increase of RPM on commercial Biostat 10L Bioreactor system

4.1.1.4 Discussion of Impact of Impeller speed on kLa

The increase of kLa per RPM differs from system to system and even in the same system, in table 4.4 below it is possible to compare the different increase of kLa per RPM, as well as see the tip speed of the corresponding impeller, which is going to be used to compare with literature equations.

From analysing the graphs we can see that the relationship between RPM and kLa seems to be linear for the Spinner Flask system and exponential for the Stirred Tank and Biostat. The kLa values obtained in the last two systems show an increasing kLa increase per RPM, showing the nature of exponential growth, as opposed to the results in the Spinner Flask system. The increase of kLa due to increase in agitation rate is as expected, but the specific relationship between both has been studied in multiple studies [194–197].

Table 4.4: Increase of kLa per RPM in Spinner Flask, Stirred Tank and Biostat systems

Experiment	N (RPM)	Tip speed (m/s)	kLa (h-1)	kLa Increase by 1 RPM (%)	Total kLa Increase (%)
Spinner Flask system	100	0.21	0.75	-**	-**
	150	0.31	0.89	0.4	18
	200	0.42	0.96	0.2	8
	250	0.52	0.97	0.01	0.8
	300	0.63	1.03	0.1	6
	350	0.73	1.06	0.1	3
Stirred Tank system	150	0.31	2.49	-**	-**
	250	0.52	2.93	0.2	18
	350	0.73	3.99	0.4	37
	500	1.05	6.96	0.5	74
Biostat 10L system *	50	0.20	8.32	-**	-**
	150	0.59	10.40	0.3	25
	250	0.98	18.84	0.8	82
	350	1.37	32.97	0.8	75

*The Biostat system has two Rushton impellers, the shown tip speed only correlates to one.
**Values require two points to calculate, therefore there are no values just for the first point.

The main issue with using equation 3.2 is fitting the experimental data using the constants and also the measurement of the power input which can prove to be too difficult, and for this study the power drawn and input was not measured. Nonetheless using equations 2.6, 2.7 and 2.8 from General Introduction section we can see that kLa with a 35% uncertainty is proportional to the total power input (P_T) to the power of 0.78. Rhe total power input itself is the sum of the gas expansion power (P_G) and the dissipated agitation power in aerated vessel (P), which itself is proportional to the mixing power input (P_C) to the power of 0.94. This last power input is itself proportional to the agitation speed (N (RPS)) to the power of 3 and the diameter of the agitator (Di) to the power of 5. As can be seen, using these equations requires more data than the available and still includes a great deal of uncertainty.

The simpler correlation 3.3, presented in the Methods section, can be used for bioreactors to compare systems of the same geometry and culture medium. By using this equation the results we have obtained in each system were compared and the error between this equation and the experimental results was observed. In table 4.5 we can see the proportionality between experimental kLa and RPM and compare it to the relation shown of power of 3.

As can be seen in the table above the calculated kLa increase shows a high error percentage from the actual increase measured experimentally. This could be due to the uncertainty of the oxygen probe used.Most likely the approximation has a low percentage of certainty and was developed for other ranges of the used parameters. When looking at the average proportionality constant obtained in Spinner Flask we can see that the kLa is

Table 4.5: Comparison of experimental data proportionality with literature proportionality

Experiment	N (RPM)	kLa (h-1)	Proportionality constant (kla vs RPM)	Average Proportionality constant (kla vs RPM)	Calculated kla1/kl2 *	Experimental kla1/kla2	Error in kLa values (%)
Spinner Flask system	100	0.75	-**	0.24	-**	-**	-**
	150	0.89	0.4		2.5	1.2	52
	200	0.96	0.3		1.9	1.1	43
	250	0.97	0.03		1.6	1.1	39
	300	1.03	0.3		1.5	1.1	30
	350	1.06	0.2		1.4	1.0	27
Stirred Tank system	150	2.49	-**	0.93	-**	-**	-**
	250	2.93	0.3		3.1	1.2	62
	350	3.99	0.9		2.1	1.4	35
	500	6.96	1.6		2.2	1.7	21
Biostat 10L system	50	8.32	-**	0.24	-**	-**	-**
	150	10.40	0.4		2.5	1.2	52
	250	18.84	0.3		1.9	1.1	43
	350	32.97	0.03		1.6	1.0	39

*Calculated using the proportionality shown in equation 3.3.
**Values require two points to calculate, therefore there are no values just for the first point.

proportional to RPM to the power of 0.2 approximately. In the Biostat and Stirred Tank reactor the proportionality constant calculated changes a lot in the different ranges of RPM used. This could be due to the aspect ratio presented and the volume of the vessel, which leads to a higher importance of superficial aeration. It is important to note also that in the Biostat system there were two rushton impellers, which means that the mixing was different from the other two systems which used smaller elephant ear impellers. Nonetheless the average proportionality constant is almost equal to two times the one on the single impellers systems, which would make sense if you consider the power input as a determining factor for the increase of kLa with increase of RPM.

Within this study we can conclude that the Biostat system shows the highest kLa for given RPM, but this does not mean that the system is better. The different impeller and mixing, which will be mentioned below, affect the values deeply. As well as the different aeration rates and the power draw, which unfortunately was not a parameter that was estimated.

4.1.2 Impact of Impeller Geometry on kLa

The shape, geometry and size of the impeller greatly influence the mixing profile, mass coefficient and whole hydrodynamics of the system. Three different impellers were studied: Elephant Ear Impellers, Toroidal Impeller and Rushton Impeller. Experiments

with Elephant Ear and Toroidal impellers were carried out in the Spinner Flask System, under similar conditions. Unfortunately the study with Rushton was only done in the commercial Biostat System, which makes it less reliable to compare. Nonetheless there is a possibility to evaluate the efficiency of it. In this part we will also include the kLa measurements in the Vibromixer system. For the Vibromixer system, two different plates were studied, as previously mentioned in the Materials and Methods section. The two types of plates are namely the perforated plate and the trapdoor plate.

4.1.2.1 Spinner Flask System Results

Table 4.6: Results for impact of Impeller Geometry with Elephant Ear impeller in the Sparged Spinner Flask system

N (RPM)	**kLa (h-1) Method 6**	**Uncertainty of kLa when compared to all methods' average (%)**
100	0.71	0.1
150	0.66	2
200	0.92	4
250	0.83	8
300	1.00	2
350	1.08	4

The values used for RPM in the graph and table above were done up to the system's limit of 350 RPM. The uneven increase against RPM does not correspond to the expected reality, this could be due to the accuracy of the measurements and calculations. Since the increase between data points is not too large.

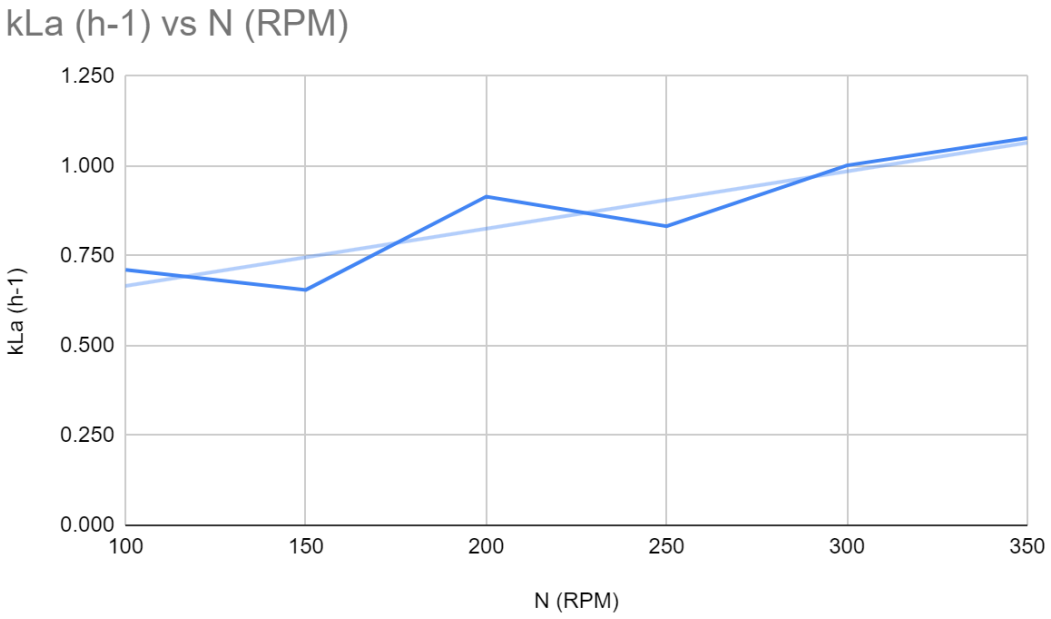

Figure 4.4: Change in kLa with increase of RPM on Spinner Flask system sparged, with Elephant Ear impeller

Table 4.7: Results for impact of Impeller Geometry increase in kLa with RPM, Elephant Ear, not sparged in Spinner Flask system

N (RPM)	**kLa (h-1) Method 6**	**Uncertainty of kLa when compared to all methods' average (%)**
250	0.92	11
350	1.22	12

In table 4.7 it is seen that only two RPM values were used, these values were chosen with a difference of 100 and high enough to produce high kLa. There were no more RPMs done in this setup since the impact of aeration was studied in this system in greater detail in a later part of this study.

Table 4.8: Results for impact of Impeller Geometry increase in kLa with RPM,Toroidal impeller, sparged and not sparged in Spinner Flask system

Experiment	**N (RPM)**	**kLa (h-1) Method 6**	**Uncertainty of kLa when compared to all methods' average (%)**
Not Sparged	100	0.84	11
	150	1.17	9
	200	1.45	7
	250	1.87	5
	300	2.57	10
	350	2.42	10
Sparged	100	1.31	6
	150	1.72	5
	200	2.44	6
	250	3.70	3
	300	4.08	9

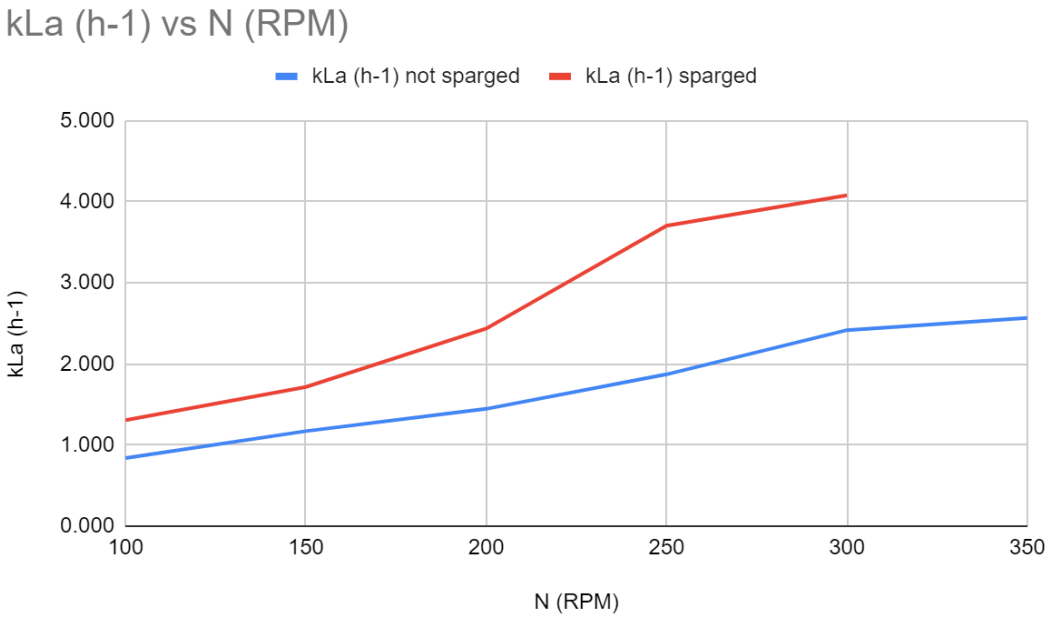

Figure 4.5: Change in kLa with increase of RPM on Spinner Flask system sparged, with Toroidal impeller, sparged and not sparged

As expected, in table 4.8, the sparged system presented a much higher kLa, the growth in both cases was different, the sparged system seemed to be more exponential, hinting at the possibility of the aeration causing a change in how the value increases with RPM.

4.1.2.2 DIscussion of Results for Elephant Ear, Toroidal and Rushton Impellers

To better compare the results in table 4.9 we can see the increase in kLa with RPM for the different experiments mentioned above as well as for the Biostat system that used the two rushton impellers.

Table 4.9: Increase of kLa in percentage by RPM increase in different systems with different impeller geometries

Experiment	N (RPM)	Tip speed (m/s)	kLa (h-1)	kLa Increase by 1 RPM (%)	Total kLa Increase (%)
Sparged Elephant Ear - Spinner Flask	100	0.4	0.71	-*	-*
	150	0.6	0.66	-0.2	-8
	200	0.8	0.92	0.8	40
	250	1.0	0.83	-0.2	-9
	300	1.2	1.00	0.4	20
	350	1.4	1.08	0.2	8
Non Sparged Elephant Ear - Spinner Flask	250	1.0	0.92	0.2	-15
	350	1.37	1.22	0.3	33
Sparged Toroidal - Spinner Flask	100	0.39	1.31	-*	-*
	150	0.59	1.72	0.6	31
	200	0.79	2.44	0.8	42
	250	0.98	3.70	1.0	52
	300	1.18	4.08	0.2	10
Non Sparged Toroidal - Spinner Flask	100	0.39	0.84	-*	-*
	150	0.59	1.17	0.8	40
	200	0.79	1.45	0.5	24
	250	0.98	1.87	0.6	30
	300	1.18	2.57	0.7	37
	350	1.37	2.42	-0.1	-6
Sparged Rushton - Biostat 10L	50	0.20	8.32	-*	-*
	150	0.59	10.40	0.3	25
	250	0.98	18.84	0.8	81
	350	1.37	32.97	0.8	75

*Values require two points to calculate, therefore there are no values just for the first point.

In table 4.9 we can observe that the increase per RPM in the kLa value is similar, even though some of the data acquired proved inconsistencies, like decreasing kLa with increasing RPM, which could be due to measuring mistakes or oxygen probe uncertainty. The similar percentage increase leads to belief that the proportionality is similar as well, even though the Biostat system was mixed using two impellers and not just one. It is important to note that, contrary to logic, the non-sparged elephant ear impeller mixed

Spinner Flask system showed less kLa than the sparged one.This is impossible due to the fact that mass transfer increases with sparging, which leads to believe there were mistakes in the data gathering in this two experiments. Another logic and possible explanation is that the increase of 50 RPM does not produce enough change in kLa for the uncertainty of the measuring method to gather reliable results, since the lower is the change in oxygen per measurement the more you notice the error of oxygen measurement.

This can be confirmed in the Toroidal impeller experiments that show that in the sparged experiment kLa was on average 65% higher than non sparged experiment. The objective of these experiments was to compare the kLa of different impeller geometries, and it can be estimated that for the same conditions the Toroidal impeller shows higher kLa than the elephant ear impeller, and possibly Rushton gives even higher. It is not certain from the data because the system with Rushton is different from the other system. As we saw in equations 2.8 and 2.9, we can confirm that kLa depends on power input, and the power input by mixing depends linearly with the adimensional parameter known as Power number, which is specific for each impeller geometry.

4.1.2.3 Power Number Estimation and Correlation

Using equation 3.5 we could calculate the power number for each impeller used knowing the physical conditions, geometry and the power input, but in these experiments the power input was not empirically measured. By rearranging the equation we see that the Power input by mixing is linearly proportional to Power Number, to the stirring speed by a power of 3 and to the impeller's diameter to a power of 5. The first two impellers have blades at an angle less than 90°, (45° in the case of elephant ear) which produce downwards axial flow [198] while Rushton produces radial flow, the changes in flow also affect the bubble time residency thus affecting the kLa.

Using the power number available in multiple studies [199–201] for the 6 blade Rushton impeller the power number is around 5.75; for the 45° angled 3 blades elephant ear the power number is estimated to be around 1.9. As for the Toroidal impeller, due to being a recent and different geometry the power number is not known but using equation 3.5 we can estimate the power number using the kLa data from the Spinner Flask experiments. By using the kLa data obtained from the toroidal and elephant ear without sparging we can estimate the RPM needed for both of them to have the same kLa, and as the conditions are the same except for mixing we can correlate that the total power input of mixing must be the same this way we can equal both expressions leaving only the Toroidal Impellers power number as the unknown variable.

Non-sparged kLa for Elephant Ear at 350 RPM is 1.22 h^{-1}; using the linear equation for Toroidal:

$$k_L a = 7.32 \times 10^{-3} \times N + 0.0713 = 1.22 \equiv N = 156.9 RPM \tag{4.1}$$

It can be seen that 157 RPM with Toroidal impeller should give the same kLa as 350 RPM in elephant ear, since all other conditions are the same we can say that the power input of mixing is the same thus arriving at the following equation 4.2:

$$N_{P,Toroidal} \cdot \rho \cdot D^5_{Toroidal} \cdot N^3_{Toroidal} = N_{P,ElephantEar} \cdot \rho \cdot D^5_{ElephantEar} \cdot N^3_{ElephantEar} \tag{4.2}$$

By rearranging the equation in order of $N_{P,Toroidal}$, and substituting the variables by their value and cutting the liquid density since it's equal on both side we reach the value of 2.8, thus confirming that even though the diameter is different the power number of the Toroidal impeller is higher than Elephant Ear used and a bit less than half of the Rushton impeller used. Of course we cannot forget that the mixing properties also change as well as the flow type and shear stress. Which means that there are more parameters to take into account before confirming that either of these impellers are better than the others for sensible cell cultivation, such as mammalian cells.

4.1.2.4 Vibromixer System Results

Table 4.10: Results for impact of different mixing and different plate's geometry in Vibromixer system

Experiment	N (RPM)	kLa (h-1) Method 6	Uncertainty of kLa when compared to all methods' average (%)
Perforated Plate	150	1.15	8
	200	1.45	3
	250	1.64	8
	300	1.98	8
	350	2.06	8
Trapdoors Plate	150	1.71	9
	200	1.78	4
	250	1.61	6
	300	2.19	8
	350	2.31	9

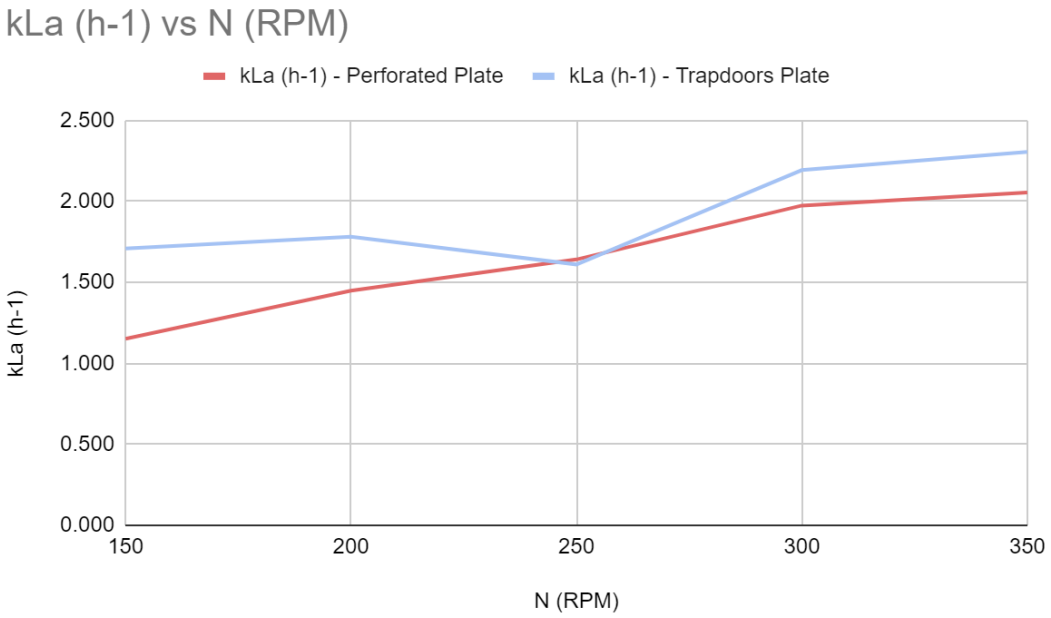

Figure 4.6: Change in kLa with increase of RPM on Vibromixer system, comparing different plates

The observed decrease in kLa at 250 RPM, in table 4.10, for the Trapdoors Plate can most likely be explained by the same reason as the above mentioned unexpected drops, which were caused by the fact that the increase was too low for the accuracy of the methods used. But overall the performance of both plates were distinguished.

4.1.2.5 Discussion of Results for Vibromixer mixing with different plates

The mixing in the Vibromixer system is completely different from the rest of the studied systems, since the movement of the shaft is different. To better understand the changes in kLa with RPM and between both different plate geometries mentioned above, table 4.11 summarises the changes observed.

Table 4.11: Increase of kLa in percentage by RPM increase in Vibromixer system with different plate geometries

Experiment	N (RPM)	kLa (h-1)	kLa Increase by 1 RPM (%)	Total kLa Increase (%)
Perforated Plate	150	1.15	-*	-*
	200	1.45	0.5	26
	250	1.64	0.3	13
	300	1.98	0.4	20
	350	2.06	0.1	4
Trapdoors Plate	150	1.71	-*	-*
	200	1.78	0.1	4
	250	1.61	-0.2	-10
	300	2.19	0.7	36
	350	2.31	0.1	5

*Values require two points to calculate, therefore there are no values just for the first point.

Analysing the increase we can see that the perforated plate has on average a bigger increase in kLa per RPM increase, nonetheless the kLa values fall shorter of the trapdoors plate. On average both of them produce higher kLa than the results observed on the Spinner Flask system with Elephant Ear and Toroidal impeller. The comparison using only the kLa values is not enough since the mixing itself and the vessel is different. And it is also observed that the difference per increase of RPM is lower than on the Stirred Tank and Biostat Systems. The fluid dynamics of this system and the estimation of its power input is more complex than the common stirred tank vessel, there have been a few studies on it but most agree that there is a higher need for studies on this system [202], since it is not as common as the stirred tank system observed in the Spinner Flask, Stirred Tank and Biostat systems studied. The flow and mixing is easier to control since it depends mostly on the orientation and shape of the holes in the plate.The created flux is explained by the Bernoulli effect [203, 204]. There have been some studies about joining the principles of stirred tank to Vibromixer [205] nonetheless due to its complexity and general less use in industry a proper evaluation of the kLa produced and its correlation with the geometry is hard to make.

Nonetheless a comparison between both plates used can be discussed and the difference in kLa can be described using the flow properties that both create. Since both experiments were sparged at the same rate the longer the residence time of bubbles the higher the kLa

observed. According to studies the existence of perforated holes creates a mixing profile based on the orientation of the conic holes and the number of them as well as size [206]. This mixing is created due to the difference in pressure when moving up and down the plate. The percentage of plate area that is not perforated is also an important factor, in this case both plates had a similar ratio of almost 40% area perforated. Due to lack of data and literature reviews on this system the explanation obtained for this difference was mostly due to the fact that the trapdoors plate produces a mixing with higher bubble entrapment rate, allowing for longer residence times thus increasing the oxygen mass transfer, kLa.

4.1.3 Impact of Impeller Position on kLa

Another impactful change on the mixing profile and the effect on the system itself, in the case of multiple impellers, is the distance between them. To better understand the effect on kLa this change in distance between impellers was performed in three different systems.

4.1.3.1 Stirred Tank System Results

Table 4.12: Results for impact on kLa of different impeller position, at different RPM values, for Stirred Tank system using 4 cm diameter elephant ear impellers

Experiment	N (RPM)	kLa (h-1) Method 6	Uncertainty of kLa when compared to all methods' average (%)
15.5 cm between Impellers	150	2.36	0.2
	250	2.59	14
	350	3.21	13
	450	3.92	12
	550	5.19	15
14.5 cm between Impellers	350	3.08	13
	450	4.26	15
	550	5.97	15
13.5 cm between Impellers	350	3.07	14
	450	4.21	15
	550	5.76	16
12.5 cm between Impellers	350	3.35	13
	450	4.05	14
	550	5.49	16
11.5 cm between Impellers	350	2.90	13
	450	3.47	14
	550	4.72	15

The N values used in this system were consistent for all measurements except the first distance setup. In this case a complete set of data was done using two lower values. In the next distances only the higher values were used. The choice of these two higher values

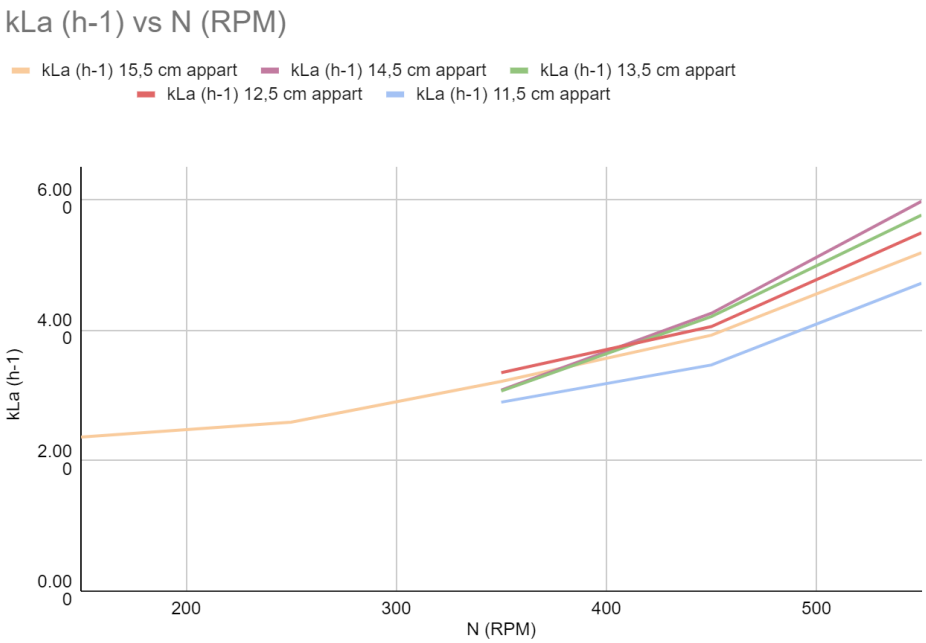

Figure 4.7: Changes in kLa with increase of RPM and change in distance between two 4 cm diameter elephant ear impellers on Stirred Tank system

was due to the growth observed in this system being close to exponential. This means that the lower values would have a lower increase than the higher ones, therefore the impact of the uncertainty of the measurements would be higher if lower values were used.

4.1.3.2 Discussion of Results for Stirred Tank System

To understand how the distance between impellers affects the kLa tables 4.13 and 4.14 summarise the results as well as the increase observed.

From this first table we can see that the increase in kLa value per increase in RPM seems to stay constant for each distance. Nonetheless we can also see that the increase of kLa is not proportional to increase or decrease of the distance, confirming that the relationship is more complex than a simple linear one. The distance values chosen represent the possible setups in the system, as well as in comparison with the diameter of the vessel the relationships are from 0.9 to 1.3 times the diameter of the vessel.

From the results above we can conclude that the increase per distance is similar for different RPM values, and it is non-linear. Meaning that the change from 12.5 cm apart to 11.5 cm resulted usually in up to 3 times as big an impact than the change from 13.5 to 12.5 cm. Due to the existence of 5 points we can conclude that for the range studied the distance of 14.5 cm proves to be the best distance. But since the range was not large this is only a local maximum, and the real best distance even for this range can only be confirmed after extra measurements at distances between 15.5 and 13.5 to find if 14.5 cm is really the best distance for kLa. According to literature the distance between impellers is correlated with the vessel diameter, for better result of mixing and efficiency the impellers

Table 4.13: Results for impact on kLa of different impeller position, at different RPM values, for Stirred Tank system and the kLa increase per RPM

Experiment	N (RPM)	kLa (h-1)	kLa Increase by 1 RPM (%)	Total kLa Increase (%)
15.5 cm between Impellers	150	2.36	-*	-*
	250	2.59	0.1	10
	350	3.21	0.2	24
	450	3.92	0.2	22
	550	5.19	0.3	32
14.5 cm between Impellers	350	3.08	-*	-*
	450	4.26	0.4	38
	550	5.97	0.4	40
13.5 cm between Impellers	350	3.07	-*	-*
	450	4.21	0.4	37
	550	5.760	0.4	37
12.5 cm between Impellers	350	3.347	-*	-*
	450	4.053	0.2	21
	550	5.489	0.4	35
11.5 cm between Impellers	350	2.895	-*	-*
	450	3.465	0.2	20
	550	4.718	0.4	36

*Values require two points to calculate, therefore there are no values just for the first point.

Table 4.14: Results for impact on kLa of different impeller position, difference in kLa by distance for the same RPM

N (RPM)	Distance between impellers (cm)	kLa (h-1)	kLa Increase for 1 cm distance (%)
350	15.5	3.21	-
	14.5	3.08	-4
	13.5	3.07	-0.4
	12.5	3.35	9
	11.5	2.90	-14
450	15.5	3.92	-
	14.5	4.26	9
	13.5	4.21	-1
	12.5	4.05	-4
	11.5	3.47	-15
550	15.5	5.19	-
	14.5	5.97	15
	13.5	5.76	-4
	12.5	5.49	-5
	11.5	4.72	-14

should be in the range of $\frac{1}{2}$ and $\frac{2}{3}$ of the vessel's diameter [207]. This is explained as when

the distance is lower than $\frac{1}{3}$ of the vessel's diameter the vortices created by each impeller connect in counterflow meaning that there is a loss of two individual vortices that increase mixing and more energy is wasted for mixing. In the case of distance being bigger than $\frac{2}{3}$ of the stirring tank's diameters the existence of non-homogeneous flow appears as zones of disconnection to the main vortices cause compartmentalization of mixing zones. The Stirred Tank vessel has a diameter of 12 cm meaning that all of the distances studied were above the optimal range thus having inconsistency of mixing. In literature there was also a study which correlated the distance between impellers and the diameter of each impeller as well as the position (symmetric or asymmetric) between them and the effect on power input which affects both mixing and mass transfer. It was stated that the optimal power input was found for three rushton impellers with the distance between them to be equal to 1.5 times the diameter of each impeller [208]. It was also found that the existence of sparging is correlated with the decrease in power input due to the higher chance of compartmentalization of mixing profiles and main vortices, in general the range should be between 1 and 2 times the diameter of the impeller. If we look at the results and the diameter of the impellers being 4 cm, the ideal should be between 4 cm and 8 cm, thus being too small for the values used or in case of the correlation to the vessel's diameter it should be between 6 cm and 8 cm, even more reduced range.

4.1.3.3 Biostat System Results

Table 4.15: Results for impact on kLa of different impeller position, at different RPM values, for Biostat system using 7.5 cm diameter Rushton impellers

Experiment	N (RPM)	kLa (h-1) Method 6	Uncertainty of kLa when compared to all methods' average (%)
10 cm between Impellers	150	9.36	16
	250	15.80	11
	350	47.41	3
15 cm between Impellers	150	8.32	12
	250	10.40	16
	350	18.84	24
20 cm between Impellers	150	12.32	21
	250	18.72	23
	350	32.88	22

In this system, even though the growth of kLa with increase of N is exponential as well; or at least appears to be; the values after optimisation were separated by 100 RPM without any negligible impact and the difference was high enough for the uncertainty of the methods to have minimal impact on the results, nonetheless the 10 cm and 20 cm distance do have similar results. The distance between impellers used in this setup are within the interval of 0.45 to 0.91 times of the vessel diameter.

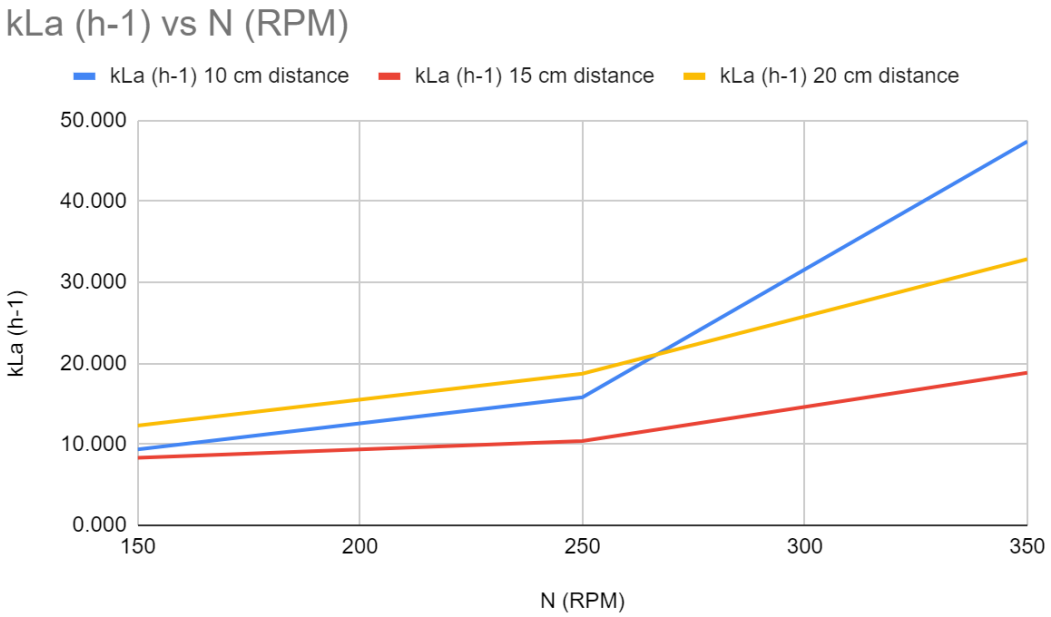

Figure 4.8: Changes in kLa with increase of RPM and change in distance between two 7.5 cm diameter Rushton impellers on Biostat system

4.1.3.4 Discussion of Results for Biostat System

As done above for the Stirred Tank system, the results of change in kLa are summarised in tables 4.16 and 4.17.

Table 4.16: Results for impact on kLa of different impeller position, difference in kLa by distance for the same RPM

Experiment	N (RPM)	kLa (h-1)	kLa Increase by 1 RPM (%)	Total kLa Increase (%)
10 cm between Impellers	150	9.36	-*	-*
	250	15.80	0.7	69
	350	47.41	2	200
15 cm between Impellers	150	8.32	-*	-*
	250	10.40	0.3	25
	350	18.84	0.8	81
20 cm between Impellers	150	12.32	-*	-*
	250	18.72	0.5	52
	350	32.88	0.8	76

*Values require two points to calculate, therefore there are no values just for the first point.

Comparing the results of the Stirred Tank system above, we can clearly see that the kLa values are much higher. It is happening due to the fact that Rushton impellers have a much higher power number than elephant ear, even with smaller RPM and higher volume of water. Following the same principles stated above, the distance between impellers

Table 4.17: Results for impact on kLa of different impeller position, difference in kLa by distance for the same RPM

N (RPM)	Distance between impellers (cm)	kLa (h-1)	kLa Increase for 1 cm distance (%)
150	10	9.36	-*
	15	8.32	-2
	20	12.32	10
250	10	15.80	-*
	15	10.40	-7
	20	18.72	16
350	10	47.41	-*
	15	18.84	-12
	20	32.88	15

*Values require two points to calculate, therefore there are no values just for the first point.

should be in the range of either 1 to 2 times the impeller diameter (in the case of rushton normally 1.5 is the best value) or in the range of $\frac{1}{2}$ to $\frac{2}{3}$ of the vessel's diameter. In this system the impellers used have 7.5 cm of diameter and the vessel has 22 cm of diameter. So according to literature the best value should be at 11.25 cm, or in the range between 11 and 15 cm. Looking at the results we see that it is not as stated, this can be due to lack of more measurements and more distances and RPM values, nonetheless for the lower two RPM values the biggest distance of 20 cm delivered the biggest kLa, but for higher RPM the smallest distance of 10 cm (close to 11.25 cm stated as best distance in literature), revealed a 40% higher value than the biggest difference and more than two times the value of kLa for 15 cm. This proves that for higher agitation the correlations shown in literature appear to be correct.

4.1.3.5 Vibromixer System Results

Table 4.18: Results for impact on kLa of different plate position, at different RPM values, for Vibromixer system using trapdoor plates

Experiment	N (RPM)	kLa (h-1) Method 6	Uncertainty of kLa when compared to all methods' average (%)
3 cm between plates	300	2.58	6
	350	3.22	3
5 cm between plates	300	2.63	9
	350	2.76	9
7 cm between plates	300	2.61	9
	350	2.61	16

In the Vibromixer system only two high values of RPM were used. Due to time

constraints using the system. Unfortunately some of the values were too close to each other, and due to mechanical limitations it was not possible to achieve higher N values.

4.1.3.6 Discussion of Results for Vibromixer System

As mentioned before, the mixing of Vibromixer systems is not well studied, nonetheless like for the previously shown systems the effect of having a different distance between the mixing plates and the impact on kLa is shown in tables 4.19 and 4.20.

Table 4.19: Results for impact on kLa of different distance between plates, difference in kLa by distance for the same RPM

Experiment	N (RPM)	kLa (h-1)	kLa Increase by 1 RPM (%)	Total kLa Increase (%)
3 cm between plates	300 350	2.58 3.22	-* 0.5	-* 25
5 cm between plates	300 350	2.63 2.76	-* 0.1	-* 5
7 cm between plates	300 350	2.61 2.61	-* -0.01	-* -0.3

*Values require two points to calculate, therefore there are no values just for the first point.

Table 4.20: Results for impact on kLa of different distance between plates, difference in kLa by distance for the same RPM

N (RPM)	Distance between plates (cm)	kLa (h-1)	kLa Increase by 1 cm distance (%)
300	3 5 7	9.36 8.32 12.32	-* -6 24
350	3 5 7	15.80 10.40 18.72	-* -17 40

*Values require two points to calculate, therefore there are no values just for the first point.

Following the same criteria as above we can see that this time the decrease and increase with RPM and with distance is more non-linear. We can see that the biggest distance shows the highest kLa and the increase when compared with the lower distances is really high (up to 40% increase in kLa per cm of increase). Using the same ranges as before, the system has the same 12 cm of diameter of the vessel and 5 cm of diameter for each plate. The mixing process might be completely different from stirred tank, nonetheless, the reasoning behind the impact of distance between impellers is due to the confluence or compartmentalization of the mixing profiles and the vortices. For this reason it is also

interesting to check if the ranges mentioned above are true for this case. According to literature the range should be from 5 cm to 10 cm, or combining the both ranges mentioned above, it should be restricted to 6 cm to 8 cm, and according to the values we have the 7 cm measurement proves to be the best in terms of kLa, as expected.

4.1.4 Impact of aeration flow rate on kLa

Another important parameter to approach in the optimization and study of oxygen kLa is the aeration flow rate. This parameter could be called the main one as the more air you sparge in the more oxygen it will have, thus increasing the mass transfer rate. For testing how this parameter is correlated with kLa there were three different setups done in 3 different systems.

4.1.4.1 Stirred Tank System Results

Table 4.21: Results for impact on kLa of changing the aeration rate using Stirred Tank system

Aeration rate (VVM)	**kLa (h-1) Method 6**	**Uncertainty of kLa when compared to all methods' average (%)**
0.08	3.89	19
0.16	6.96	11
0.28	11.33	10

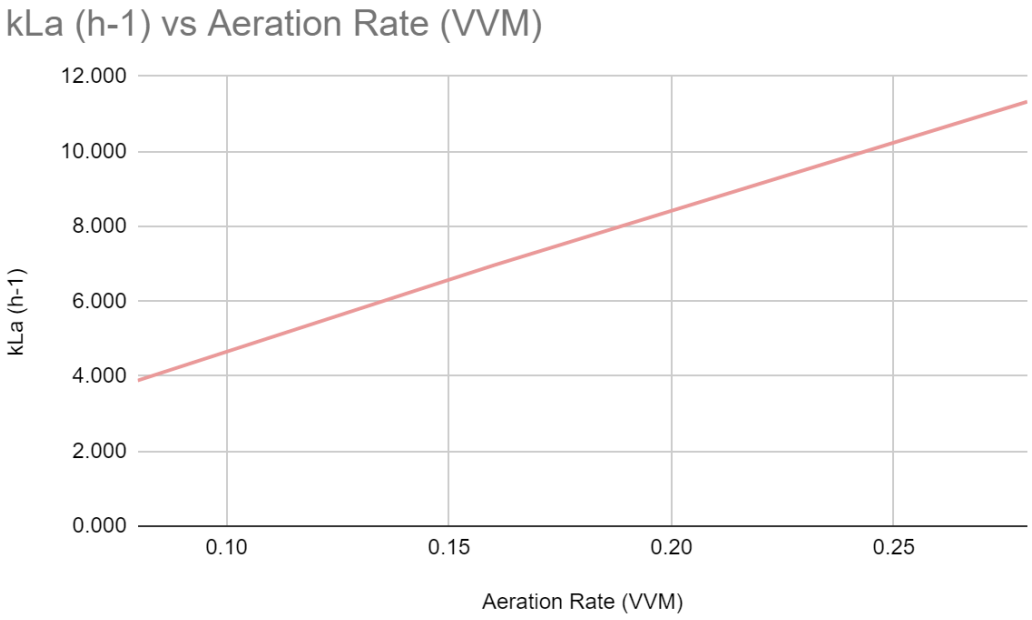

Figure 4.9: Changes in kLa with increase of aeration rate in Stirred Tank system

The graph 4.9 and values in table 4.21 show a seemingly perfect linear relationship in the Stirred Tank system, the aeration rates used were chosen in a way that the increase between the values is not the same step size. And the highest value corresponds to the limit of the used pump.

4.1.4.2 Vibromixer System Results

Table 4.22: Results for impact on kLa of changing the aeration rate using Vibromixer system

Aeration rate (VVM)	kLa (h-1) Method 6	Uncertainty of kLa when compared to all methods' average (%)
0.02	1.80	8
0.04	2.06	8
0.06	2.39	10
0.08	2.68	8

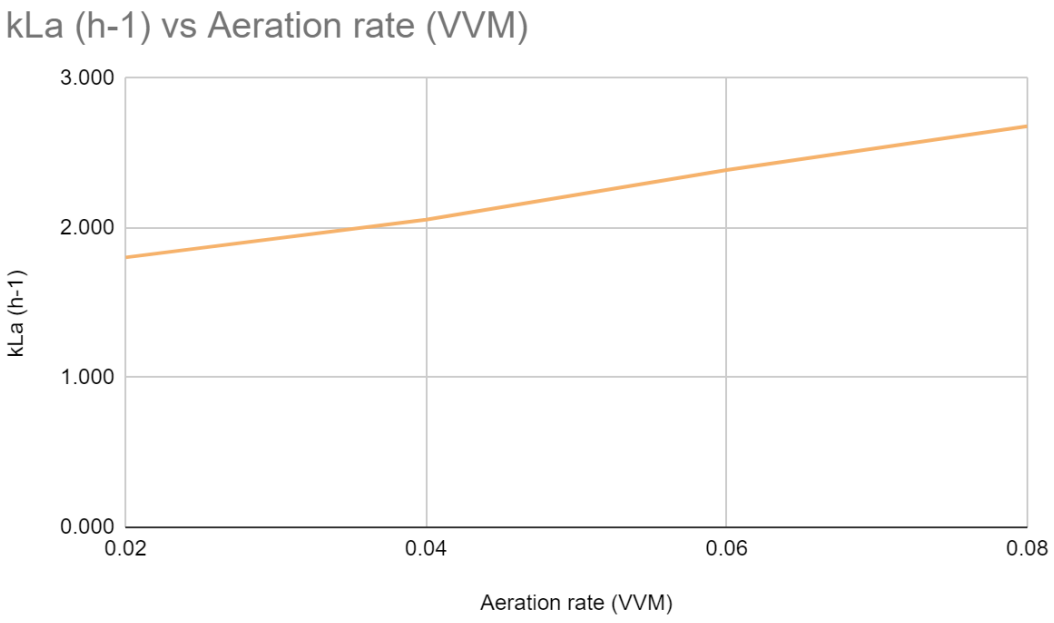

Figure 4.10: Changes in kLa with increase of aeration rate in Vibromixer system

In this system the number of data points was increased and the increase step was the same, having the last value equal to the limit of the used pump. Even with four different data points the linear growth corresponds to a 0.97 coefficient of determination (R^2).

4.1.4.3 Spinner Flask System Results

Table 4.23: Results for impact on kLa of changing the aeration rate using Spinner Flask system with stainless steel sintered spargers

Aeration rate (VVM)	kLa (h-1) Method 6	Uncertainty of kLa when compared to all methods' average (%)
0.08	5.31	8
0.16	8.18	7
0.32	12.46	5

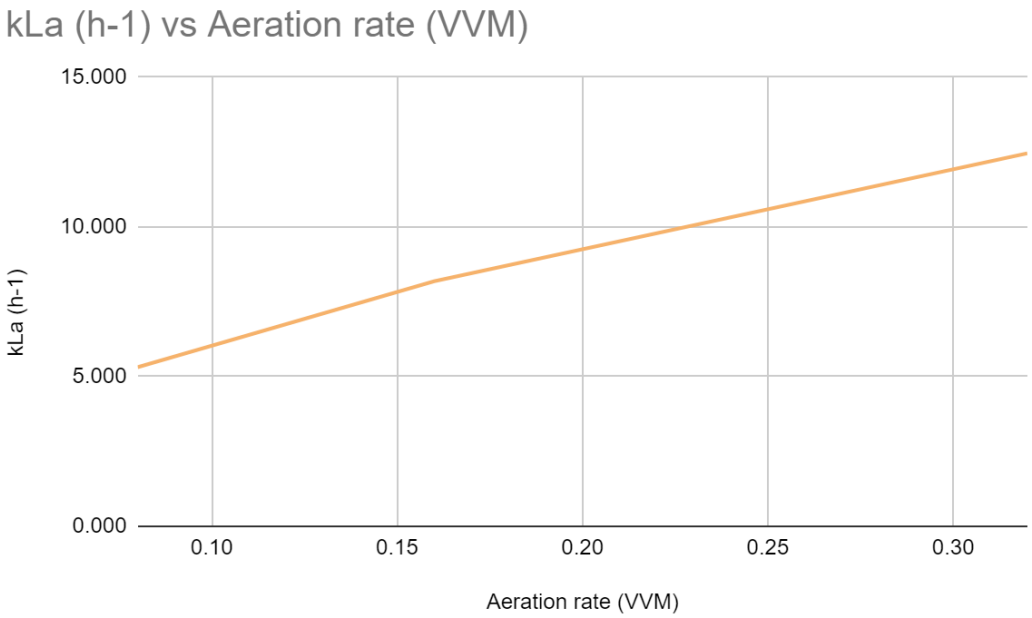

Figure 4.11: Change in kLa with increase of RPM on commercial Biostat 10L Bioreactor system

These setups showed a slight deviation from the linearity of the relationship observed above. This could be due to the nature of the system, as the relationship between N and kLa was also different from the other systems.

4.1.4.4 Changes in kLa with increase of aeration rate in Spinner Flask system with stainless steel sintered spargers

The discussion of the three different systems and the results obtained will be done together, since the increase of VVM shows to be linear in each one of them. In table 4.24 we can see a summary of the increase observed.

As can be seen above the increase in kLa with an increase of 0.01 VVM is similar across all systems, averaging at a 6.6% increase. According to the graphs shown for each system and the linear regression equations we can confirm that the increase of kLa is linearly

Table 4.24: Results for increase in kLa with increase in aeration rate for Stirred Tank, Vibromixer and Spinner Flask systems

Experiment	Aeration rate (VVM)	kLa (h-1)	kLa Increase for 0.01 VVM increase (%)	Total kLa Increase (%)
Stirred Tank system	0.08	3.89	-*	-*
	0.16	6.96	10	80
	0.28	11.33	5	63
Vibromixer system with Perforated Plate	0.02	1.80	-*	-*
	0.04	2.06	7	14
	0.06	2.39	8	17
	0.08	2.68	6	12
Spinner Flask system	0.08	5.31	-*	-*
	0.16	8.18	7	54
	0.32	12.46	3	52

*Values require two points to calculate, therefore there are no values just for the first point.

proportional to the increase of VVM, with the R-squared factor being higher than 0.99 in all systems studied. Comparing the results with equation 3.3 it is mentioned that kLa is proportional to superficial gas velocity to the power of 0.28. Therefore we can use an example from each system and compare it, as shown in table 4.25.

Table 4.25: Proportionality constant calculation between kLa and Vg for the studied systems

Experiment	Vg (m/s)	kLa (h-1)	Proportionality Constant
Stirred Tank system	1.8×10^{-5}	3.89	0.9
	6.1×10^{-5}	11.33	
Vibromixer system	4.4×10^{-6}	1.80	0.3
	1.8×10^{-5}	2.68	
Spinner Flask system	1.0×10^{-4}	5.31	0.6
	4.0×10^{-4}	12.46	

From the results it is noticeable that the proportionality constants are much more different than the one in literature. Nonetheless, said constants depend on the system's characteristics and mainly on the geometry, which is why we can see the big differences. One unexpected result is that the Vibromixer system which has the same geometry as Stirred Tank shows a different constant, and even more unexpected is really close to the one from literature, even though this system has a completely different mixing regime from normal stirring tank. Even with the proportionality constants being different the results clearly show that there is a linear correlation between VVM or superficial velocity and kLa.

4.1.5 Membrane Aeration and kLa

As mentioned in the General Introduction section, there are multiple ways to aerate a bioreactor.Sparging is the most commonly used method but it still has its disadvantages, for example the existence of bubbles has been linked to cell damage, as mentioned above. Therefore, what seems to be a promising solution being researched and developed is the use of membrane aerated bioreactors. In this study we also study the possibility of using a simple silicone tubing as a membrane and compare the effectiveness of this membrane aeration technique with calculations of kLa.

4.1.5.1 Spinner Flask System Results

The multiple setups done in this study were optimised until a clear increase in kLa was observed, which can be seen below in table 4.26.

Table 4.26: Results of kLa calculations from the best membrane aeration setup, using the Spinner Flask system

Experiment	kLa (h-1) Method 6	Uncertainty of kLa when compared to all methods' average (%)
Control (no pumping)	0.81	25
Final optimised setup	0.88	5

4.1.5.2 Discussion of Results for Spinner Flask System

In this experiment we had only one positive result from the final testing, with increased pressure, nonetheless the kLa obtained is much lower than that of sparging, as expected. The increase from the sparging through the membrane with increased pressure only showed an increase of about 0.069 in kLa, which corresponds to roughly 8% increase from no sparging. Of course that in this small scale, as mentioned before, the surface aeration has a big impact on the overall observed kLa, thus in larger scale this membrane aeration could probably prove to be better. To better understand the impact the oxygen transfer per area of tubing was calculated as the ratio between the kLa and the total submerged superficial area, rounding up the increase to 0.07 in kLa, when compared to the control without sparging. According to the specified conditions of the optimised setup; presented in Methods; we conclude that for the material and thickness used the oxygen mass transfer per area submerged equals 4.6×10^{-4} $h^{-1}.cm^{-2}$ or 4.6 $h^{-1}.m^{-2}$. It means that in order to achieve similar results to normal sparged reactors with sintered spargers in the same system for the same RPM, we would need to reach around a kLa value of 7 h^{-1}. The control value without the sparging is 0.81 h^{-1}. It means it would need an increase of

6.2 h^{-1}, for that the area needed would be 1.35 m^2. It corresponds to 7 metres of tubing, assuming the same dimensions and material, which would be impossible to fit inside the system. This shows some of the limitations and challenges posed by the membrane aeration system when compared to the commonly available sparged bioreactors. It is important to remember that the system was not optimal, and that with higher pressure, lower thickness and better material higher values can be reached, nonetheless from the results shown the use of membrane aeration has no clear way to compete with bubble aeration.

4.1.6 Impact of Baffles on kLa

As seen above, intense mixing caused by high stirring velocity leads to the production of the effect of vortexing.As it was explained above, it has a negative impact on the culture. Therefore most bioreactors come equipped with baffles.

4.1.6.1 Spinner Flask System Results

Table 4.27: Results for impact of having baffles on kLa in Spinner Flask bioreactor system

Experiment	kLa (h-1) Method 6	Uncertainty of kLa when compared to all methods' average (%)
Without Baffles	1.40	54
With Baffles	1.80	79

4.1.6.2 Discussion of Results for Spinner Flask System

The main reason for why this study was only done with absence of baffles or two baffles was due to previous results with the exact same system that showed no appreciable increase when going from 2 to 3 or 4 baffles, and even less for higher than that. In general there is an increase in kLa from the existence of baffles, which is a common known fact in literature, and the use of baffles in any large scale bioreactor is a must. The increase seen in this experiment is 29%, according to literature [209] normal vertical baffles can increase up to 38% the kLa based on estimations, when compared to unbaffled vessels. It is important to note that the shear strain also increases, meaning that the reduced vortexing also causes changes in the fluid speed and movement that can cause some stress to cells, but according to literature it is too low to affect CHO cells negatively, which can be compared to the mammalian cells used. The shape and number of baffles is also something being studied but since the effect from unbaffled to baffled is much more noticeable than improvements in baffles shape and number it still needs to be further studied. As well as possible equations or empirical equations correlating the kLa and power input for

different conditions of baffled vessels, since most of the empirical correlations only state normally that they were developed for baffled vessels and don't present some parameters that change with baffles characteristics, a part from complex CFD models [210–212].

4.1.7 Impact of Bubble size on kLa

The impact of bubble size on the aeration of the bioreactor is mentioned in the General Introduction section of this study, the impact of it and how important it is to make a good model for kLa calculation is still not conclusive. Nonetheless in this study, five different sintered spargers with different pore size distribution were used both for analysing the change in kLa values with pressure, which is known to be correlated with the number and size of bubbles [213] produced, and for bubble size and number estimation using image analysis.

4.1.7.1 Spinner Flask System Results

Table 4.28: Results for different pore size and different aeration flow rate in kLa on Spinner Flask system with sintered spargers

Pore Size (μm)	**Aeration rate (VVM)**	**kLa (h-1) Method 6**	**Uncertainty of kLa when compared to all methods' average (%)**
20-30	0.08	5.31	8
	0.16	8.18	7
	0.32	12.46	5
10-15	0.08	7.55	6
	0.16	10.90	8
	0.32	12.99	4
3-5	0.08	7.27	11
	0.16	8.30	10
	0.32	13.69	8
2	0.08	4.95	10
	0.16	8.77	6
	0.28	11.42	4
0.5	0.08	5.69	5
	0.16	9.30	9
	0.28	12.34	6

As could be seen the values used were almost the same in all setups, except for the last two sizes, due to pump constraints. As can be clearly seen in the graph, all values are close to each other even though there is a great difference in pore size.

As for the bubble number and size distribution for different aeration rates, the experimental setup used a ruler next to the sparger and the capture of video footage, allowing for frames like figure 4.13. The results of size and number distribution can be found below, in table 4.29.

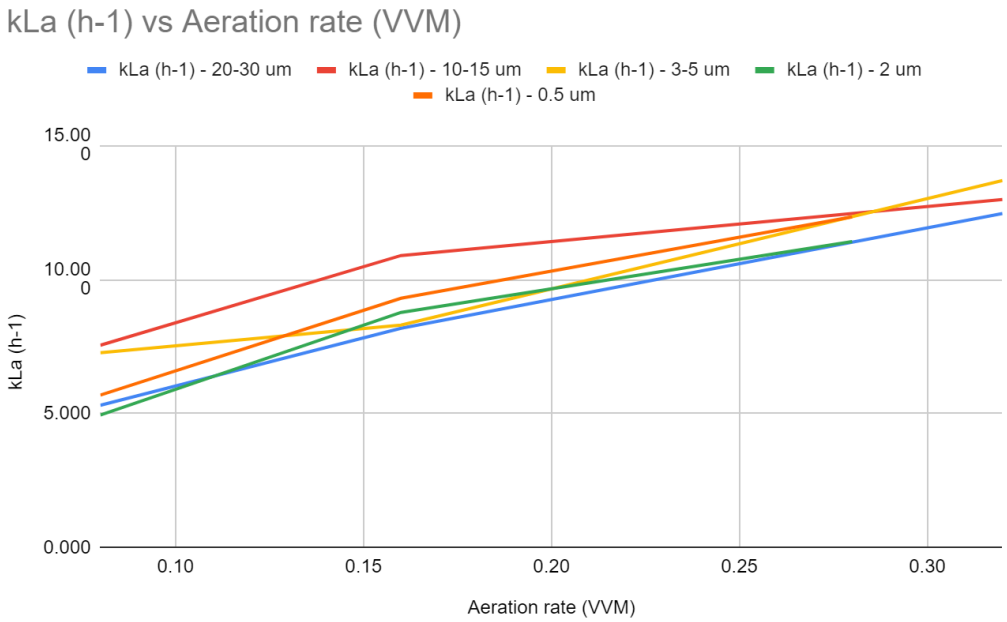

Figure 4.12: Changes in kLa with increase of aeration rate and different pores sizes sintered spargers in Spinner Flask bioreactor system

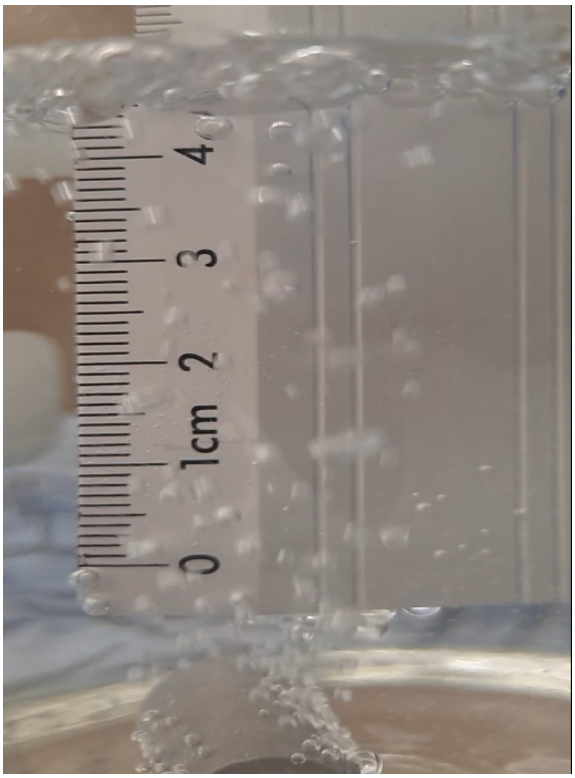

Figure 4.13: Frame from video capture used to analyse bubble size distribution

Table 4.29: Bubble number and size distribution in Spinner Flask system with different aeration rate and pore size spargers

Pore size (μm)	aeration rate (VVM)	number of bubbles	Average Size (mm)	Size deviation (%)
20-30	0.08	41	3.1	-52 to +19
	0.16	45	2.9	-62 to +10
	0.28	58	2.4	-50 to +13
10-15	0.08	24	2.4	-29 to +38
	0.16	36	2.3	-43 to +48
	0.28	54	2.1	-52 to +52
3-5	0.08	21	2.3	-52 to +35
	0.16	26	1.9	-37 to +37
	0.28	46	1.7	-47 to +41
2	0.08	22	2	-55 to +30
	0.16	21	1.9	-42 to +26
	0.28	32	2.1	-43 to +24
0.5	0.08	26	1.9	-42 to +63
	0.16	34	1.8	-33 to +28
	0.28	56	1.2	-42 to +33

From the results we can see the size deviation, which represents in percentage how much the lowest and highest bubble diameter observed varies from the average size. In most results it can be seen clearly that the size deviation towards smaller bubble diameter is much bigger than for the larger bubble, which corresponds to the fact that larger bubbles exist in bigger quantities than the smallest ones (for most cases studied).

4.1.7.2 Discussion of Results for Spinner Flask System

The impact of bubble size on kLa and how the different pore sizes produced different sized bubbles based on flow rate has been summarised in table 4.30. From the graphs above we see the aforementioned clearly linear relationship between kLa and sparging flow rate (with R^2 always above 0.9).Nonetheless there are a few odd cases, and the exact distribution of sizes and number of bubbles obtained shows a high degree of uncertainty due to the method used.

It is seen that with the increase of flow rate the size of bubbles tends to decrease and the number increase, the rate of which is completely different from each pore size. We can see that the increase of aeration rate results in a smaller impact on kLa the higher the value of VVM used. Meaning that even though from 0.08 to 0.16 VVM there was an increase of 0.08 and in the last pair of values from 0.16 to 0.32 there was an increase of 0.16, the increase of kLa was larger in the first one. According to literature [65, 214, 215] and the already mentioned facts in the General Introduction section. The smaller the bubble the higher the oxygen mass transfer rate is observed, nonetheless the smaller the bubbles the higher the damage to cells, due to high pressure and the behaviour of “solid-like”

Table 4.30: Change in bubble size, number of bubbles and kLa with VVM for different pore sizes

Pore size (μm)	Aeration Rate (VVM) for size analysis	Change in Average Size by 0.01 VVM (%)	Change in Number of bubbles by aeration rate (%)	Aeration Rate (VVM) for kLa	Change in kLa by 0.01 VVM(%)
20-30	0.08	-	-	0.08	-
	0.16	-7	10	0.16	7
	0.28	-21	29	0.32	3
10-15	0.08	-	-	0.08	-
	0.16	-4	50	0.16	6
	0.28	-10	50	0.32	1
3-5	0.08	-	-	0.08	-
	0.16	-21	24	0.16	1
	0.28	-12	77	0.32	4
2	0.08	-	-	0.08	-
	0.16	-5	-5	0.16	10
	0.28	10	52	0.28	3
0.5	0.08	-	-	0.08	-
	0.16	-6	31	0.16	8
	0.28	-50	65	0.28	3

particles. In general we can see that with the decrease in pore size, the expected size of bubbles also decreases and the kLa increases. Nonetheless the last two (2 and 0.5 μm), smaller pore sizes show lower kLa than the previous size (3-5 μm), this could be due to the fact that with the decreasing of pore size the needed flow rate to achieve the necessary pressure to produce bubbles is higher [216]. An important note to this parameter is also that the system where it was more closely studied was small scale. With the increase of volume and scale bubbles have more residence time thus having higher chance of coalescing and forming bigger bubbles that offer less kLa and carry cells to the top layer of the media. With this in mind for larger scales it is important that the flow created pulls the bubbles towards the impeller and the impellers break the bubbles into smaller ones. This procedure makes it less relevant to have specific control over bubble size production in the sparger, and reaffirms that it is of higher importance the mixing and the superficial gas velocity or sparging rate, which are correlated with each other.

4.1.8 Impact of Additives on kLa

The composition of the media; as aforementioned in the General Introduction and Materials and Methods sections of this study; is of great importance when it comes to its physical properties. The addition of some compounds, as the ones shown below, can have a great impact on the rheology of the given mixture used.

4.1.8.1 Spinner Flask System Results

Table 4.31: Results of kLa calculations from different additives concentrations and different temperatures in the Spinner Flask system

Experiment	Aeration rate (VVM)	Temperature (°C)	kLa (h-1) Method 6	Uncertainty of kLa when compared to all methods' average (%)
Distilled water	0.05	25	1.82	3
	0.05	37	2.59	17
	0.1	37	3.15	16
CMC 0.04%	0.05	25	1.09	5
	0.05	37	1.51	18
	0.1	37	2.11	18
PEG 0.1 %	0.05	25	1.72	2
	0.05	37	2.55	14
	0.1	37	2.93	29

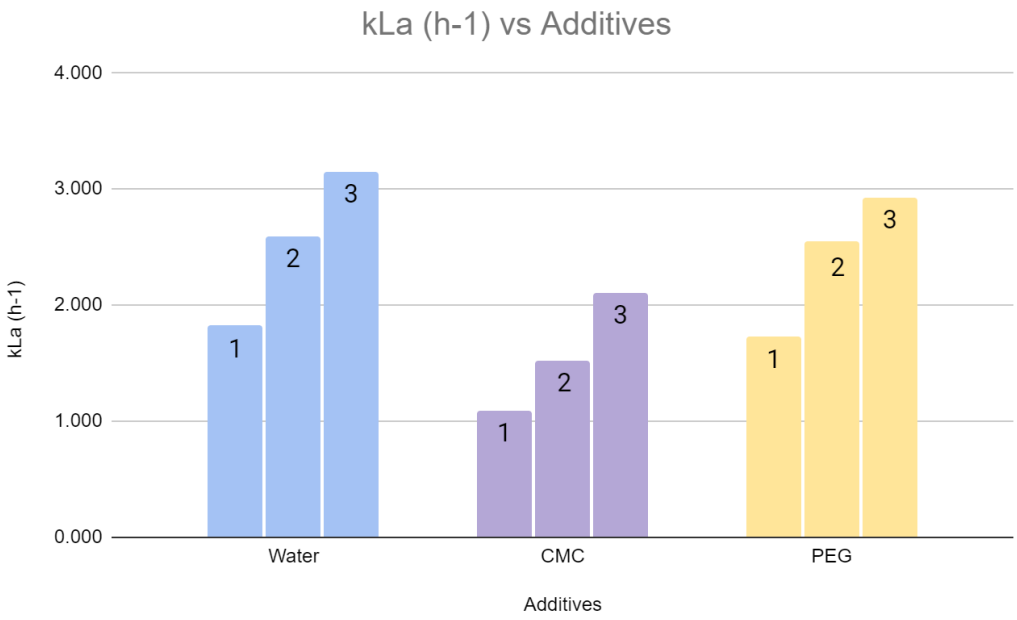

Figure 4.14: Change in kLa with temperature for different concentrations of additives in Spinner Flask system. It is presented 0.05 VVM at 25°C (1); 0.05 VVM at 37°C (2) and 0.1 VVM at 37°C (3)

A clear difference between the values of different temperatures and fluid composition can be seen in the above shown graph and table. The use of the increased temperature was done to simulate the temperature in cultivation and to test the physical changes that a higher temperature would have.

4.1.8.2 Discussion of Results for Spinner Flask System

In this experiment we have the addition of commercially available shear protectants, and we can see the effect they have on the properties of the media and mainly on the transfer of oxygen. Table 4.32 summarises the main results and the impact of the different additives on the kLa.

Table 4.32: Impact of Temperature and Additives on the kLa in Spinner Flask system

Experiment	Aeration rate (VVM)	Temperature (°C)	kLa (h-1)	Change in kLa by Temperature (%)	Change in kLa with addition of additives (%)
Distilled water	0.05 0.05 0.1	25 37 37	1.82 2.59 3.15	42	-*
CMC 0.04%	0.05 0.05 0.1	25 37 37	1.09 1.51 2.11	39	-40 -42 -33
PEG 0.1 %	0.05 0.05 0.1	25 37 37	1.72 2.55 2.93	48	-5 -2 -7

*Values are compared with Distilled water results, therefore there are no comparisons with the values of reference.

As we can see, the increase in temperature from 25°C to 37°C, on average translates into an increase of 40% in kLa and this can be misleading. When the temperature increases [217, 218] the diffusivity increases, with the decrease in surface tension and viscosity, this way the kLa is higher. But if we compare the OTR (oxygen transfer rate) in mass/time it is actually much lower. This is explained by the decrease in solubility, and as we know both OTR and kLa depend on the driving force being the difference between concentration in liquid and saturation concentration. Since the saturation is lower the overall amount of oxygen getting into the liquid is lower as well. We can see that at 25°C the solubility of oxygen in water is approximately 8.25 mg/L and at 37°C only 6.72 mg/L [219].

When we look at the additives, we can see that even though PEG is at a higher concentration the decrease in kLa is actually lower than the decrease caused by CMC. Averaging a decrease of 5% when compared to distilled water for PEG and 40% for CMC. This difference is due to two main factors: the density and viscosity of the additives. As mentioned above, with the increase of temperature the viscosity decreases thus helping increase the diffusion rate and overall kLa [220]. When looking at the viscosity of both additives when present in a water solution [221, 222] we find that for ambient temperature (20-25°C) at 4% concentration CMC exhibits a range of viscosity from 50-200 cp (reminding that water viscosity is approximately 1 cp at ambient temperature) while PEG for a concentration of 50% shows 210-260 cp of viscosity. So even though the concentration

of PEG is more than 12 times that of CMC; in the given example; the viscosity observed is only up to 5 times higher, or possibly even less given the range shown. This means that CMC impacts the solution's viscosity much more than PEG, which can explain the decrease in kLa.

4.2 Optimization of Bioreactors for Cell Viability

In this subchapter different parameters will be approached that have an impact on cell culture in bioreactors. When it comes to producing biomass or products that stem from cells in bioreactors there are two important parameters that should be considered: cell viability and cell doubling time [223, 224].

4.2.1 Impact of different parameters on Cell Viability

There are a large number of parameters that affect cell viability directly or indirectly. One of the most noticeable and complicated to predict is the effect of shear stress caused either by agitation or aeration bubble bursting. Nonetheless there are several models and equations in multiple studies that correlate these parameters with shear stress on cells [225–227]. In this subchapter cell cultivation experiments were done to understand the limits of our cell lines as well as the efficiency of PEG as shear protectant at a given concentration for different mixing conditions. The second set of experiments correlated to the damage that bubble bursting causes on cells, namely the impact of foaming and how it can be prevented on a large scale.

4.2.1.1 Shear Stress Evaluation

To evaluate the shear stress effect on cells we used different setups using the Stirred Tank bioreactor system as shown in Methods section.For these experiments we used both of the cell lines mentioned before: Cell Line A and B.

Cell Line A Cultivation Results

Table 4.33: Results of cell viability and density over cultivation time in 0.1% PEG medium and 900 RPM with Cell Line A in Stirred Tank bioreactor system

Time (hours)	Time (days)	Dead cells (%)	Live cells (%)	N (RPM)	viability (%)
0	0	11	15	250	89
17	1	5	29	250	95
23	1	10	25	900	90
41	2	12	34	900	88
49	2	4	40	900	96
65.5	3	6	63	900	94
72.5	3	3	68	900	97
101	4	2	100	900	98

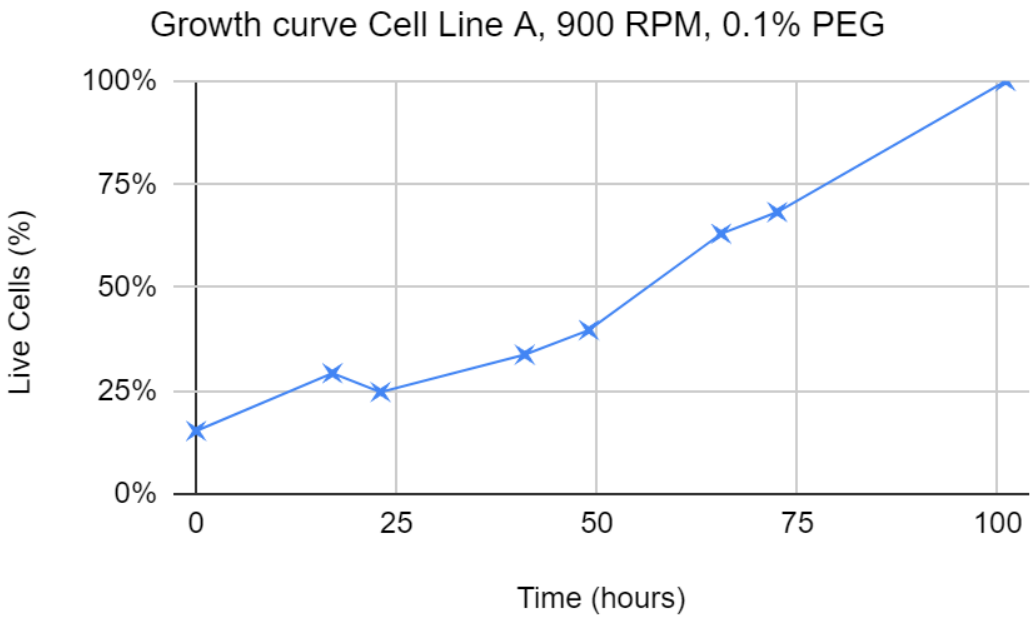

Figure 4.15: Viable cell growth over time of cultivation in 0.1% PEG medium and 900 RPM with Cell Line A in Stirred Tank bioreactor system

In figure 4.15 above, we can see that the cells kept growing in an almost constant linear way, instead of the expected death of cells. The first day of cultivation at 250 RPM was done in order to adapt them to stirring conditions as well as to let them resuspend back into suspension after centrifuging for inoculation. The 900 RPM value was chosen due to being the highest value that can be safely used in the given setup.

In Table 4.34, there is a summary of results from experiments with 0% PEG. The 900 RPM was firstly used to test if the cells could survive it without shear protectant, as they have survived in the presence of it. There was no period of adaptation in 250 RPM due to it not showing any changes in the first experiment.

Table 4.34: Results of cell viability and density over cultivation time in medium without shear protectant and 900 RPM with Cell Line A in Stirred Tank bioreactor system

Time (hours)	Time (days)	Dead cells (%)	Live cells (%)	N (RPM)	viability (%)
0	0	7	100	900	93
19	1	100	0	900	0
46.5	1	100	0	900	0

Table 4.35: Results of cell viability and density over cultivation time in medium without shear protectant and 600 RPM with Cell Line A in Stirred Tank bioreactor system

Time (hours)	Time (days)	Dead cells (%)	Live cells (%)	N (RPM)	viability (%)
0	0	13	100	600	87
20.5	1	100	0	600	0

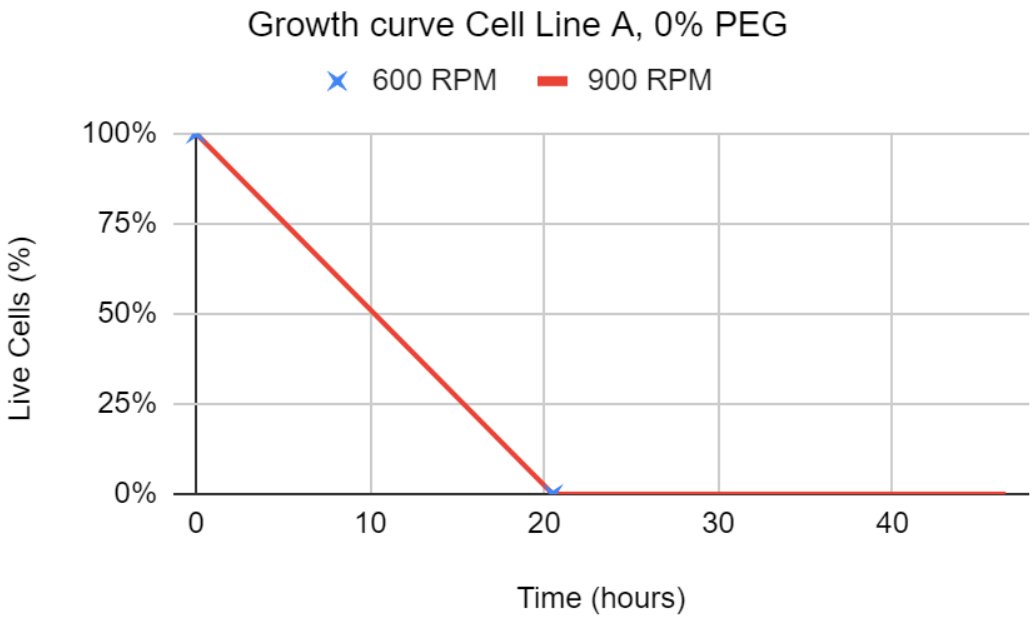

Figure 4.16: Viable cell growth over time of cultivation in medium without shear protectant, at 900 and 600 RPM with Cell Line A in Stirred Tank bioreactor system

Similar behaviour of the cell suspension can be observed in the experiment with lower RPM without shear protectant. Results are summarised in Table 4.35 and visualised Fig 4.16.

Discussion for Cell Line A Cultivation Results

Based on the results found we were able to confirm that with just 0.1% PEG concentration, the cells were able to survive and grow at 900 RPM. The doubling time observed (via cytometry) was similar to the literature and observed in other cultivation, close to 24h. With this information we can conclude that even for such high RPM a small concentration

of PEG allows Cell Line A to survive.

Cell Line B Cultivation Results

Table 4.36: Results of cell viability and density over cultivation time in medium with 0.01% PEG and slow increase to 650 RPM with Cell Line B cells in Stirred Tank bioreactor system

Time (hours)	Time (days)	Dead cells (%)	Live cells (%)	N (RPM)	viability (%)
0.00	0	10	28	250	90
16.00	1	9	29	250	91
23.25	1	6	35	600	94
23.50	1	7	37	600	93
42.00	2	7	65	600	94
47.00	2	7	74	600	93
64.00	3	10	71	650	90
72.00	3	10	80	650	90
92.00	4	12	100	650	88
136.00	6	55	32	650	45

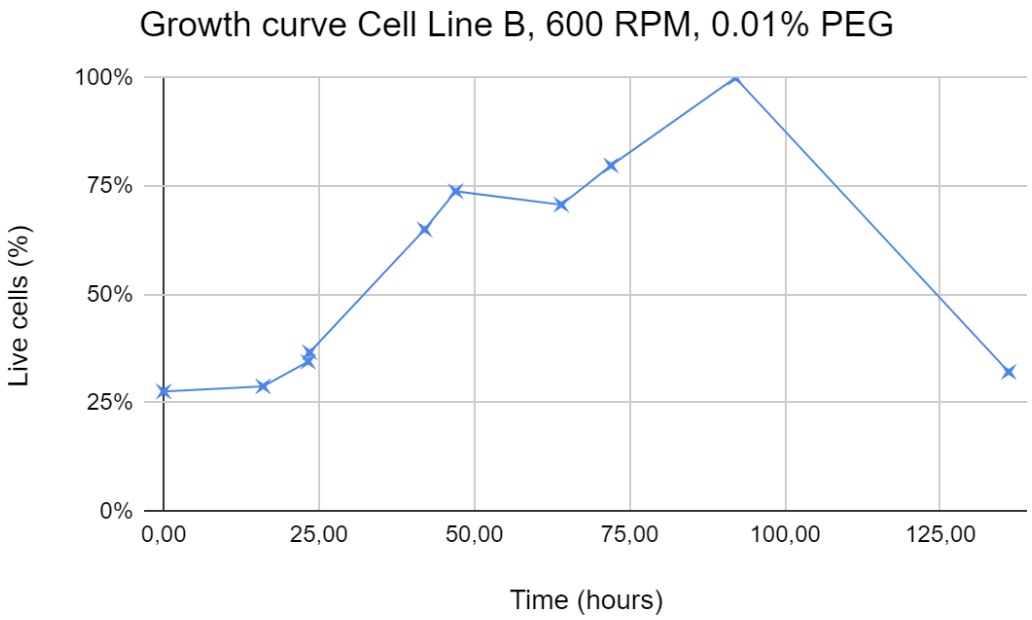

Figure 4.17: Viable cell growth over time of cultivation in medium with 0.01% PEG and slow increase to 650 RPM with Cell Line B in Stirred Tank bioreactor system

Similarly to how it was done with A cell line, the experiments with Cell line B were carried out. For the comparison of all results, as expected, cells died almost instantaneously after being in the presence of 900 and 600 RPM without PEG. The amount of PEG present in the media was decreased to 0.01%, the first increasing step was done to 600 RPM instead of 900 RPM. Both changes were in order to test optimised conditions that would minimise the costs of production.

There was no shear protectant present in the media, the goal was to start at 150 RPM, which should be minimal shear stress for cells and let them adapt to this mixing, and increase 100 RPM each day, unfortunately both experiments turned out dying in the first day, the results can be seen in table 4.37.

Table 4.37: Results of cell viability and density over cultivation time in medium without shear protectant and slow increase from 150 RPM with Cell Line B in Stirred Tank bioreactor system

Experiment	Time (hours)	Time (days)	Dead cells (%)	Live cells (%)	N (RPM)	viability (%)
First Run	0 22	0 1	7 100	100 0	150	93 0
Second Run	0 18.5	0 1	6% 98%	100% 1%	150	94 2

Discussion for Cell Line B Cultivation Results

For Cell Line B the characteristics of shear stress resistance should be the same, nonetheless we can see that using PEG at 0.01%, which is 10 times less than the previously used concentration allowed cells to survive up to 650 RPM and grow with high viability and doubling time close to the expected 24 hours. Nonetheless when the experiment was done without any PEG, cells weren't even able to survive 150 RPM, which produces much lower shear stress, and should be within both mammalian cell lines (A and B) capability of survival. This also leads to posing the question that maybe cells have changed after multiple cultivations with the presence of PEG, leading to a need for adaptation without it.

Shear Stress Estimation

Using the equations 2.2, 2.3 and 2.4 for the conditions used, it can be estimated that the energy dissipated in the system at 900 RPM, should be close to 1.03x105 m^2/s^3, which corresponds to a Kolmogoroff eddy size close to 1.8 μm. This size is about 10 times smaller than the size of a cell, which according to literature causes destruction of cells. The shear stress in these conditions comes out to 574 N/m^2. This number is way too high when compared with mentioned limits of CHO cells [228] (which are well researched and comparable to the studied cells), namely between 0.59 and 1.19 N/m^2. Both cell lines should have similar shear stress resistance due to similarities between size and other characteristics. Using 600 RPM and even 150 RPM we can also estimate the shear stress and eddy size. For 600 RPM the shear stress comes to 174 N/m^2 and 21 N/m^2 for 150 RPM. Both of these values are much lower but still quite bigger than the aforementioned limits, which explains the obtained results. Nonetheless the shear stress dissipation and the eddies produced damage tends to be weaker the further away from the impeller cells are. Even though the exact mechanism that PEG has on cells is still a topic of discussion, and

depends highly on the molecular weight of it, some studies [229] purpose that PEG shields cells from bubble bursting damage, by changing the way cells attach to bubbles and the properties of the liquid (increasing viscosity for example) that allow for less damage from bubbles. This theory can help formulate a possible reason for cell survival in such harsh conditions, that being that as we saw in both equations, for eddy size and shear stress the increase in kinematic viscosity negatively affects both, meaning that PEG would allow them to survive.

4.2.1.2 Antifoaming and Defoaming

In these experiments, as explained in the General Introduction and Methods sections, the effect of foaming will be studied in bioreactor cultivation and the use of PEMF stimulation as an Antifoaming or Deafoaming technique was also studied.

PEMF Stimulation in Spinner Flask System Results

In the optimised experimental setup, everything was kept the same except the increase in airflow mentioned above and an increase in density and viscosity of the media by addition of PEG, with the final concentration of 1.25%.

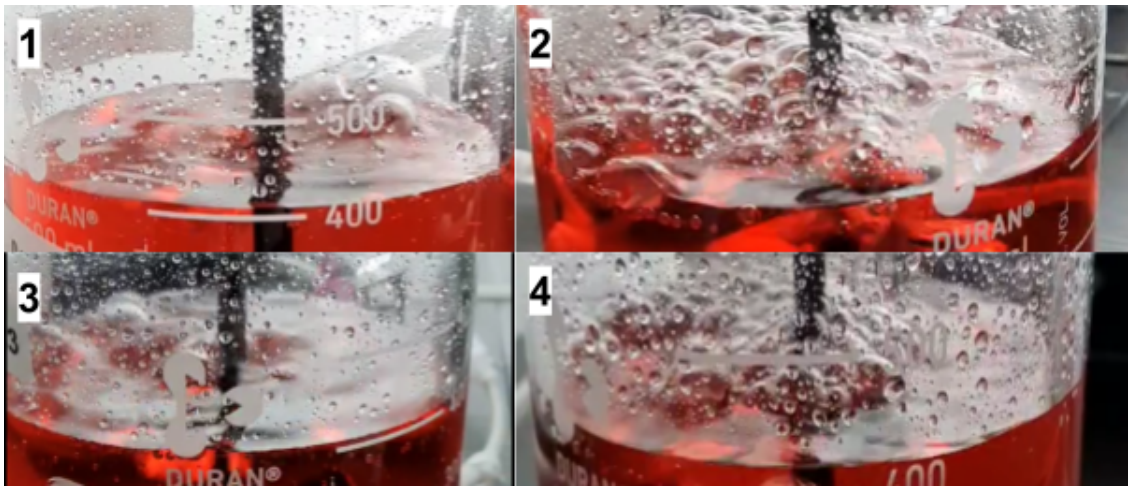

Figure 4.18: Results of one of the setups of PEMF treatment as antifoaming and defoaming technique. (1) The result of the PEMF treated bioreactor surface free of bubbles after 2 hours, (2) the surface of the non PEMF treated bioreactor surface with bubbles/foam after 2 hours. (3) The result of 2 hours after the second treatment and (4) the result after another 2 hours in the non-treated one

The results in one of the setups showed that the PEMF treated bioreactor had less bubbling/foam formation in the surface. In another setup both bioreactors exhibited a lack of visible bubbles/foam in the surface and there was no clear distinction between both of them as can be seen in figure 4.19 below.

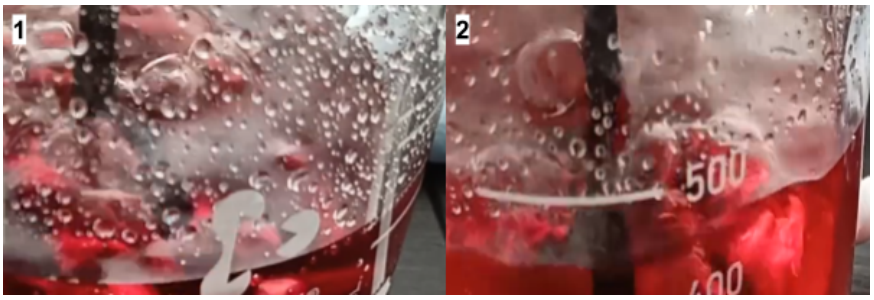

Figure 4.19: Results of experiment with PEMF treatment, (1) the PEMF treated vessel surface and (2) the non-treated vessel surface

The next step was to simulate a larger amount of foaming to better visualise the efficiency of PEMF treatment. Therefore in the experiment shown below, the changes were only two: decrease in RPM and addition of 0.2 mL of liquid soap to improve foaming. These changes were done to ensure the creation of enough foaming to be able to see differences between both bioreactors. The results can be seen in figure 4.20.

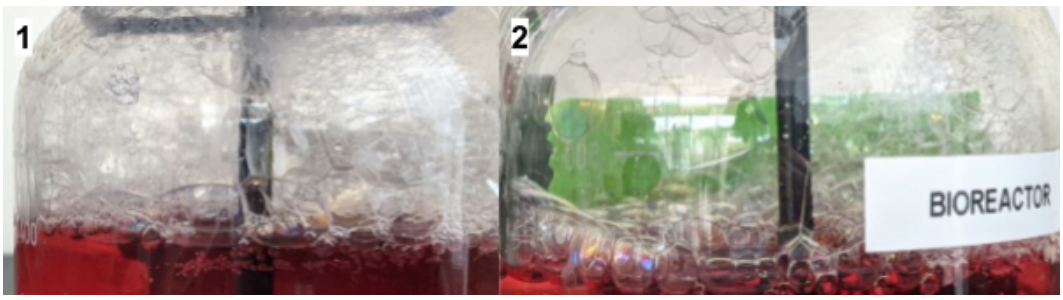

Figure 4.20: Results of experiment with PEMF treatment with induced foaming, (1) PEMF treated surface and (2) non-treated surface

As can be seen above, there was creation of a large layer of large frail bubbles, after the first two hours there was no visual difference between both bioreactors. After two hours the second treatment the PEMF treated one had more foam layer than the non-treated one. Since we had observed visual denser foam being made in our cell cultivations we decided for the last experiment to be done with cells from Cell Line B.

The procedure was the same as the fourth experiment except there was no liquid soap addition and there was a seeding density of more than 300 cells/μL. Furthermore, to cultivate the cells this experiment was done inside an incubator, where the temperature was kept at 37 °C. The results can be seen in figure 4.21 below.

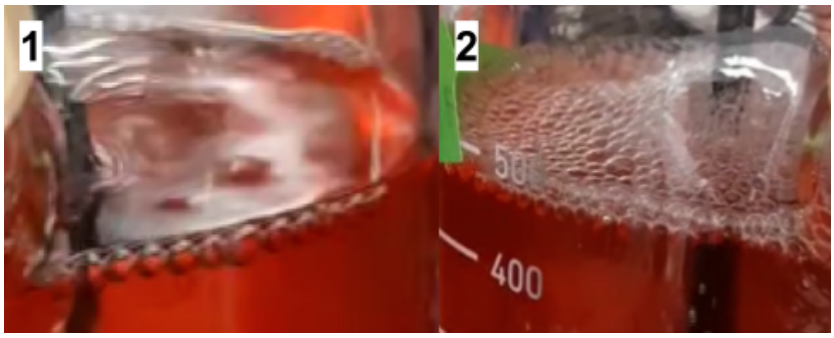

Figure 4.21: Results from PEMF stimulation experiment with cells, (1) PEMF stimulated surface and (2) non-stimulated surface

Discussion of PEMF Stimulation Effect

Unfortunately, this experiment proved to be quite difficult when it comes to interpretation of results. In some cases the PEMF treated vessel produced visible less foaming, but in others the contrary was observed. In general further optimisation of medium composition and a wider range of PEMF treatment setups would provide better results. Nonetheless this topic is still not widely researched, and it might turn out to be an interesting way to stimulate property changes in the media reducing foaming if a more customisable system is used, with possibly higher intensities.

4.2.2 Experimental consumption of nutrients

For the cultivation of cells to be a competitive way to produce meat, and even in other biotechnology applications, it is important to ensure that the yield of product desired is as high as possible without being too expensive. Therefore, it is necessary to strive to always optimise the production process and the cultivation regime. In this subchapter of this study we will study the way to produce higher cell density, using fed-batch cultivation experiments, where the feeding process, solution and the bioreactor conditions will be evaluated using cell density, viability and doubling time as the main parameters to judge success.

4.2.2.1 Fed-Batch Experiment

The production and consumption of amino acids will be the main focus of this experiment, in this particular study. Below in table 4.38 the results of cell density and growth can be seen, and in table 4.39 the results for amino acids, glucose and lactate concentration over time.

Fed-Batch Cultivation in Stirred Tank System Results

Table 4.38: Growth of cells and viability results in Fed-Batch experiment in Stirred Tank bioreactor system

Experiment	Time (hours)	Time (days)	Dead cells (%)	Live cells (%)	N (RPM)	viability (%)
Pre Feeding	0	0	9	31	250	91
	23.7	1	22	46	250	78
	47.4	2	15	57	250	85
	71	3	6	100	250	94
Post Feeding	95	4	15	86	250	85
	119	5	31	72	250	69
	143	6	100	0	250	0.2

Table 4.39: Concentration of amino acids, glucose and lactate over time in Fed-Batch experiment in Stirred Tank bioreactor system

Time (days)	0	1	2	3 - Pre feeding	3 - Post feeding	4	5	6
Time (hours)	0	23.7	41.4	71	71	95	119	143
Asp (%)	100	97	107	49	97	88	80	91
Glu (%)	100	118	295	122	176	149	151	155
Asn (%)	100	72	34	7	60	22	12	13
Ser (%)	100	71	55	39	82	58	50	55
Gln (%)	100	32	32	12	87	10	11	18
His (%)	100	97	109	69	69	77	71	66
Gly (%)	100	187	258	171	166	243	254	275
Thr (%)	100	102	113	69	73	78	77	77
Arg (%)	100	101	112	66	71	76	72	72
Ala (%)	100	129	138	60	64	131	135	136
Tyr (%)	100	103	113	61	65	67	66	66
Trp (%)	100	103	110	53	56	52	47	48
Phe (%)	100	102	108	61	65	68	66	65
Ile (%)	100	95	91	41	43	40	37	41
Leu (%)	100	90	83	34	35	30	26	27
Lys (%)	100	101	108	60	66	69	67	73
Pro (%)	100	144	135	56	95	106	186	294
Glucose (%)	100	82	56	31	79	71	66	57
Lactate (%)	100	227	404	555	509	558	589	610
Osmolality (%)	100	99	99	116	89	90	92	91

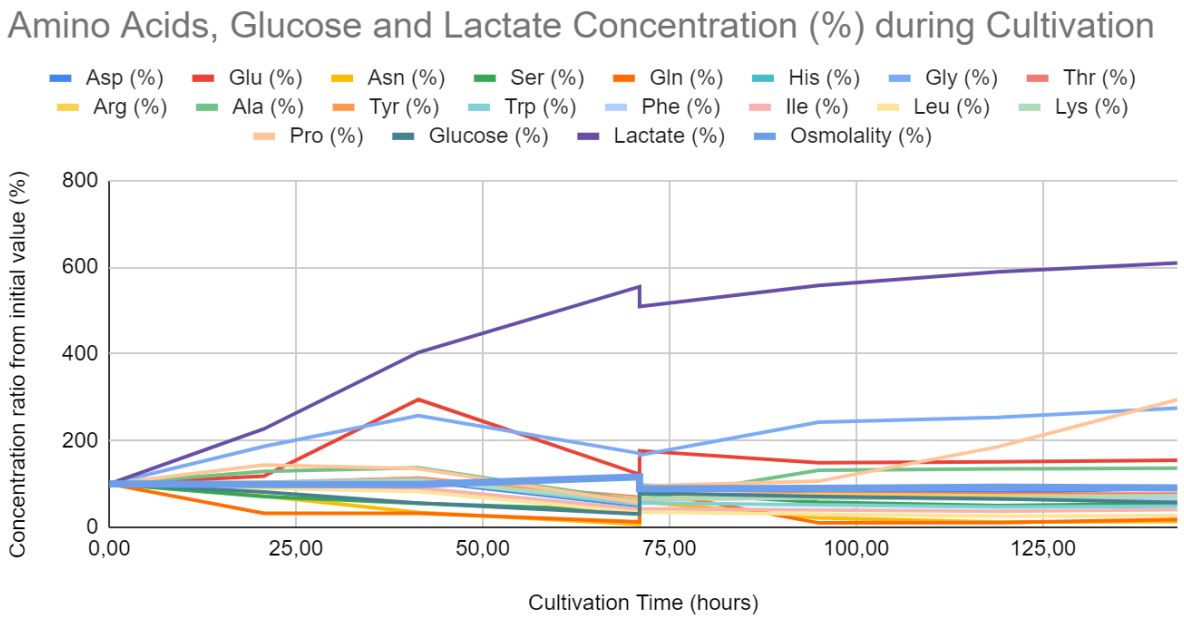

Figure 4.22: Amino Acid, Glucose and Lactate concentration, as percentage of initial concentration, during fed-batch cultivation of Cell Line B

Discussion of Results for Fed-Batch Cultivation in Stirred Tank System

In this experiment we were able to observe how there was a slow growth in the beginning, due to the adaptation of cells, but from 57% to 100%; of the largest number of cells achieved; the doubling time was faster, and closer to 24h and also there was a big increase in viability. Nonetheless the feeding regime was not optimised, after feeding there was a great decrease in cell viability, even though there was more concentration of the necessary nutrients. One possible reason might be that lactate was too high, but for other cultivations that didn't prove to be the point. Another curious result is the increase in osmolality, before feeding the osmolality was much higher, had increased up to 16% more than the starting value, which is 17% more than the previous measurement, this also coincides with the highest density and viability measured in the experiment. According to previous studies, experiments and literature [230], the optimal osmolality for Cell Line B should be in the range of 290-340. So the high osmolality might have been the reason for the decrease in cells, but there is still no clear reason for this sudden increase. One possible reason could be the lactate, but the increase and production of it has been constant as could be seen, and the osmolality remained stable. When it comes to amino acid consumption, according to the previous studies [231–233], the most consumed amino acids are supposed to be serine, asparagine, proline and cysteine. When looking at these amino acids we see that just before feeding there was a big decrease in concentration of asparagine and proline and that overall these were among the most consumed as expected. Nonetheless, this study proves to show the complexity and amount of parameters that need to be taken into

account. There might have been physical changes due to failure in control systems that were not noticed or even the lack of other compounds not measured, such as vitamins.

4.2.3 Predictive python metabolic model estimations of nutrient consumption and growth

In this study a python metabolic model was used and optimised in order to predict the behaviour of CHO cells. The most important parts of the used code are present below as results and also the simulations that resulted from them.

```
import cobra
import pandas as pd
import numpy as np
from scipy.integrate import solve_ivp
import csv
import matplotlib.pyplot as plt

# Load the metabolic matrix CSV file
metabolic_matrix = pd.read_csv('metabolic_matrix.csv', index_col=0)

# Create an empty COBRApy model object
model = cobra.Model()

# Add metabolites to the model
for metab in metabolic_matrix.index:
    model.metabolites.add(cobra.Metabolite(metab))

# Add reactions to the model
for rxn in metabolic_matrix.columns:
    reaction = cobra.Reaction(rxn)
    reaction.add_metabolites({model.metabolites.get_by_id(metabolic_matrix.index[i]):
                              metabolic_matrix.iloc[i, j]
                              for i in range(len(metabolic_matrix.index))
                              for j in range(len(metabolic_matrix.columns)) if metabolic_matrix.columns[j] == rxn})
    model.add_reactions([reaction])
```

Figure 4.23: First part of the python code used, the required imports and loading and reading the metabolic matrix

The first objective was to use data from experiments with Cell Line B cultivation to compare the simulated data by the model and change it until the simulated data is closely similar to the experimental data. In order to do so it is necessary to better understand what each part of the above shown python code does. It is necessary so that the following different optimization steps, simulations and python code written can be well understood.

The metabolic network defined by Robitaille et al, present in figure 3.8, presents 45 chemical species, 21 intracellular and 24 extracellular and a total 34 reactions, of which 20 are intracellular and 14 are extracellular. In the first part of the python code present in figure 4.23, six different functions and libraries are imported and pandas is used to read the metabolic matrix present in csv format. Cobra.model is used for creating the matrix model using the metabolites and reactions present in the metabolic matrix csv file that was read. And the model made with Cobra.model function is converted into a stoichiometric matrix to be used by the following functions.

```
def kinetics(t,state,Const):

  [ACCOA, ADP, AKG, AMP, ATP, CIT, F6P, G6P, GAP, GLU, MAL, NAD, NADH, NADP, NADPH, OX

  [aAMP, aF6P, bAMP, bF6P, KAAMP, KAF6P, KdCIT, KdEGLN, KdG6P, KdLAC, KdPEP, KdPYR, Kd

 #rates

  if NADH<1e-10:
    NADRatio=0
  else:
    NADRatio = NAD/NADH

  if NADPH<1e-10:
    NADPRatio=0
  else:
    NADPRatio = NADP/NADPH

 VGROWTH = Vmaxgrowth * (G6P / (KmG6Pg + G6P)) * (R5P / (KmR5Pg + R5P)) * (LYS / (

 rates = np.array([[VPDH], [VCS], [VPFK], [VPGK], [VPK], [VSDH], [VPC], [VATPASE],

 return rates
```

Figure 4.24: Second part of the python code used, the function kinetics, used for computing the flux rates equations (only a part of the function's code is present in the figure)

In the second part of the code, which a small part is present in figure 4.24, the kinetics function is defined. This function receives a "t" parameter which is a real integer representing the time of cultivation, state parameter which is the concentrations of the different intracellular and extracellular chemical species present in the matrix. "Const" parameter represents the value of each Michaelis-Menten constant for the kinetic equations that will define the fluxes of the 34 reactions present in the model and in the stoichiometric matrix.

In the third part of the code the function ode is defined, which can be seen above in figure 4.25. It receives the same three parameters that the kinetics function receives and calculates the flux rates using matrix multiplication of the stoichiometric matrix by the kinetic equations matrix. obtained from the kinetics function. The resulting matrix comprise the fluxes at the given time point t, represented by a system of ODEs.

```
def ode(t,state,Const):
  for i in range(len(state)):
    if state[i]<0:
      state[i]=2.48*10**-10
    else:
      continue
  [ACCOA, ADP, AKG, AMP, ATP, CIT, F6P, G6P, GAP, GLU, MAL, NAD, NADH, NADP, NADPH, OXA, PEP, PYR, R5P, SUC, X5
  rates = kinetics(t,state,Const); #A vector containing the all rates

  #feed
  i=int(t)

  MU = rates[-1]*1; #1/h

  #death rate
  kdMin=2.6e-6; #h-1
  kdMax=2e-2; #h-1
  beta = 1e-3; #h-1

  KdX=kdMin + kdMax*(beta/(beta+rates[-1]))**2;

  #ODEs
  ODEs = matrixS@rates; #stoichiometry ODEs
  ODEs = np.squeeze(ODEs);
  ODEs[-1] = ODEs[-1]-KdX;#ODEs with death rate on biomass
  for i in range(21,45):
    ODEs[i] = ODEs[i]*X; #Extracellular components need to be multiplied to X to obtained the correct units

  for i in range(0,45):
    if state[i] == 0 and ODEs[i] <=0:
      ODEs[i]=0

  return ODEs
```

Figure 4.25: Third part of the used python code, defining the ode function that used the kinetic equations from the previous function to compute the ODEs system

The fourth and last part of the code is where the imported function solve-ivp is used as a linear programming integration solver for the ODEs system. In this last part, which can be seen in image 4.26, the initial concentrations of each compound are set as well as the different constants used in the kinetics function, and also the time interval used for the simulation.

In this adaptation of the existing model in order to obtain an optimization of the culture media there were two main sets of experimental data. Both the first and second sets of data were obtained during a characterization experiment using Cell Line A and Cell Line B, respectively. The second set of data was more reliable, coming from an experiment with replicates and better results from the analysis of chemical concentrations. For the first set of available data the first step was to compare the normal result of the model adapted from Robitaille using python and compare it to the said experimental data. In order to do that x0, which is a set of numbers that represent the initial concentrations of the 45 compounds in the model, was changed accordingly to the concentrations found in the media used for the experiment from which the data came from.

```
# Define the initial state of the system
#    ACCOA      ADP      AKG      AMP      ATP      CIT      F6P      G6P      GAP      GLU
x0=[ 1.4e-7,  6.7e-5,  1e-7,  3.1e-7,    7e-6,   1e-6,  2.2e-7,   1.6e-7, 4e-7,  2.2e-4,

#        aAMP, aF6P, bAMP, bF6P, KAAMP, KAF6P, KdCIT, KdEGLN,    KdG6P,   KdLAC, KdPEP, Kd
VariC = [0.47, 4.1, 10.46, 1.7, 0.09, 4.9e-06, 0.00074, 3.5, 1.710841e-08, 5.412, 3.7e-07,

# Define the time vector for integration
time_span = (0, 241)
t_points = np.linspace(0, 240, 241)

abs_tol = 1e-6
rel_tol = 1e-5

# Solve the system of ODEs using the dFBA approach
sol = solve_ivp(ode, time_span, x0, method='RK45',t_eval =t_points,atol = abs_tol, rtol =

t = sol.t

ACCOA = sol.y[0]
ADP = sol.y[1]
AKG = sol.y[2]
AMP = sol.y[3]
#Save file
# open the file in the write mode
f = open('Results', 'w')

# create the csv writer
writer = csv.writer(f)
writer.writerow(["t(h)","ACCOA(mM)","ADP(mM)","AKG(mM)","AMP(mM)","ATP(mM)","CIT(mM)","F6P(
# write a row to the csv file
for i in range(0,241):
  writer.writerow([t[i],ACCOA[i],ADP[i],AKG[i],AMP[i],ATP[i],CIT[i],F6P[i],G6P[i],GAP[i],GLU

# close the file
f.close()
```

Figure 4.26: Fourth and final part of the python code used for the model defined by Robitaille et al, the definition of initial conditions and solving the system and saving the simulated data points

Below we can see in table 4.40 and table 4.41 the results obtained of amino acid concentration and cell growth over time in both the experimental data and the first simulation. All simulations were done for 240 hours or 10 days, since all of the experimental data used never went above 10 days of cultivation.

Table 4.40: Experimental results from Cell Line A experiment for concentration of cells and amino acids over cultivation time

Cultivation Time	**Day 0**	**Day 1**	**Day 2**	**Day 3**	**Day 4**	**Day 5**	**Day 6**
Asp (mg/L)	7.1	7.0	0.0	0.0	0.0	0.0	0.0
Glu (mg/L)	8.7	11.0	0.0	0.0	0.0	0.0	0.0
Asn (mg/L)	7.5	6.5	5.4	4.1	3.0	0.0	0.0
Ser (mg/L)	26.7	23.6	21.7	17.0	12.6	8.0	6.8
Gln (mg/L)	313.9	264.0	223.8	161.6	96.7	16.9	1.3
His (mg/L)	23.1	20.9	20.4	19.5	18.4	17.2	16.4
Gly (mg/L)	19.7	19.0	22.9	25.1	29.0	33.7	34.6
Thr (mg/L)	49.6	46.2	46.6	45.5	44.7	42.8	41.7
Arg (mg/L)	148.8	136.0	139.7	136.6	135.8	133.2	129.0
Ala (mg/L)	4.8	8.3	16.4	28.6	48.6	74.7	82.5
Tyr (mg/L)	34.3	31.1	30.8	29.9	29.2	27.5	25.6
Met (mg/L)	15.9	14.2	13.7	13.0	11.9	10.0	8.6
Val (mg/L)	49.4	45.2	44.8	43.4	42.8	40.1	36.7
Cys (mg/L)	25.5	20.6	38.2	36.7	35.9	31.3	22.4
Trp (mg/L)	8.4	7.1	6.6	6.2	5.9	5.1	4.3
Phe (mg/L)	33.8	30.7	30.4	28.8	27.8	25.4	23.6
Ile (mg/L)	49.2	43.0	41.5	39.1	37.5	32.5	28.1
Leu (mg/L)	54.6	47.8	46.2	42.5	39.9	33.1	27.6
Lys (mg/L)	79.0	72.2	87.4	82.6	80.4	74.9	70.2
Pro (mg/L)	27.9	26.1	24.3	20.8	18.7	14.9	11.9
Live cells per μL	99	102	270	510	714	1107	720

Table 4.41: Amino acids concentration and cell density over cultivation time from first simulation using the metabolic python model

Cultivation Time	Day 0	Day 1	Day 2	Day 3	Day 4	Day 5	Day 6
Asp (mg/L)	7.8	5.5	3.7	2.1	0.8	0.3	0.1
Glu (mg/L)	8.7	8.8	8.9	9.0	9.2	9.5	9.7
Asn (mg/L)	7.5	7.4	7.3	7.3	7.2	7.1	7.0
Ser (mg/L)	26.7	26.3	25.9	25.3	24.7	24.0	23.3
Gln (mg/L)	313.9	311.7	308.9	305.6	301.6	297.2	292.9
His (mg/L)	23.1	23.2	22.9	22.8	22.6	22.4	22.3
Gly (mg/L)	19.7	19.6	19.6	19.5	19.5	19.4	19.4
Thr (mg/L)	49.6	49.6	49.5	49.5	49.4	49.4	49.4
Arg (mg/L)	148.8	148.6	148.3	147.8	147.4	146.9	146.5
Ala (mg/L)	4.8	8.2	12.4	16.6	22.2	28.3	33.6
Tyr (mg/L)	34.3	33.7	32.9	31.8	30.5	29.3	28.1
Met (mg/L)	15.9	16.0	15.9	15.9	15.9	15.9	15.9
Val (mg/L)	49.4	48.9	48.4	47.6	46.8	46.0	45.2
Cys (mg/L)	25.5	25.5	25.5	25.5	25.5	25.5	25.5
Trp (mg/L)	8.4	-	-	-	-	-	-
Phe (mg/L)	33.8	33.8	33.7	33.7	33.6	33.6	33.6
Ile (mg/L)	49.2	48.7	48.1	47.3	46.3	45.4	44.6
Leu (mg/L)	54.6	54.1	53.5	52.6	51.6	50.7	49.9
Lys (mg/L)	79.0	78.4	77.7	76.8	75.7	74.7	73.7

After this first simulation the results gathered showed as expected a big difference both in cell growth and density as well as in all amino acids concentrations overall. The first step towards optimization was to understand what parameters to change. Since the cells were from different cell lines but the model used to describe the kinetics should be similar the idea used was to only change the constants in each optimization attempt. The model used has 140 kinetic constants that control the kinetic equations generated in the kinetics function, that end up ultimately defining the flux balance over time in accordance with the metabolic matrix used. For the first optimization the thought process was to focus on one amino acid and reduce the difference between simulated data and experimental data for that specific amino acid. The amino acid chosen was Glutamine since it is one of the amino acids with highest concentration in the media, one of the most consumed and had a big difference between the experimental and simulated data. To do this optimization the first step was to identify the reactions in which Glutamine was directly involved using the metabolic stoichiometric matrix described in the model, after doing so the first constant that was changed/optimised was VfmaxGLNT, which is defined as the maximum flux of Glutamine.

The optimization of the constant was done using two python functions, one which computes the squared difference between the simulated data (using the kinetic constant given to it) and the experimental data, and the second function is from scipy.optimize

python package, this function is called minimise and it changes the given parameter for a given function over a specified interval for a specified range of values and iterations until it reaches the specified result, as close to 0 as possible, thus minimising the function. An example of this code used can be found in figure 4.27, a similar version to this code was used for all optimizations, only normally changing the number of iterations and variables/constants that were optimised.

```
from scipy.optimize import minimize

#        aAMP, aF6P, bAMP, bF6P, KAAMP, KAF6P, KdCIT, KdEGLN,    KdG6P,   KdLAC, KdPEP, KdPYR,  KdLACg, KdNH4g,
VariF1 = [0.47, 4.1, 10.46, 1.7, 0.09, 4.9e-06, 0.00074, 3.5, 1.710841e-08, 6.3, 3.7e-07, 4.5e-07, 170.0, 4.44,

def Objt(ValNew):
  VariF1[66]=ValNew

  sol1 = solve_ivp(ode, time_span, x0, method='RK45',t_eval =t_points,atol = abs_tol, rtol = rel_tol,args=(VariF
  Diff1 = (sol1.y[27][24] - 1.806122411)**2
  Diff2 = (sol1.y[27][48] - 1.531314216)**2
  Diff3 = (sol1.y[27][72] - 1.10583633)**2
  Diff4 = (sol1.y[27][96] - 0.6619207064)**2
  Diff5 = (sol1.y[27][120] - 0.1154381009)**2
  Diff6 = (sol1.y[27][144] - 0.009002383989)**2
  DiffT = Diff1 + Diff2 + Diff3 + Diff4 + Diff5 + Diff6
  return DiffT

bnds = ((0.00012,0.01),)
solF = minimize(Objt,0.00015,bounds = bnds,options = {"maxiter" : 2})
```

Figure 4.27: Example of the python code used for optimization of the different kinetic constants in the metabolic mode

After this first optimization of VfmaxGLNT a big improvement was observed in the way that the glutamine levels changed in the simulated results. Nonetheless, the squared differences of the other concentrations also changed, and it became clear that most likely a lot of the 140 parameters were going to be changed in order to achieve lower error. For this reason multiple simulations were done and analysed, the main results and changes from one simulation to the next can be seen in tables 4.42 to 4.43 below.

Table 4.42: Summary table of the results and conclusions of the 2nd optimization of parameters and simulation

2nd optimization - optimization of 5 variables (kinetic parameters) doing 15 iterations (evaluations of the function using new input). The variables were chosen based on the Glutamine consumption equation: KmASP, KmEGLN, KmR5P, VfmaxGLNT and VmaxPPRIBP							
Squared difference between experimental concentration of amino acids and simulation results over all data points							
Asp	4.8×10^{1}	His	2.1×10^{3}	Tyr	5.0×10^{3}	Ile	8.2×10^{3}
Glu	1.2×10^{2}	Gly	4.6×10^{3}	Met	8.6×10^{2}	Leu	9.5×10^{3}
Asn	9.5×10^{1}	Thr	1.2×10^{4}	Val	1.1×10^{4}	Lys	3.6×10^{4}
Ser	1.5×10^{3}	Arg	1.1×10^{5}	Cys	5.9×10^{3}	Pro	2.4×10^{3}
Gln	1.5×10^{5}	Ala	1.6×10^{4}	Phe	4.6×10^{3}	Total	3.8×10^{5}
Time of cultivation	Day 0	Day 1	Day 2	Day 3	Day 4	Day 5	Day 6
Experimental live cells	99	102	270	510	714	1107	720
Simulated live cells	100	118	146	173	199	214	201
Conclusion: The difference was lower than the one obtained in the first optimization for Glutamine, the next step was to increase the number of iterations, but the error in cell growth was still too big.							

Table 4.43: Summary table of the results and conclusions of the 3rd optimization of parameters and simulation

3rd optimization - optimization of 5 variables doing 1000 iterations. The variables were chosen based on the Glutamine consumption equation: KmASP, KmEGLN, KmR5P, VfmaxGLNT and VmaxPPRIBP							
Squared difference between experimental concentration of amino acids and simulation results over all data points							
Asp	4.8×10^{1}	His	2.1×10^{3}	Tyr	5.0×10^{3}	Ile	8.2×10^{3}
Glu	1.2×10^{2}	Gly	4.6×10^{3}	Met	8.6×10^{2}	Leu	9.5×10^{3}
Asn	9.5×10^{1}	Thr	1.2×10^{4}	Val	1.1×10^{4}	Lys	3.6×10^{4}
Ser	1.5×10^{3}	Arg	1.1×10^{5}	Cys	5.9×10^{3}	Pro	2.4×10^{3}
Gln	1.5×10^{6}	Ala	1.6×10^{4}	Phe	4.6×10^{3}	Total	3.8×10^{5}
Time of cultivation	Day 0	Day 1	Day 2	Day 3	Day 4	Day 5	Day 6
Experimental live cells	99	102	270	510	714	1107	720
Simulated live cells	100	118	147	175	204	224	217
Conclusion: The difference was actually higher, which showed that doing this many iterations did not improve the difference total. The next step was to decrease the number of iterations and increase the number of variables.							

Table 4.44: Summary table of the results and conclusions of the 4th optimization of parameters and simulation

4th optimization - optimization of 29 variables doing 50 iterations. The variables were chosen based on the Glutamine consumption equation and all the reactions that glutamine was a part of. *							
Squared difference between experimental concentration of amino acids and simulation results over all data points							
Asp	1.8×10^{1}	His	7.2×10^{1}	Tyr	1.7×10^{1}	Ile	6.1×10^{2}
Glu	4.4×10^{2}	Gly	5.7×10^{2}	Met	1.2×10^{2}	Leu	1.1×10^{3}
Asn	1.3×10^{2}	Thr	1.6×10^{2}	Val	1.5×10^{2}	Lys	2.1×10^{2}
Ser	7.3×10^{2}	Arg	9.8×10^{2}	Cys	4.6×10^{2}	Pro	5.6×10^{2}
Gln	2.3×10^{6}	Ala	6.5×10^{3}	Phe	2.4×10^{2}	Total	2.4×10^{5}
Time of cultivation	Day 0	Day 1	Day 2	Day 3	Day 4	Day 5	Day 6
Experimental live cells	99	102	270	510	714	1107	720
Simulated live cells	100	129	176	211	260	290	268
Conclusion: The overall differences dropped 36%, nonetheless there was an increase in Glutamine difference, in this simulation the optimization program took into account the differences between all concentrations, instead of just glutamine. This was used for all the following simulations. The next step was to test again a higher number of iterations							

*The 29 parameters optimised were: KdLACg, KdNH4g, KmASP, KmATP, KmEGLN, KmGLY, KmR5P, VfmaxGLNT, Vmaxgrowth, VmaxPPRIBP, KmALAg, KmARGg, KmASNg, KmASPg, KmATPg, KmCITg, KmEGLNg, KmG6Pg, KmEGLUg, KmGLYg, KmHISg, KmILEg, KmLYSg, KmPHEg, KmPROg, KmR5Pg, KmTHRg, KmTYRg and KmVALg.

Table 4.45: Summary table of the results and conclusions of the 5th optimization of parameters and simulation

5th optimization - optimization of 29 variables doing 150 iterations. The variables chosen were the same as in the 4th simulation.							
Squared difference between experimental concentration of amino acids and simulation results over all data points							
Asp	1.8×10^{1}	His	7.3×10^{1}	Tyr	2.9×10^{1}	Ile	6.7×10^{2}
Glu	4.3×10^{2}	Gly	5.7×10^{2}	Met	1.2×10^{2}	Leu	1.2×10^{3}
Asn	1.3×10^{2}	Thr	1.6×10^{2}	Val	1.7×10^{2}	Lys	2.1×10^{2}
Ser	7.4×10^{2}	Arg	9.8×10^{2}	Cys	4.6×10^{2}	Pro	5.6×10^{2}
Gln	2.3×10^{5}	Ala	6.4×10^{3}	Phe	2.4×10^{2}	Total	2.4×10^{5}
Time of cultivation	Day 0	Day 1	Day 2	Day 3	Day 4	Day 5	Day 6
Experimental live cells	99	102	270	510	714	1107	720
Simulated live cells	100	130	176	210	245	262	244
Conclusion: The differences increased in total and decreased in some concentrations, the next step was to try to use all relevant parameters at the same time to test the efficiency of the optimization program with a higher number of parameters. Cell growth remains mostly unchanged throughout the simulations, even if the concentration of each amino acid changes a lot.							

Table 4.46: Summary table of the results and conclusions of the 6th optimization of parameters and simulation

6th optimization - optimization of 120 variables doing 400 iterations. The variables chosen were all constants not related to mAb production since our cell line does not have those reactions. *							
Squared difference between experimental concentration of amino acids and simulation results over all data points							
Asp	2.0×10^{1}	His	7.8×10^{1}	Tyr	4.4×10^{1}	Ile	7.2×10^{2}
Glu	4.5×10^{2}	Gly	5.7×10^{2}	Met	1.2×10^{2}	Leu	1.2×10^{3}
Asn	1.3×10^{2}	Thr	1.6×10^{2}	Val	2.0×10^{2}	Lys	1.9×10^{2}
Ser	7.8×10^{2}	Arg	1.0×10^{3}	Cys	4.6×10^{2}	Pro	5.6×10^{2}
Gln	5.2×10^{4}	Ala	6.3×10^{3}	Phe	2.4×10^{2}	Total	6.6×10^{4}
Time of cultivation	Day 0	Day 1	Day 2	Day 3	Day 4	Day 5	Day 6
Experimental live cells	99	102	270	510	714	1107	720
Simulated live cells	100	64	147	179	214	232	222
Conclusion: The high number of parameters and iterations proved to be efficient but only 6 of the 120 parameters were actually changed. The overall total differences got reduced by 73% by only changing these 6 parameters, which led to the conclusion that for this model and data those parameters are the most sensible ones, that have the biggest impact with less change to them. The next step was to run a simulation focused on these six parameters, but as it could be seen, the cell density and growth is still unchanged throughout simulations.							

* The 120 parameters changed were: aAMP, aF6P, bAMP, bF6P, KAAMP, KAF6P, KdCIT, KdEGLN, KdG6P, KdLAC, KdPEP, KdPYR, KdLACg, KdNH4g, KmACCOA, KmADP, KmAKG, KmALA, KmAMP, KmARG, KmASP, KmASN, KmATP, KmCIT, KmEGLC, KmEGLN, KmEGLU, KmF6P, KmG6P, KmGAP, KmGLU, KmGLY, KmHIS, KmILE, KmLAC, KmLEU, KmLYS, KmMAL, KmNADH, KmNADPH, KmNH4, KmOXA, KmPEP, KmPYR, KmR5P, KmSER, KmSUC, KmTYR, KmVAL, KmX5P, KdALA, Pratio, VfmaxAK, VrmaxAK, VmaxAKGDH, VfmaxALATA, VrmaxALATA, VmaxASN, VmaxASTA, VmaxATPASE, VmaxCITS, VmaxCS, VmaxEP, VmaxG6PDH, VfmaxGLDH, VrmaxGLDH, VfmaxGLNT, VrmaxGLNT, VfmaxGLUT, VrmaxGLUT, Vmaxgrowth, VmaxHISARGTA, VmaxHK, VfmaxLDH, VrmaxLDH, Vmaxleak, VmaxAATOSUC, VmaxMAB, VmaxME, VmaxMLD, VmaxNADPHOX, VmaxPC, VmaxPDH, VmaxPFK, VfmaxPGI, VrmaxPGI, VmaxPGK, VmaxPK, VmaxPPRIBP, Vmaxresp, VmaxSDH, VmaxSDHH, VmaxTK, KmALAg, KmARGg, KmASNg, KmASPg, KmATPg, KmCITg, KmCYSg, KmEGLNg, KmG6Pg, KmEGLUg, KmGLYg, KmHISg, KmILEg, KmLYSg, KmMETg, KmPHEg, KmPROg, KmR5Pg, KmSERg, KmTHRg, KmTYRg, KmVALg, KmADPATP, KmATPADP, KmNADNADH, KmNADHNAD and KmNADPNADPH.

Table 4.47: Summary table of the results and conclusions of the 7th optimization of parameters and simulation

7th optimization - optimization of 6 variables doing 100 iterations. The variables chosen were all the constants that suffered a change during the last optimization, namely: KdLAC, KmASP, KmEGLN, KmR5P, VfmaxGLNT and VmaxPPRIBP							
Squared difference between experimental concentration of amino acids and simulation results over all data points							
Asp	3.5×10^{1}	His	8.2×10^{1}	Tyr	4.4×10^{1}	Ile	7.2×10^{2}
Glu	4.4×10^{2}	Gly	5.7×10^{2}	Met	1.2×10^{2}	Leu	1.2×10^{3}
Asn	1.3×10^{2}	Thr	1.6×10^{2}	Val	2.0×10^{2}	Lys	1.9×10^{2}
Ser	7.9×10^{2}	Arg	1.0×10^{3}	Cys	4.6×10^{2}	Pro	5.6×10^{2}
Gln	1.4×10^{3}	Ala	6.9×10^{3}	Phe	2.4×10^{2}	Total	1.5×10^{4}
Time of cultivation	Day 0	Day 1	Day 2	Day 3	Day 4	Day 5	Day 6
Experimental live cells	99	102	270	510	714	1107	720
Simulated live cells	100	64	139	166	198	229	245
Conclusion: This simulation reduced the total differences by 76% from the previously mentioned simulation, nonetheless there is still a big difference in general and specially in the growth and death rate of cells.							

The presented simulations above were not all the simulations done for the Cell Line A experimental data used, rather, the ones shown are either the ones that had the biggest impact or the ones that led to biggest changes in the optimization approach and code. In general from this set of simulations and optimizations we can conclude that using a high number of iterations (for example higher than 500) can lead to the code running for more than 24 hours without having better results than a simulation which takes 3 hours using less iterations. The number of parameters can also be increased to understand which are changed by the program and that could be the most sensible ones in the model, as seen in the last two simulations. Nonetheless it is necessary to employ bigger changes to the code and model in order to achieve better results, specifically in cell growth and death rate. For this data, even though the model is not perfect the total differences between experimental and simulated concentrations of amino acids over cultivation time decreased a total of 96% when comparing the first simulation with the last and best result achieved.

Due to the data used being from Cell Line A and the concentrations not having a high degree of certainty (due to possible analytical errors), the model was also fitted and optimised to a second set of data, this time using Cell Line B, specifically adapted for our process and the optimised media for it. This second set of data was acquired in duplicate, meaning that the experiment was run in two different vessels with the same conditions at the same time. The samples were also taken in duplicates and measured twice allowing for more reliable results, statistically speaking. The number of datapoints was also increased

to 10, instead of the previous 7 used in Cell Line A, which increases the difference value but also allows for more accurate optimization. And two other compounds were used to optimise the model, namely glucose concentration and lactated concentration, which are deeply connected with cell growth, which was the biggest issue observed in the previous optimization of the model.

The first step was to calculate the error obtained when optimising the model with this new data from Cell Line B cultivation, using the last parameters, which showed the best overall result. The summary of the first optimization can be seen in table 4.48 below.

Table 4.48: Summary table of the results and conclusions of the 1st optimization of parameters and simulation with Cell Line B cultivation data

1st optimization with Cell Line B data - optimization of 6 variables doing 250 iterations. The variables chosen were the same used in the best simulation of Cell Line A, namely: KdLAC, KmASP, KmEGLN, KmR5P, VfmaxGLNT and VmaxPPRIBP							
Squared difference between experimental concentration of amino acids and simulation results over all data points							
Asp	1.08×10^{3}	His	5.43×10^{4}	Tyr	5.85×10^{4}	Ile	9.97×10^{5}
Glu	7.31×10^{4}	Gly	1.26×10^{4}	Met	4.68×10^{4}	Leu	3.87×10^{5}
Asn	2.99×10^{5}	Thr	1.81×10^{5}	Val	1.11×10^{5}	Lys	3.59×10^{4}
Ser	4.78×10^{4}	Arg	6.39×10^{4}	Cys	1.34×10^{4}	Pro	1.75×10^{4}
Gln	8.65×10^{3}	Ala	3.91×10^{5}	Phe	2.13×10^{4}	Total	1.93×10^{6}
Glucose	399	Lactose	393				
Time of cultivation	Day 0	Day 1	Day 2	Day 3	Day 4	Day 5	Day 6
Experimental live cells	307	373	830	1198	1385	1888	2042
Simulated live cells	300	327	371	393	417	434	444
Conclusion: This simulation has a much higher difference, in both cell growth and in all concentrations when compared to the previous dataset this dataset shows ten times more difference than the best result obtained in the last simulations.							

Due to the difference between simulated data and experimental data being much higher, the optimization code for the parameters was changed, the optimization function was changed from minimise function [234], from scipy.optimize python library to cma.f2min function [235], which receives similar parameters but changes the way it chooses the values it tries to optimise. This function is part of the cma python library [236]. CMA stands for Covariance Matrix Adaptation; the function used uses a specific type of this technique called CMA-ES, which stands for Covariance Matrix Adaptation Evolution Strategy. CMA-ES is a numerical optimization algorithm strategy that is useful for optimization problems where the function is nonlinear and the relationship between parameters is complex and not well defined [237]. Evolutionary algorithms are broadly based on biological evolution principles, meaning that the way the optimization happens is with repeated interplay

of variation, recombination and mutation [238]. In other words in each iteration new individuals or possible solutions are generated in a stochastic way. This way the solutions that are closer to the goal are selected as the "new generation" meaning that new solutions will originate from random changes in the "parent" solutions [239, 240]. An example of the used code, derived from the shown code in figure 4.27 but with the new function as well as more data points evaluation can be found below in figure 4.28.

```
def Objt(ValNew):
    VariF1[11]=ValNew[0] #KmASP -- KdLAC -- SENSIBLE 0,79% VmaxASTA -- SENSIBLE 0,56% kdPYR
    VariF1[27]=ValNew[1] #KmEGLN -- KmASP -- SENSIBLE 0,77% VmaxATPASE -- SENSIBLE 0,55% KmF6P
    VariF1[48]=ValNew[2] #KmR5P -- KmEGLN -- SENSIBLE 0,79% VmaxHISARGTA -- SENSIBLE 0,52% KmVAL
    VariC[58]= ValNew[3] #KmASP -- KdLAC -- SENSIBLE 0,79% VmaxASTA
    VariC[59]= ValNew[4] #KmEGLN -- KmASP -- SENSIBLE 0,77% VmaxATPASE
    VariF1[70]=ValNew[5] #VfmaxGLNT -- KmR5P -- SENSIBLE 0,63% VMaxNADPHOX -- SENSIBLE 0,50% VmaxGrowth
    VariC[71]= ValNew[6] #KmR5P -- KmEGLN -- SENSIBLE 0,79% VmaxHISARGTA
    VariC[80]= ValNew[7] #VfmaxGLNT -- KmR5P -- SENSIBLE 0,63% VMaxNADPHOX
    VariC[82]= ValNew[8] #VmaxPPRIBP -- VfmaxGLNT -- SENSIBLE 0,62% VMaxPDH
    VariC[98]= ValNew[9] # VmaxPPRIBP -- SENSIBLE 0,6% KM CITg[9]= 5.41199999623080 #KmASP -- KdLAC
    VariF1[138]=ValNew[10] #VmaxPPRIBP -- VfmaxGLNT -- SENSIBLE 0,62% VMaxPDH -- SENSIBLE 0,50% kmNADHNAD
    VariF1[139]=ValNew[11] # VmaxPPRIBP -- SENSIBLE 0,6% KM CITg -- SENSIBLE 0,51% KmNADPNADPH

    sol1 = solve_ivp(ode, time_span, x0, method='RK45',t_eval =t_points,atol = abs_tol, rtol = rel_tol,args=(
    DiffT = 0
    TIMe = [0,9,17,25,33,42,50,58,67,120]

    for i in TIMe:
      if i == 0:
        ax = 0
      DiffT15 = (AnickaData['Phe'][ax]-sol1.y[37][i])*1000
      DiffT16 = (AnickaData['Ile'][ax]-sol1.y[31][i])*1000
      DiffT17 = (AnickaData['Leu'][ax]-sol1.y[33][i])*1000
      DiffT18 = (AnickaData['Lys'][ax]-sol1.y[34][i])*1000
      DiffT19 = (AnickaData['Pro'][ax]-sol1.y[38][i])*1000
      DiffT20 = (AnickaData['Lac'][ax]-sol1.y[32][i])
      #print(DiffT20)
      DiffT21 = (AnickaData['Gluc'][ax]-sol1.y[26][i])
      DiffT = DiffT + DiffT1**2 + DiffT2**2 + DiffT3**2 + DiffT4**2 + DiffT5**2 + DiffT6**2 + DiffT7**2 + Dif
    return DiffT

bnds = ((0.1,10),(0.01,1),(0.1,10),(1e-09,1e-06),(0.0001,0.01),(1e-10,1e-07),)
solF = cma.fmin2(Objt,ValNew,0.000001,options={'maxfevals': 1500})
solF
```

Figure 4.28: A snippet of the code used for the optimization of parameters for Cell Line B model using CMA-ES approach

Using this new approach, which runs much faster and based on the explained behaviour is beneficial for longer runs, with higher number of iterations, the first optimization was done with the same 6 variables and 1000 iterations, the results can be seen below in table 4.49.

Table 4.49: Summary table of the results and conclusions of the 2nd optimization of parameters and simulation with Cell Line B cultivation data

2nd optimization with Cell Line B data - optimization of 6 variables doing 1000 iterations, using the CMA-ES approach.							
Squared difference between experimental concentration of amino acids and simulation results over all data points							
Asp	1.10×10^3	His	5.42×10^4	Tyr	5.95×10^4	Ile	1.01×10^5
Glu	7.31×10^4	Gly	1.26×10^4	Met	4.68×10^4	Leu	3.90×10^5
Asn	2.99×10^5	Thr	1.81×10^5	Val	1.13×10^5	Lys	3.66×10^4
Ser	4.80×10^4	Arg	6.41×10^4	Cys	1.34×10^4	Pro	1.75×10^4
Gln	8.71×10^3	Ala	4.24×10^5	Phe	2.13×10^4	Total	1.97×10^6
Glucose	399	Lactose	413				
Time of cultivation	Day 0	Day 1	Day 2	Day 3	Day 4	Day 5	Day 6
Experimental live cells	307	373	830	1198	1385	1888	2042
Simulated live cells	300	321	363	384	408	425	438
Conclusion: This simulation proved to be faster than the previously used method, but the results were slightly worse, meaning that the parameters used had to be different.							

After multiple simulations that led to similar results, the sensibility of each parameter was better assessed, since the 6 variables that were thought to be the most sensitive were obtained in the optimization of 120 variables at the same time. To compare the different parameters in terms of sensitivity in the model, a python program was written that keeps all parameters the same and changes one at the time, increasing and decreasing it by 5%. The resulting total differences in concentrations in each simulation was then compared with the difference using the starting values for the constants shown in Robitaille's et al model. Using this method the most sensitive variables were then tested in multiple simulations, the best results were obtained using: KmCITg, VmaxHISARGTA, VmaxNADPHOX, VmaxPDH, VrmaxALATA, VmaxASN. The best results can be seen below in table 4.50.

Table 4.50: Summary table of the results and conclusions of the best optimization of parameters and simulation with Cell Line B cultivation data

Best optimization with Cell Line B data - optimization of 6 variables doing 1000 iterations, using the CMA-ES approach. The variables used were: KmCITg, VmaxHISARGTA, VmaxNADPHOX, VmaxPDH, VrmaxALATA, VmaxASN.							
Squared difference between experimental concentration of amino acids and simulation results over all data points							
Asp	2.22×10^4	His	3.21×10^4	Tyr	3.95×10^4	Ile	7.25×10^4
Glu	6.98×10^4	Gly	1.26×10^4	Met	4.68×10^4	Leu	3.31×10^5
Asn	2.99×10^5	Thr	1.82×10^5	Val	8.20×10^4	Lys	2.27×10^4
Ser	4.77×10^4	Arg	1.55×10^5	Cys	1.34×10^4	Pro	1.76×10^4
Gln	8.69×10^3	Ala	6.72×10^4	Phe	2.12×10^4	Total	1.54×10^6
Glucose	398	Lactose	384				
Time of cultivation	Day 0	Day 1	Day 2	Day 3	Day 4	Day 5	Day 6
Experimental live cells	307	373	830	1198	1385	1888	2042
Simulated live cells	300	323	366	389	415	436	457
Conclusion: This simulation, even though it had the best results, only decreased the difference by 22% when compared to the first simulation using CMA-ES approach.							

The objective of this fitting of Robitaille's et al model was to later use it with FBA to optimise the cultivation conditions, namely the initial cultivation media concentrations. Both attempts, with either the data from Cell Line A and with the data from Cell Line B, ended up not showing good enough results to reach this goal. Due to the higher degree of quality from the data set of Cell Line B, due to having duplicate results, the expected results would have been that the model would be better fitted to this data, but as we could see the error displayed by the squared differences between the concentrations of amino acids over time is much higher in the Cell Line B data set than in the Cell Line A. To better illustrate this figure 4.29 and 4.30 show the graphs of the concentrations of some amino acids in the experimental data against the simulated data.

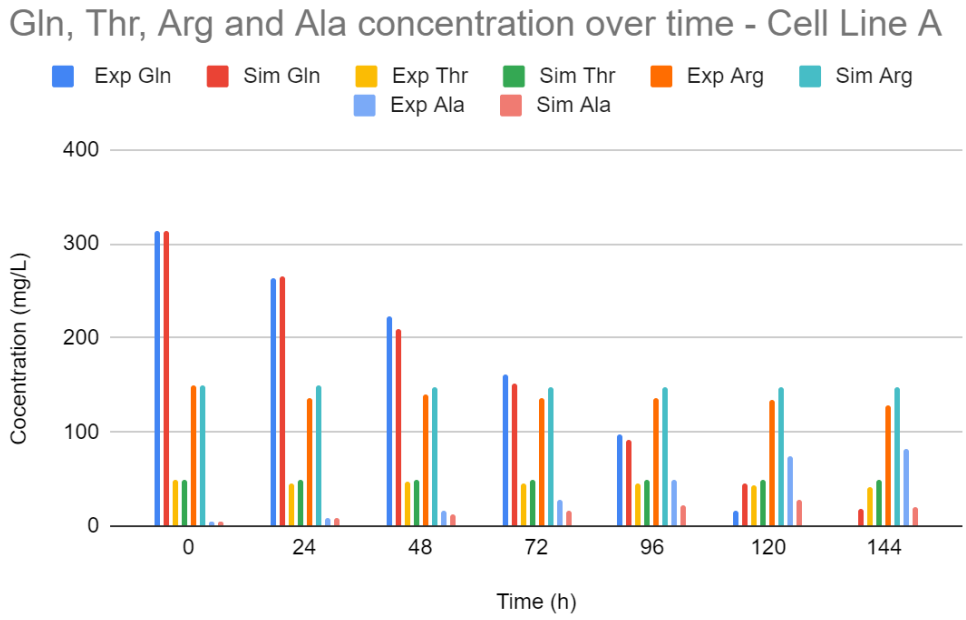

Figure 4.29: Glutamine (Gln), Threonine (Thr), Arginine (Arg) and Alanine (Ala) concentration over cultivation time with Cell Line A. "Exp" data refers to experimental data and "Sim" to Simulated data

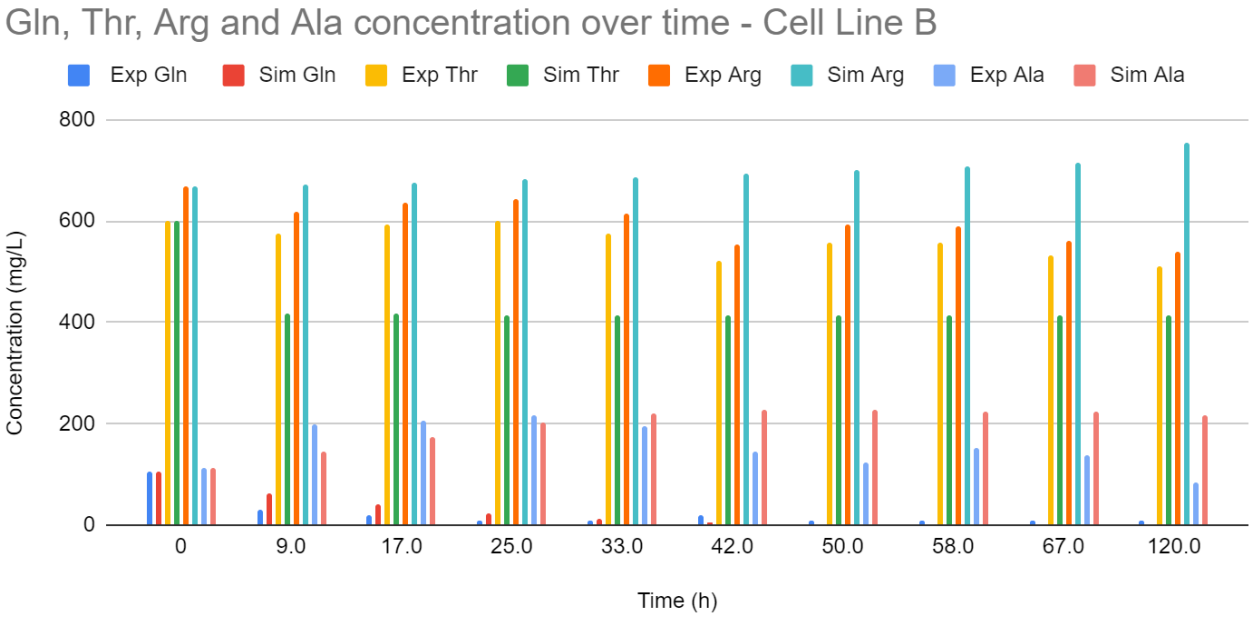

Figure 4.30: Glutamine (Gln), Threonine (Thr), Arginine (Arg) and Alanine (Ala) concentration over cultivation time with Cell Line B. "Exp" data refers to experimental data and "Sim" to Simulated data

As seen above the results are not close enough to allow for the use of the model for optimising the media. The main issues might be due to the fact that the cell death rate was not among the kinetic parameters that was optimised due to it being added separately in the ode function that defines the ODEs system. Another potential issue could be the optimization function not being clear enough for the CMA-ES or minimising function to achieve better results. Nonetheless it was shown that metabolic models can get results close to the behaviour of cell cultures as long as properly optimised and fitted to experimental data. An important note is that the model used was also developed for a different cell line, which means that to produce reliable data the equations of the model should be changed as well.

5

Conclusions

In this study, multiple approaches and parameters that influence the growth of mammalian cells in bioreactors were tested and studied. In order to better understand the overview of the results obtained. This section will shortly mention the main conclusions for each experimental test, as well as in general for each subtopic studied. Future steps that might be taken in this topic and study are also given.

5.1 Optimization of kLa in Bioreactors

In the experiments for the optimization of kLa in the Bioreactors, the main goal was to study the different conditions and how they affect the oxygen mass transfer, since this is one of the most important parameters in bioreactor operation. The conclusions reached about each parameter studied are as such:

- **Impact of Impeller Speed -** In these experiments, it was confirmed the relationship of impeller tip speed and RPM with the increase of kLa, and it was compared with the existing literature. The conclusion is that the proportionality constants differ from system to system, and even within the same system some large changes can be observed. The analysed systems exhibited proportionality constants that differed from the examples in the literature.

- **Impact of Impeller Geometry and Mixing Profile -** In these experiments, it was discussed different impeller geometries. The simple correlations used in literature were tested and used to compare the results. It was estimated and confirmed that the used Toroidal Impeller must have a higher power number when compared to Elephant Ear, which was one of the first conclusions reached. The different mixing of Vibromixer was concluded to be worse in times of kLa, and the proper estimation of power input by this mixing has been concluded as a topic to be further researched, due to lack of existing studies. It was also observed that the surface aeration has a big influence on the kLa in this smaller scale since the non-sparged experiments presented showed a similar but lower (in general) kLa than the sparged ones. This

was also proposed as an explanation for the changes in results when compared to literature at this scale.

- **Impact of Impeller Position -** These setups and experiments were meant to be used as a way to study the effect of the different position of impellers along the shaft, namely the distance between two impellers in a two impeller system. It was confirmed that, in accordance with literature, the best distance should follow one of two ranges. The relationship between impeller diameter and distance between each other, and the relationship between vessel diameter and distance between each other.

  The first is said that the best distance should be between 1 and 2 times the diameter of the impeller, showing better results for 1.5 in general. The second was shown that the range of distances should be between $\frac{1}{2}$ and $\frac{2}{3}$ of the vessel's diameter. The Vibromixer system was the best setup since the distances used improved and the final and best result was equal to the last distance used which was 7 cm, and the literature range was between 6 and 8 cm.

  The Stirred Tank was done with higher values than the range in literature, the best distance for this system was bigger than the vessel's diameter, and the other distances showed similar results. For the Biostat, the distance that was closer to the mentioned range was the highest kLa, by 40% more than the second best distance, but only for the highest RPM.

- **Impact of Aeration Flow Rate -** The objective of this experiment was to determine the relationship between the air flow rate and kLa, and the simple conclusion is that for all cases the relationship is linear, with a R-squared value higher than 0.99, with a proportionality constant for the Vibromixer system similar to literature values, while the other systems showed a much higher proportionality constant, which might be related to the mixing profile of the other systems and its having a higher impact on the kLa.

- **Impact of Baffles -** The study of baffles is still a topic that needs to be further developed, nonetheless the study showed a clear increase from unbaffled to baffled vessel, in terms of kLa. But, according to literature and to previous experiments, it was also concluded that the increase by increasing the number of baffles or changing or optimising the shape and placement is several orders of magnitude lower than the impact of going from unbaffled to baffled.

- **Impact of Bubble Size -** The impact of bubble size is a topic widely researched but extremely complex to simulate, as multiple literature equations were mentioned. Nonetheless, in the end the conclusion is that defined bubble size is hard to produce and that in general the factors that contribute to it are the pore size, flow rate and pressure. The main conclusion is that in smaller scale it is important to keep this in

mind, but at larger scale bubble coalescence becomes an issue and the use of high agitation to break bubbles becomes more effective than making extremely precise bubble size optimization and generation.

- **Impact of Membrane Aeration -** The use of silicone tubing as membrane proved to be ineffective, the goal was to reduce the impact of bubbles and the stress they produce by using diffusion through a membrane, in this study only one simple tube of silicone was used to develop a prototype. According to the results, the kLa in general was too low to produce good enough data, nonetheless, the comparison between control and the highest kLa obtained with membrane showed that it would be estimated a surface area too large to fit in the bioreactor. Other issues with this method include maintenance, as such the use of normal sparging has been accepted as the main method of aeration, or the easiest to optimise.

5.1.1 Final Conclusions

The different bioreactor systems studied showed, as expected, differences that show that the largest reactor used, the Biostat, achieved the highest kLa, mostly due to the impellers used in said system. The stirred tank setup, and the use of rushton proved to be the most reliable. In the future, the optimization and cultivation experiments should continue to be done in stirred tank systems that ensure the necessary and previously stated conditions for mammalian cell cultivation. The potential gaps in the results obtained were due to optimisation of the setups used and the gradual evolution of the design and functionalities of the bioreactor system used.

5.2 Optimization of Bioreactors for Cell Viability

In these experiments, the goal was to run multiple tests on possible causes of shear stress and issues on cells, for example trying to find the limit of protection that shear protectants allow at a given concentration, checking the multiple parameters and changes that happen during cultivation and what factors could be behind the multitude of parameters that need to be studied and kept in mind, even outside of just bioreactor apparatus, such as the media composition. As done above, the main conclusions will be described per experiment as such:

- **Shear Stress Evaluation -** In this experiment, the shear stress resistance of cells was tested, as well as calculated the shear stress and eddy size near the impeller, which should be a close estimation to the max shear stress that cells can feel in the given system. It was confirmed that the mammalian cells used were not able to survive any cultivation at the mixing conditions without PEG, it was also noticed that even a really low amount of PEG was enough to keep the cells alive, yet the doubling time was not consistent, due to the adaptation of cells to extreme conditions, there

is the possibility of cells being adapted with higher PEG and this would be lower and lower with each passage to adapt them to survive without PEG.

- **Foaming, Defoaming and use of PEMF -** The impact of foaming in chemical processes including fermentation is known, in the experiments a new external stimulation technique was studied, namely Pulsed Electromagnetic Fields. The intensity of the treatment was always the maximum allowed by the machine used, nonetheless it was concluded that further experiments and a more customizable and stronger pulse machine should be used to gather better results and conclusions.

- **Fed-Batch Cultivation -** This experiment was done to understand and compare the behaviour of cells in a fed batch cultivation environment. Conclusion on further needs of adaptation and optimization of feeding rates and composition was reached. The doubling time and maximum density were lower than those found in stock cultivations in shake flasks. The rate of consumption of amino acids, glucose and lactate were also evaluated, and the main amino acids and changes in density can be connected to changes in the amino acids.

- **Predictive Python Metabolic Model -** Based on the needs of the above mentioned fed batch experiment, the use of Metabolic Engineering Models was approached, namely the use of a FBA based model and the adaptation to experimental growth and amino acid consumption was made through repetition of simulations and optimization using different iterations of python code and expressions. For the first data set, Cell Line A, a good reduction of the error between estimations of amino acid concentrations made by the model and the experimental data was achieved. Nonetheless the same was not the case in the second data set, a bigger one with more data points, but also more reliable data based on duplicates and better analytical methods. Both times the model was unable to reach optimised cell growth and the difference in it was not reduced significantly in both cases.

5.2.1 Final Conclusions

To better understand cellular growth, more extensive cultivation experiments should be done in order to assess the conditions mentioned above that show the best results. The results obtained point to a need for further research on stirring speed and aeration in stirred tanks, which are shown to be easier to change and control conditions. With the increase of experimental data the development of predictive metabolic models can be further improved, and the effectiveness of it increased as well.

6

Future Directions

6.1 Optimization of kLa in Bioreactors

In general, the main future steps in this topic is to do more testing and replicates to gather increasingly more data, to compare to a higher number of existing models and, eventually, to create novel models. The use of AI might be a possibility given enough data for machine learning and development of robust CFD models that would allow a more rigorous interpretation of data and estimation of fluid dynamics which in turn correlates with the studied parameters.

- **Impact of Impeller Speed -** Trying new impellers, replicating data and using more measurements for lower ranges of increments of RPM.
- **Impact of Impeller Geometry and Mixing Profile -** Testing and developing new impellers that are focused on CFD modelling of the necessary parameters, for example by modelling shear stress in one impeller and how the velocity profile changes we can upgrade those parts of the impeller geometry, needs more shear stress data from cells for better understanding of limitations in power input, flow pattern or in an easier way, the relationship between Power Number and Flow Number in aerated vessels.
- **Impact of Impeller Position -** This seems to be close to the already established equations, since the results followed the predicted best values, nonetheless it is important to understand and to study the effect of flow dynamics better, by doing more testing using multiple geometries in the same shaft and the change of the position and also the correlation to the liquid level and it's changes should be studied for fed batch possibilities.
- **Impact of Aeration Flow Rate -** Another study that was conclusive and linearly changed as expected, nonetheless the repeatability of data should be done as well as study the impact in different mixing profiles and the changes in the flow dynamics due to having increased flooding/cavitation for higher flow rate and the possible economic implications of higher flow rate.

- **Impact of Baffles -** The shape of baffles and the number of baffles could and should be further developed, even if the impact is not as great as having just baffles, possibility of using different positions and geometry might also help reducing the shear stress or strain from the varying velocity gradients.

- **Impact of Bubble Size -** This topic was greatly studied in theory and literature, nonetheless as future steps it makes total sense to increase the number of aeration, sparging techniques studied and develop into the delivery of bubbles into the system, doing experiments that correlate flow number/power input/mixing and bubble size and sparging efficiency.

- **Impact of Membrane Aeration -** The use of different materials and structures and higher pressure can help achieve the higher oxygenation needed without using the sparging techniques, nonetheless this is actively being studied since it has many advantages. Main future steps in this field would go into material and diffusion studies and membrane engineering for further development.

- **Other topics -** The specific measurement of power input with different techniques should be done in order to better understand the existing models. This will also allow for the creation of new empirical models for the studied systems, with a higher degree of certainty.

6.2 Optimization of Bioreactors for Cell Viability

In general, the future steps and directions, is to increase the number of experiments, repeatability in order to get statistically relevant data and results. Study implementation of different models and use big data to optimise with the use of machine learning and AI. Overall, a greater development and study of control systems and protocols that will be directly linked to viability, experiment with different parameter ranges to find optimal values and study control.

- **Shear Stress Evaluation -** In general, the next steps would be to repeat experiment with cells from the same culture for different ranges of RPM, aeration rates and possibly change the experimental testing, use different machine/vessel for testing. Compare more existing models and empirical equations with CFD models.

- **Foaming, Defoaming and use of PEMF -** This topic is still unclear, the approach of different techniques should be done such as the use of commercially available chemical antifoams, check the concentrations, if they are easy to remove or allowed in food. There should be a bigger focus on other physical stimulations such as ultrasound or even mechanical defoamers or drainage of foaming. The PEMF technique should be tested further in more setups and with a more versatile machine.

- **Fed-Batch Cultivation - Cultivation** tests with different techniques, optimised feeding regime and time and the control protocols should be tested and studied, including the different yields to optimise the final goal of economic viability of industrial production of meat in bioreactors.

References

[1] FAO and WHO. "Food safety aspects of cell-based food". In: *FAO and WHO* (2023), pp. 9–119. ISSN: 978-92-5-137723-9. DOI: https://doi.org/10.4060/cc4855en (cit. on pp. 3, 6).

[2] M. J. Post. "Cultured beef: medical technology to produce food". In: *Journal of the Science of Food and Agriculture* 94.6 (2014), pp. 1039–1041. DOI: https://doi.org/10.1002/jsfa.6474. eprint: https://onlinelibrary.wiley.com/doi/pdf/10.1002/jsfa.6474. URL: https://onlinelibrary.wiley.com/doi/abs/10.1002/jsfa.6474 (cit. on p. 4).

[3] S. Bailey. "5 challenges faced by the cultured meat industry". In: *Kilburn & amp; Strode* (2021-11). URL: https://www.kilburnstrode.com/knowledge/european-ip/5-challenges-cultured-meat-industry (cit. on pp. 4, 5).

[4] V. Company. "The companies removing fetal bovine serum to make ethical, slaughter-free meat - vegconomist - The Vegan Business Magazine". In: *vegconomist* (2023-06). URL: https://vegconomist.com/cultivated-cell-cultured-biotechnology/companies-removing-fetal-bovine-serum-slaughter-free-meat/ (cit. on p. 4).

[5] M. Siegrist and C. Hartmann. "Consumer acceptance of novel Food Technologies". In: *Nature News* (2020-06). URL: https://www.nature.com/articles/s43016-020-0094-x#citeas (cit. on p. 4).

[6] *Making Meat Affordable: Progress Since The $330,000 Lab-Grown Burger*. 2022-03. URL: https://www.forbes.com/sites/lanabandoim/2022/03/08/making-meat-affordable-progress-since-the-330000-lab-grown-burger/ (cit. on p. 4).

[7] *Will I See Lab-Grown Meat in Supermarkets Any Time Soon?* 2023-01. URL: https://www.bonappetit.com/story/lab-grown-meat (cit. on pp. 4, 5).

[8] *BioBetter has the key to scale-up cultivated meat: An innovative approach to growth factors could cut cultured meat costs*. 2022-09. URL: https://www.foodnavigator.com/Article/2022/09/12/biobetter-s-growth-factor-innovation-cuts-cost-of-cultured-meat (cit. on p. 4).

[9] *Lab-grown meat would 'cut emissions and save energy*. 2011-06. URL: https://www.ox.ac.uk/news/2011-06-21-lab-grown-meat-would-cut-emissions-and-save-energy (cit. on p. 5).

[10] H. L. Tuomisto and M. J. Teixeira de Mattos. "Environmental Impacts of Cultured Meat Production". In: *Environmental Science & Technology* 45.14 (2011). PMID: 21682287, pp. 6117–6123. DOI: 10.1021/es200130u. URL: https://doi.org/10.1021/es200130u (cit. on p. 5).

[11] *Biotechnologies: Commission seeks open debate on New Genomic Techniques as study shows potential for sustainable agriculture and need for new policy*. 2021-04. URL: https://ec.europa.eu/commission/presscorner/detail/en/ip_21_1985 (cit. on p. 5).

[12] *Lab Grown Meat - An Emerging Industry*. 2021-10. URL: https://www.colorado.edu/ecenter/2021/10/20/lab-grown-meat-emerging-industry (cit. on p. 5).

[13] *Italy moves to ban lab-grown meat to protect food heritage*. 2023-03. URL: https://www.bbc.com/news/world-europe-65110744 (cit. on p. 5).

[14] D. Humbird. "Scale-up economics for cultured meat". In: *Biotechnology and Bioengineering* 118.8 (2021), pp. 3239–3250. DOI: https://doi.org/10.1002/bit.27848. URL: https://onlinelibrary.wiley.com/doi/abs/10.1002/bit.27848 (cit. on p. 5).

[15] S. Bohn, D. Ung, and T. Moses. "How to overcome the challenges of cost-effective cultured meat production at scale". In: *crbgroup* (2023). URL: https://www.crbgroup.com/insights/food-beverage/cultured-meat (cit. on p. 5).

[16] *Plant-based and cultivated meat innovation | GFI*. 2023-09. URL: https://gfi.org/ (cit. on p. 6).

[17] *World's first lab-grown burger is eaten in London*. 2023-09. URL: https://www.bbc.com/news/science-environment-23576143 (cit. on p. 6).

[18] *U.S. regulators approve sale of cell-cultured chicken by two startups*. 2022-05. URL: https://www.cnbc.com/2023/06/21/us-approves-sale-of-cell-cultured-chicken-to-two-start-ups.html (cit. on p. 6).

[19] *Mosa Meat opens new facility in Maastricht, sees 'a clear path towards price parity' for cultivated meat*. 2023-05. URL: https://agfundernews.com/mosa-meat-opens-facility-sees-a-clear-path-towards-price-parity (cit. on p. 6).

[20] *Mosa Meat's new home*. 2023-06. URL: https://mosameat.com/blog/mosa-meats-new-home (cit. on p. 6).

[21] *Space F Claims Korea's First Cultivated Chicken And Beef Prototypes Alongside New Pork 2.0*. 2022-02. URL: https://www.greenqueen.com.hk/space-f-korea-first-cultivated-beef-chicken/ (cit. on p. 6).

[22] *This German Startup Has Made A Slaughter-Free Schnitzel To Break With Convention But Maintain Tradition*. 2022-03. URL: https://www.greenqueen.com.hk/afine-foods-debuts-cultivated-pork-schnitzel/ (cit. on p. 6).

[23] *Mogale Meat Unveils Africa's First Cultivated Chicken Breast*. 2022-04. URL: https://vegconomist.com/cultivated-cell-cultured-biotechnology/mogale-meat-unveils-africas-first-cultivated-chicken-breast/ (cit. on p. 6).

[24] *South African Startup Unveils Continent's First Cultivated Beef Burger*. 2022-04. URL: https://www.greenqueen.com.hk/africa-gets-first-cultivated-beef-burger/ (cit. on p. 6).

[25] J. Camphuijsen, F. J. C. Rivera, G. Potter, C. Clark, J. Chen, S. Kahan, and B. Aguilar. "Modeling the biomechanics of cells on microcarriers in a stirred-tank bioreactor". In: *bioRxiv* (2022). DOI: 10.1101/2022.08.31.505282. URL: https://www.biorxiv.org/content/early/2022/09/03/2022.08.31.505282 (cit. on p. 6).

[26] *Author Correction: Spontaneous immortalization of chicken fibroblasts generates stable, high-yield cell lines for serum-free production of cultured meat*. 2023-01. URL: https://www.nature.com/articles/s43016-023-00692-2 (cit. on p. 7).

[27] *Cultivated meat cell culture media | Deep dive | GFI*. 2023-09. URL: https://gfi.org/science/the-science-of-cultivated-meat/deep-dive-cultivated-meat-cell-culture-media/ (cit. on p. 7).

[28] T. A. Wyrobnik, S. Oh, A. Ducci, and M. Micheletti. "Engineering characterization of the novel Bach impeller for bioprocessing applications requiring low power inputs". In: *Chemical Engineering Science* 252 (2022), p. 117263. ISSN: 0009-2509. DOI: https://doi.org/10.1016/j.ces.2021.117263. URL: https://www.sciencedirect.com/science/article/pii/S0009250921008289 (cit. on p. 7).

[29] *Cellmotions - THE BATCH IMPELLER SOLUTION*. 2023-09. URL: https://www.cellmotions.com/pages/technology (cit. on p. 7).

[30] F. J. Cantarero Rivera and J. Chen. "Computational fluid dynamics modeling of cell cultures in bioreactors and its potential for cultivated meat production—A mini-review". In: *Future Foods* 6 (2022), p. 100195. ISSN: 2666-8335. DOI: https://doi.org/10.1016/j.fufo.2022.100195. URL: https://www.sciencedirect.com/science/article/pii/S266683352200082X (cit. on p. 7).

[31] *Cultivated meat bioprocess design | Deep dive | GFI*. 2023-09. URL: https://gfi.org/science/the-science-of-cultivated-meat/deep-dive-cultivated-meat-bioprocess-design/ (cit. on p. 7).

[32] E. A. Rosado-Olivieri and A. H. Brivanlou. "Gastruloids Gain Muscle: Somite Formation in Embryo-Like Structures". In: *Cell Stem Cells* 26 (2020). DOI: https://doi.org/10.1016/j.stem.2020.03.011. URL: https://www.cell.com/cell-stem-cell/fulltext/S1934-5909(20)30103-X?_returnURL=https%3A%2F%2Flinkinghub.elsevier.com%2Fretrieve%2Fpii%2FS193459092030103X%3Fshowall%3Dtrue#%20 (cit. on p. 7).

[33] M. K. Saad, J. John SK Yuen, C. M. Joyce, X. Li, T. Lim, T. L. Wolfson, J. Wu, J. Laird, S. Vissapragada, O. P. Calkins, A. Ali, and D. L. Kaplan. "Continuous Fish Muscle Cell Line with Capacity for Myogenic and Adipogenic-like Phenotypes". In: *bioRxiv* (2022). DOI: 10.1101/2022.08.22.504874. URL: https://www.biorxiv.org/content/early/2022/08/22/2022.08.22.504874 (cit. on p. 7).

[34] *Scomber scombrus Myoblast Cell Line (MACK1) - KeraFast*. 2023. URL: https://www.kerafast.com/item/5885/scomber-scombrus-myoblast-cell-line-mack1 (cit. on p. 7).

[35] Y. Tsuruwaka and E. Shimada. "Reprocessing seafood waste: challenge to develop aquatic clean meat from fish cells". In: *npj Science of Food* 6.1 (2022-01), p. 7. ISSN: 2396-8370. DOI: 10.1038/s41538-021-00121-3. URL: https://doi.org/10.1038/s41538-021-00121-3 (cit. on p. 7).

[36] T. Messmer, I. Klevernic, C. Furquim, E. Ovchinnikova, A. Dogan, H. Cruz, M. J. Post, and J. E. Flack. "A serum-free media formulation for cultured meat production supports bovine satellite cell differentiation in the absence of serum starvation". In: *Nature Food* 3.1 (2022-01), pp. 74–85. ISSN: 2662-1355. DOI: 10.1038/s43016-021-00419-1. URL: https://doi.org/10.1038/s43016-021-00419-1 (cit. on p. 7).

[37] A. Kolkmann, A. Van Essen, and P. Moutsatsou. "Development of a Chemically Defined Medium for in vitro Expansion of Primary Bovine Satellite Cells". In: (2022-08). DOI: 10.3389/fbioe.2022.895289. URL: https://pubmed.ncbi.nlm.nih.gov/35992337/ (cit. on p. 7).

[38] R. Mitić, F. Cantoni, C. S. Börlin, M. J. Post, and L. Jackisch. "A simplified and defined serum-free medium for cultivating fat across species". In: *iScience* 26.1 (2023-01). ISSN: 2589-0042. DOI: 10.1016/j.isci.2022.105822. URL: https://doi.org/10.1016/j.isci.2022.105822 (cit. on p. 7).

[39] D. Liu, E. Xu, and R. Niu. "Tissue-like cultured fish fillets through a synthetic food pipeline". In: (2022-11). URL: https://doi.org/10.21203/rs.3.rs-2274508/v1 (cit. on p. 7).

[40] *Algae2fish*. 2023-09. URL: https://algae2fish.wixsite.com/algae2fish (cit. on p. 7).

[41] D. M. C. Marques, J. C. Silva, A. P. Serro, J. M. S. Cabral, P. Sanjuan-Alberte, and F. C. Ferreira. "3D Bioprinting of Novel & kappa;-Carrageenan Bioinks: An Algae-Derived Polysaccharide". In: *Bioengineering* 9.3 (2022). ISSN: 2306-5354. DOI: 10.3390/bioengineering9030109. URL: https://www.mdpi.com/2306-5354/9/3/109 (cit. on p. 7).

[42] A. Zernov, L. Baruch, and M. Machluf. "Chitosan-collagen hydrogel microparticles as edible cell microcarriers for cultured meat". In: *Food Hydrocolloids* 129 (2022), p. 107632. ISSN: 0268-005X. DOI: https://doi.org/10.1016/j.foodhyd.2022.107632. URL: https://www.sciencedirect.com/science/article/pii/S0268005X22001527 (cit. on p. 7).

[43] Y. Kong, S. Ong, M. H. Liu, H. Yu, and D. Huang. "Functional composite microbeads for cell-based meat culture: effect of animal gelatin coating on cell proliferation and differentiation". In: *Journal of Physics D: Applied Physics* 55.34 (2022-06), p. 345401. DOI: 10.1088/1361-6463/ac7011. URL: https://dx.doi.org/10.1088/1361-6463/ac7011 (cit. on p. 7).

[44] M. Ogawa, J. Moreno Garcia, N. Nitin, K. Baar, and D. E. Block. "Assessing Edible Filamentous Fungal Carriers as Cell Supports for Growth of Yeast and Cultivated Meat". In: *Foods* 11.19 (2022). ISSN: 2304-8158. DOI: 10.3390/foods11193142. URL: https://www.mdpi.com/2304-8158/11/19/3142 (cit. on p. 7).

[45] Y. Liu, R. Wang, S. Ding, L. Deng, Y. Zhang, J. Li, Z. Shi, Z. Wu, K. Liang, X. Yan, W. Liu, and Y. Du. "Engineered meatballs via scalable skeletal muscle cell expansion and modular micro-tissue assembly using porous gelatin micro-carriers". In: *Biomaterials* 287 (2022), p. 121615. ISSN: 0142-9612. DOI: https://doi.org/10.1016/j.biomaterials.2022.121615. URL: https://www.sciencedirect.com/science/article/pii/S0142961222002551 (cit. on p. 7).

[46] S. C. Norris, N. S. Kawecki, A. R. Davis, K. K. Chen, and A. C. Rowat. "Emulsion-templated microparticles with tunable stiffness and topology: Applications as edible microcarriers for cultured meat". In: *Biomaterials* 287 (2022), p. 121669. ISSN: 0142-9612. DOI: https://doi.org/10.1016/j.biomaterials.2022.121669. URL: https://www.sciencedirect.com/science/article/pii/S014296122200309X (cit. on p. 7).

[47] R. C. Andreassen, S. B. Rønning, N. T. Solberg, K. G. Grønlien, K. A. Kristoffersen, V. Høst, S. O. Kolset, and M. E. Pedersen. "Production of food-grade microcarriers based on by-products from the food industry to facilitate the expansion of bovine skeletal muscle satellite cells for cultured meat production". In: *Biomaterials* 286 (2022), p. 121602. ISSN: 0142-9612. DOI: https://doi.org/10.1016/j.biomaterials.2022.121602. URL: https://www.sciencedirect.com/science/article/pii/S0142961222002423 (cit. on p. 7).

[48] *Bioreactor - an overview | ScienceDirect Topics*. 2023-09. URL: https://www.sciencedirect.com/topics/earth-and-planetary-sciences/bioreactor (cit. on p. 7).

[49] V. Gold, U. internationale de chimie pure et appliquée, I. U. of Pure, and A. Chemistry. *Compendium of Chemical Terminology: IUPAC Recommendations*. Blackwell Scientific Publications, 1987. ISBN: 9780632017652. URL: https://books.google.cz/books?id=wDiMswEACAAJ (cit. on p. 7).

[50] R. Meyers. *Encyclopedia of Physical Science and Technology*. Encyclopedia of Physical Science and Technology v. 2. Academic Press, 2002. ISBN: 9780122274107. URL: https://books.google.cz/books?id=QlqfvwEACAAJ (cit. on p. 7).

[51] Y. Chisti. "Bioreactor design". In: *Basic Biotechnology*. Ed. by C. Ratledge and B. Kristiansen. 3rd ed. Cambridge University Press, 2006, pp. 181–200. DOI: 10.1017/CBO9780511802409.009 (cit. on p. 7).

[52] *Real life bioreactor Diagram*. 2023-09. URL: https://commons.wikimedia.org/wiki/File:Real_life_bioreactor.png (cit. on p. 8).

[53] *Bioreactor- Definition, Design, Principle, Parts, Types, Applications, Limitations*. 2023-09. URL: https://microbenotes.com/bioreactor/ (cit. on p. 8).

[54] *Stirred-Tank Bioreactors - an overview | ScienceDirect Topics*. 2023-09. URL: https://www.sciencedirect.com/topics/engineering/stirred-tank-bioreactors (cit. on p. 8).

[55] *Airlift Bioreactors - an overview | ScienceDirect Topics*. 2023-09. URL: https://www.sciencedirect.com/topics/engineering/airlift-bioreactors (cit. on p. 8).

[56] *Bubble Columns - an overview*. URL: https://www.sciencedirect.com/topics/chemistry/bubble-columns (cit. on p. 8).

[57] *Fluidized Bed Reactor - an overview | ScienceDirect Topics*. 2023-09. URL: https://www.sciencedirect.com/topics/chemistry/fluidized-bed-reactor (cit. on p. 9).

[58] *Photobioreactor - an overview | ScienceDirect Topics*. 2020-09. URL: https://www.sciencedirect.com/topics/immunology-and-microbiology/photobioreactor#:~:text=A%20photobioreactor%20(PBR)%20can%20be,Science%2C%20Technology%20and%20Medicine%2C%202020 (cit. on p. 9).

[59] M. Moo-Young. *Comprehensive Biotechnology*. Comprehensive Biotechnology. Elsevier Science, 2011. ISBN: 9780080885049. URL: https://books.google.cz/books?id=hPOa0_eW1_oC (cit. on p. 9).

[60] S. Yang. *Bioprocessing for Value-Added Products from Renewable Resources: New Technologies and Applications*. Elsevier Science, 2011. ISBN: 9780080466712. URL: https://books.google.cz/books?id=Sr0J08qkbxYC (cit. on p. 9).

[61] (Cit. on p. 9).

[62] J. Vanags and A. Suleiko. "Oxygen Mass Transfer Coefficient Application in Characterisation of Bioreactors and Fermentation Processes". In: *Latvian Journal of Physics and Technical Sciences* 59.5 (2022), pp. 21–32. DOI: doi:10.2478/lpts-2022-0038. URL: https://doi.org/10.2478/lpts-2022-0038 (cit. on p. 9).

[63] "Oxygen Transfer in Bioreactors". In: *Engineering Principles in Biotechnology*. John Wiley & Sons, Ltd, 2017. Chap. 8, pp. 241–264. ISBN: 9781119159056. DOI: https://doi.org/10.1002/9781119159056.ch8. eprint: https://onlinelibrary.wiley.com/doi/pdf/10.1002/9781119159056.ch8. URL: https://onlinelibrary.wiley.com/doi/abs/10.1002/9781119159056.ch8 (cit. on p. 9).

[64] M. Wild, Y. Mast, and R. Takors. "Revisiting Basics of kLa Dependency on Aeration in Bubble Columns: a Is Surprisingly Stable". In: *Chemie Ingenieur Technik* 95.4 (2023), pp. 511–517. DOI: https://doi.org/10.1002/cite.202200165. eprint: https://onlinelibrary.wiley.com/doi/pdf/10.1002/cite.202200165. URL: https://onlinelibrary.wiley.com/doi/abs/10.1002/cite.202200165 (cit. on p. 10).

[65] K. Akita and F. Yoshida. "Bubble Size, Interfacial Area, and Liquid-Phase Mass Transfer Coefficient in Bubble Columns". In: *Industrial & Engineering Chemistry Process Design and Development* 13.1 (1974-01), pp. 84–91. ISSN: 0196-4305. DOI: 10.1021/i260049a016. URL: https://doi.org/10.1021/i260049a016 (cit. on pp. 10, 81).

[66] J. J. Chalmers. "Mixing, aeration and cell damage, 30+ years later: what we learned, how it affected the cell culture industry and what we would like to know more about". In: *Current Opinion in Chemical Engineering* 10 (2015). Biotechnology and bioprocess engineering - Process systems engineering, pp. 94–102. ISSN: 2211-3398. DOI: https://doi.org/10.1016/j.coche.2015.09.005. URL: https://www.sciencedirect.com/science/article/pii/S2211339815000611 (cit. on pp. 10, 13).

[67] N. Suwartha, D. Syamzida, C. R. Priadi, S. S. Moersidik, and F. Ali. "Effect of size variation on microbubble mass transfer coefficient in flotation and aeration processes". In: *Heliyon* 6.4 (2020), e03748. ISSN: 2405-8440. DOI: https://doi.org/10.1016/j.heliyon.2020.e03748. URL: https://www.sciencedirect.com/science/article/pii/S2405844020305934 (cit. on p. 10).

[68] H. Rehm and G. Reed. *Biotechnology: Bioprocessing*. Biotechnology: A Multi-volume Comprehensive Treatise. VCH, 1993. ISBN: 9783527283101. URL: https://books.google.cz/books?id=7VBRAAAAMAAJ (cit. on pp. 10, 11, 19).

[69] M. Wild, Y. Mast, and R. Takors. "Revisiting Basics of kLa Dependency on Aeration in Bubble Columns: a Is Surprisingly Stable". In: *Chemie Ingenieur Technik* 95.4 (2023), pp. 511–517. DOI: https://doi.org/10.1002/cite.202200165. URL: https://onlinelibrary.wiley.com/doi/abs/10.1002/cite.202200165 (cit. on pp. 10, 11).

[70] K. Stewart. "Buoyancy, laws of physics". In: *Encyclopedia Britannica* (2023). URL: https://www.britannica.com/science/buoyancy (cit. on p. 10).

[71] *Do small bubbles rise at a different speed than large bubbles?* URL: https://www.thenakedscientists.com/forum/index.php?topic=47524.0 (cit. on p. 10).

[72] P. Shukla. *Applied Microbiology and Bioengineering: An Interdisciplinary Approach*. Elsevier Science, 2018. ISBN: 9780128155486. URL: https://books.google.cz/books?id=FdZwDwAAQBAJ (cit. on p. 12).

[73] A. Shahar. "14 - Cultivation of Nerve and Muscle Cells on Microcarriers". In: *Cell Culture*. Ed. by P. M. Conn. Vol. 2. Methods in Neurosciences. Academic Press, 1990, pp. 195–209. DOI: https://doi.org/10.1016/B978-0-12-185254-2.50018-8. URL: https://www.sciencedirect.com/science/article/pii/B9780121852542500188 (cit. on p. 12).

[74] M. S. Croughan and D. I. Wang. "CHAPTER 9 - Hydrodynamic Effects on Animal Cells in Microcarrier Bioreactors". In: *Animal Cell Bioreactors*. Ed. by C. S. Ho and D. I. Wang. Boston: Butterworth-Heinemann, 1991, pp. 213–249. ISBN: 978-0-409-90123-8. DOI: https://doi.org/10.1016/B978-0-409-90123-8.50015-X. URL: https://www.sciencedirect.com/science/article/pii/B978040990123850015X (cit. on pp. 12, 14).

[75] J.-J. Chiu and S. Chien. "Effects of Disturbed Flow on Vascular Endothelium: Pathophysiological Basis and Clinical Perspectives". In: *Physiological Reviews* 91.1 (2011), pp. 327–387. DOI: 10.1152/physrev.00047.2009. URL: https://doi.org/10.1152/physrev.00047.2009 (cit. on p. 12).

[76] N. Katopodes. *Free-Surface Flow: Environmental Fluid Mechanics*. Elsevier Science, 2018. ISBN: 9780128162514. URL: https://books.google.cz/books?id=vYdqDwAAQBAJ (cit. on p. 13).

[77] W. K. George. "Lectures in Turbulence for the 21st Century". In: (2013). URL: https://doi.org/10.1152/physrev.00047.2009 (cit. on p. 13).

[78] E. T. Papoutsakis. "Fluid-mechanical damage of animal cells in bioreactors". In: *Trends in Biotechnology* 9.1 (1991), pp. 427–437. ISSN: 0167-7799. DOI: https://doi.org/10.1016/0167-7799(91)90145-8. URL: https://www.sciencedirect.com/science/article/pii/0167779991901458 (cit. on p. 13).

[79] M. Eckert. "The troublesome birth of hydrodynamic stability theory: Sommerfeld and the turbulence problem". In: *http://dx.doi.org/10.1140/epjh/e2010-00003-3* 35 (2010-07). DOI: 10.1140/epjh/e2010-00003-3 (cit. on p. 14).

[80] R. Sinnott, J. Coulson, and J. Richardson. *Chemical Engineering Design*. Chemical Engineering Design v. 6. Elsevier Butterworth-Heinemann, 2005. ISBN: 9780750665384. URL: https://books.google.cz/books?id=XLzOngEACAAJ (cit. on p. 14).

[81] R. Kuboi, I. Komasawa, and T. Otake. "Fluid and particle motion in turbulent dispersion-II: Influence of turbulence of liquid on the motion of suspended particles". In: *Chemical Engineering Science* 29.3 (1974), pp. 651–657. ISSN: 0009-2509. DOI: https://doi.org/10.1016/0009-2509(74)80179-X. URL: https://www.sciencedirect.com/science/article/pii/000925097480179X (cit. on p. 14).

[82] R. S. Cherry. "Animal cells in turbulent fluids: Details of the physical stimulus and the biological response". In: *Biotechnology Advances* 11.2 (1993), pp. 279–299. ISSN: 0734-9750. DOI: https://doi.org/10.1016/0734-9750(93)90043-M. URL: https://www.sciencedirect.com/science/article/pii/073497509390043M (cit. on p. 14).

[83] *Selecting an impeller for overhead stirring*. 2023-09. URL: https://www.asynt.com/customise-your-lab/little-large/selecting-an-impeller-for-overhead-stirring/ (cit. on p. 14).

[84] *Selecting an Impeller for Your Overhead Stirrer*. 2023-09. URL: https://stirrers.net/blogs/blog/selecting-an-impeller-for-your-overhead-stirrer (cit. on p. 15).

[85] R. Brodkey and A. I. of Chemical Engineers. *Turbulence in Mixing Operations: Theory and Application to Mixing and Reaction*. Academic Press rapid manuscript reproductions. Academic Press, 1975. ISBN: 9780121344504. URL: https://books.google.cz/books?id=JAiIAAAAIAAJ (cit. on pp. 15, 16).

[86] *The Impeller: Why It Could Be Called The Heart Of The Bioreactor*. 2023-09. URL: https://www.infors-ht.com/en/blog/the-impeller-why-you-can-call-it-the-heart-of-the-bioreactor/ (cit. on p. 16).

[87] A. Nienow. "Hydrodynamics of Stirred Bioreactors". In: *Applied Mechanics Reviews - APPL MECH REV* 51 (1998-01). DOI: 10.1115/1.3098990 (cit. on pp. 16, 17).

[88] S. Jesus, J. Neto, A. Santana, and R. Filho. "Influence of Impeller Type in Hydrodynamics and Gas-Liquid Mass Transfer Characteristics in Stirred Airlift Bioreactor". In: *AIChE Journal* 61 (2015-05), n/a–n/a. DOI: 10.1002/aic.14871 (cit. on p. 17).

[89] R. Petříček, T. Moucha, F. Rejl, L. Valenz, and J. Haidl. "Prediction of power consumption in mechanically agitated gassed reactor in viscous batch". In: *Chemical Engineering & Technology* 41 (2018-02). DOI: 10.1002/ceat.201700149 (cit. on p. 17).

[90] R. Petříček, T. Moucha, J. F. Rejl, L. Valenz, J. Haidl, and T. Čmelíková. "Gas-liquid-solid volumetric mass transfer coefficient and impeller power consumptions for industrial vessel design". In: *International Journal of Heat and Mass Transfer* 121 (2018), pp. 653–662. ISSN: 0017-9310. DOI: https://doi.org/10.1016/j.ijheatmasstransfer.2018.01.041. URL: https://www.sciencedirect.com/science/article/pii/S0017931017353395 (cit. on p. 17).

[91] H. Jin, D. Liu, S. Yang, G. He, Z. Guo, and Z. Tong. "Experimental Study of Oxygen Mass Transfer Coefficient in Bubble Column with High Temperature and High Pressure". In: *Chemical Engineering & Technology* 27.12 (2004), pp. 1267–1272. DOI: https://doi.org/10.1002/ceat.200402111. URL: https://onlinelibrary.wiley.com/doi/abs/10.1002/ceat.200402111 (cit. on p. 18).

[92] A. Ferreira, C Ferreira, J. Teixeira, and F. Rocha. "Temperature and solid properties effects on gas-liquid mass transfer". In: *Chemical Engineering Journal* 162 (2010-08), pp. 743–752. DOI: 10.1016/j.cej.2010.05.064 (cit. on p. 18).

[93] J. I. Betts and F. Baganz. "Miniature bioreactors: current practices and future opportunities". In: *Microbial Cell Factories* 5.1 (2006-05), p. 21. ISSN: 1475-2859. DOI: 10.1186/1475-2859-5-21. URL: https://doi.org/10.1186/1475-2859-5-21 (cit. on p. 18).

[94] H. Kojima, J. Sawai, and H. Suzuki. "Effect of pressure on volumetric mass transfer coefficient and gas holdup in bubble column". In: *Chemical Engineering Science* 52.21 (1997), pp. 4111–4116. ISSN: 0009-2509. DOI: https://doi.org/10.1016/S0009-2509(97)00253-4. URL: https://www.sciencedirect.com/science/article/pii/S0009250997002534 (cit. on p. 18).

[95] E. Cussler. *Diffusion: Mass Transfer in Fluid Systems*. Cambridge Series in Chemical Engineering. Cambridge University Press, 2009. ISBN: 9780521871211. URL: https://books.google.cz/books?id=dq6LdJyN8ScC (cit. on p. 18).

[96] R. Bird, W. Stewart, and E. Lightfoot. *Transport Phenomena*. Transport Phenomena v. 1. Wiley, 2006. ISBN: 9780470115398. URL: https://books.google.cz/books?id=L5FnNlIaGfcC (cit. on p. 18).

[97] R. E. Treybal. *Mass-transfer Operations*. Chemical engineering series. McGraw-Hill, 1980. ISBN: 9780070651760. URL: https://books.google.cz/books?id=HLZTAAAAMAAJ (cit. on p. 18).

[98] *Aeration principles*. 2023-09. URL: https://cercell.com/bioreactor-support/cellvessel-details/aeration-principle/ (cit. on p. 19).

[99] L. Velez, R. Tarrant, A. Tait, D. Spencer, and D. Bracewell. "Impact of aeration strategy on CHO Cell performance during antibody production". In: *Biotechnology progress* 29 (2013-02). DOI: 10.1002/btpr.1647 (cit. on p. 19).

[100] H. Brod, J. Kauling, B. Frahm, and R. Rose. "Method and Apparatus for the Gassing and Degassing of Liquids, Particularly in Biotechnology, and Specifically of Cell Cultures". In: (1998) (cit. on p. 19).

[101] 2023-09. URL: http://www.zena-membranes.cz/index.php/products/immersed/module-custom (cit. on p. 19).

[102] *Aeration in Cell Culture Bioreactors with Bubble-Free Sparging: Bioreactor CO2 & O2 Control*. 2021-11. URL: https://www.permselect.com/markets/bioreactor (cit. on p. 19).

[103] *Bubble-Free Sparging & Aeration Control in Bioreactors: Gentle Agitation, Effective Gassing & CO2 Stripping*. 2021-11. URL: https://www.permselect.com/markets/bioreactor%20gas%20control (cit. on p. 19).

[104] *Tank Aeration*. 2023-08. URL: https://www.transvac.co.uk/tank-aeration/ (cit. on p. 19).

[105] *A look at unit processes in RAS systems - Responsible Seafood Advocate*. 2023-09. URL: https://www.globalseafood.org/advocate/look-at-unit-processes-in-ras-systems/ (cit. on p. 19).

[106] L.-K. Ju and W. B. Armiger. "Enhancing Oxygen Transfer in Surface-Aerated Bioreactors by Stable Foams". In: *Biotechnology Progress* 6.4 (1990), pp. 262–265. DOI: https://doi.org/10.1021/bp00004a005. URL: https://aiche.onlinelibrary.wiley.com/doi/abs/10.1021/bp00004a005 (cit. on p. 20).

[107] H. Chanson. "Chapter 1 - Introduction". In: *Air Bubble Entrainment in Free-Surface Turbulent Shear Flows*. Ed. by H. Chanson. San Diego: Academic Press, 1996, pp. 2–16. ISBN: 978-0-12-168110-4. DOI: https://doi.org/10.1016/B978-012168110-4/50005-9. URL: https://www.sciencedirect.com/science/article/pii/B9780121681104500059 (cit. on p. 20).

[108] M. J. Semmens. "Alternative MBR configurations: using membranes for gas transfer". In: *Desalination* 231 (2008-10), pp. 236–242. DOI: 10.1016/j.desal.2007.12.011 (cit. on p. 20).

[109] D. Lu, H. Bai, F. Kong, S. Liss, and B. Liao. "Recent advances in membrane aerated biofilm reactors". In: *Critical Reviews in Environmental Science and Technology* 51 (2020-03), pp. 1–55. DOI: 10.1080/10643389.2020.1734432 (cit. on p. 20).

[110] J. Wang, X. Ying, Y. Huang, Y. Chen, D. Shen, X. Zhang, and H. J. Feng. "Numerical study of hydrodynamic characteristics in a moving bed biofilm reactor". In: *Environmental Research* 194 (2021), p. 110614. ISSN: 0013-9351. DOI: https://doi.org/10.1016/j.envres.2020.110614. URL: https://www.sciencedirect.com/science/article/pii/S0013935120315115 (cit. on p. 20).

[111] P. Bongartz, I. Bator, K. Baitalow, R. Keller, T. Tiso, L. M. Blank, and M. Wessling. "A scalable bubble-free membrane aerator for biosurfactant production". In: *Biotechnology and Bioengineering* 118.9 (2021), pp. 3545–3558. DOI: https://doi.org/10.1002/bit.27822. URL: https://onlinelibrary.wiley.com/doi/abs/10.1002/bit.27822 (cit. on p. 20).

[112] *How MABR Modules Work*. 2023-09. URL: https://www.oxymem.com/how-mabr-modules-work (cit. on p. 20).

[113] C. Dupont. "OxyMem – The MABR Solution for Treating Municipal and Industrial Wastewater". 2021 (cit. on p. 20).

[114] *MABRs explained*. 2023-09. URL: https://www.thembrsite.com/mabrs/mabrs-what-is/ (cit. on p. 20).

[115] P. Bongartz, I. Bator, K. Baitalow, R. Keller, T. Tiso, L. M. Blank, and M. Wessling. "A scalable bubble-free membrane aerator for biosurfactant production". In: *Biotechnology and Bioengineering* 118.9 (2021), pp. 3545–3558. DOI: https://doi.org/10.1002/bit.27822. URL: https://onlinelibrary.wiley.com/doi/abs/10.1002/bit.27822 (cit. on p. 20).

[116] *Submerged MBR*. 2023-09. URL: https://www.lenntech.com/processes/submerged-mbr.htm (cit. on p. 21).

[117] Z. Wang, H. Guo, T. Zhou, Z. Cheng, and Z. Huang. "Influence of Sparger Type on Mass Transfer in a Pilot-Scale Internal Loop Airlift Reactor". In: *Processes* 10.2 (2022). ISSN: 2227-9717. DOI: 10.3390/pr10020429. URL: https://www.mdpi.com/2227-9717/10/2/429 (cit. on p. 21).

[118] C. Mott. "Sparging Gas-Liquid Contacting Design Guide & Part Selection". 2021 (cit. on p. 21).

[119] A. V. Kulkarni and J. B. Joshi. "Design and selection of sparger for bubble column reactor. Part I: Performance of different spargers". In: *Chemical Engineering Research and Design* 89.10 (2011), pp. 1972–1985. ISSN: 0263-8762. DOI: https://doi.org/10.1016/j.cherd.2011.01.004. URL: https://www.sciencedirect.com/science/article/pii/S0263876211000128 (cit. on p. 21).

[120] O. Basha, L. Sehabiague, A. Abdel-Wahab, and B. Morsi. "Fischer–Tropsch Synthesis in Slurry Bubble Column Reactors: Experimental Investigations and Modeling – A Review". In: *International Journal of Chemical Reactor Engineering* 0 (2015-01). DOI: 10.1515/ijcre-2014-0146 (cit. on p. 21).

[121] C. Mott. "Mott Porous Metal Micro Sparger Tips for Bench-Top Laboratory Bioreactors and Fermentors". 2019 (cit. on p. 21).

[122] *Regulating O2 & CO2 with Bioreactor Sparging*. 2023-09. URL: https://www.alicat.com/knowledge-base/scaling-challenges-of-bioreactor-sparging/ (cit. on p. 21).

[123] N. Naidoo, W. Pauck, and M. Carsky. "Effects of sparger design on the gas holdup and mass transfer in a pilot scale external loop airlift reactor". In: *South African Journal of Chemical Engineering* 37 (2021), pp. 127–134. ISSN: 1026-9185. DOI: https://doi.org/10.1016/j.sajce.2021.05.009. URL: https://www.sciencedirect.com/science/article/pii/S1026918521000317 (cit. on p. 21).

[124] *Designing Spargers | Maximize Sparger Efficiency*. 2023-08. URL: https://mottcorp.com/5-steps-to-designing-a-sparger/ (cit. on p. 22).

[125] A. V. Kulkarni, S. V. Badgandi, and J. B. Joshi. "Design of ring and spider type spargers for bubble column reactor: Experimental measurements and CFD simulation of flow and weeping". In: *Chemical Engineering Research and Design* 87.12 (2009), pp. 1612–1630. ISSN: 0263-8762. DOI: https://doi.org/10.1016/j.cherd.2009.06.003. URL: https://www.sciencedirect.com/science/article/pii/S026387620900135X (cit. on p. 22).

[126] *A Simpler Way to Reduce Foam from Industrial Chemical Production*. 2023-09. URL: https://blog.agchemigroup.eu/a-simpler-way-to-control-and-reduce-foams-and-bubbles-in-industrial-chemical-production/ (cit. on p. 22).

[127] A. Prins and K. van't Riet. "Proteins and surface effects in fermentation: foam, antifoam and mass transfer". In: *Trends in Biotechnology* 5.11 (1987), pp. 296–301. ISSN: 0167-7799. DOI: https://doi.org/10.1016/0167-7799(87)90080-1. URL: https://www.sciencedirect.com/science/article/pii/0167779987900801 (cit. on p. 22).

[128] *What Causes Foaming In Fermentation?* 2023-09. URL: https://www.wine-is.com/what-causes-foaming-in-fermentation/ (cit. on p. 22).

[129] H. Leuner, C. Gerstenberg, K. Lechner, C. McHardy, C. Rauh, and J.-U. Repke. "Overcoming unwanted foam in industrial processes of the chemical and food industry – an ongoing survey". In: *Chemical Engineering Research and Design* 163 (2020), pp. 281–294. ISSN: 0263-8762. DOI: https://doi.org/10.1016/j.cherd.2020.09.006. URL: https://www.sciencedirect.com/science/article/pii/S0263876220304688 (cit. on p. 22).

[130] v.-s. Fazilet. "Foaming and its Control in Bioprocesses". In: 1992-01, pp. 113–146. ISBN: 978-94-010-5089-0. DOI: 10.1007/978-94-011-2468-3_6 (cit. on p. 22).

[131] *Mechanical Defoamer SEMD110, Great Foam Breaker*. 2023-09. URL: https://www.sefluid.com/products/mechanical-defoamer-foam-breaker-machine/ (cit. on p. 23).

[132] L. Rapoport, T. Emmerich, and K. K. Varanasi. "Capturing Bubbles and Preventing Foam Using Aerophilic Surfaces". In: *Advanced Materials Interfaces* 7.6 (2020), p. 1901599. DOI: https://doi.org/10.1002/admi.201901599. URL: https://onlinelibrary.wiley.com/doi/abs/10.1002/admi.201901599 (cit. on p. 23).

[133] R. Mawson, J. Tongaonkar, S. Bhagwat, and A. Pandit. "13 - Airborne Ultrasound for Enhanced Defoaming Applications". In: *Innovative Food Processing Technologies*. Ed. by K. Knoerzer, P. Juliano, and G. Smithers. Woodhead Publishing Series in Food Science, Technology and Nutrition. Woodhead Publishing, 2016, pp. 347–359. ISBN: 978-0-08-100294-0. DOI: https://doi.org/10.1016/B978-0-08-100294-0.00013-4. URL: https://www.sciencedirect.com/science/article/pii/B9780081002940000134 (cit. on p. 23).

[134] A. Sulaiman and F. V. M. Silva. "Chapter Thirteen - Principles of sonication and its equipment in the food industry". In: *Non-thermal Food Processing Operations*. Ed. by S. M. Jafari and N. Therdthai. A volume in Unit Operations and Processing Equipment in the Food Industry. Woodhead Publishing, 2023, pp. 435–464. ISBN: 978-0-12-818717-3. DOI: https://doi.org/10.1016/B978-0-12-818717-3.00001-9. URL: https://www.sciencedirect.com/science/article/pii/B9780128187173000019 (cit. on p. 23).

[135] *Ultrasonic defoaming. Foam control*. 2023-09. URL: https://www.ultratecno.eu/technology/technology-high-power-ultrasound-hpu/ultrasonic-defoaming/ (cit. on p. 23).

[136] S. Khan, I. Ullah, Q. Wang, H. Xu, T. Tiso, L. Blank, and L. Liu. "Thermal and ultrasound foam control in biotechnology: a mini-review". In: *Discover Chemical Engineering* 2 (2022-12). DOI: 10.1007/s43938-022-00016-z (cit. on p. 23).

[137] M. Redouane, E. Abderrahmane, M. Salah, M. Monkade, E. B. Abdeslam, and A. Ghidan. "EFFECT OF ELECTROMAGNETIC FIELDS ON THE pH OF WATER UNDER KINETIC CONDITIONS". In: *Fresenius Environmental Bulletin* 29 (2020-07), pp. 7922–7933 (cit. on p. 23).

[138] C. J. Hartline, A. C. Schmitz, Y. Han, and F. Zhang. "Dynamic control in metabolic engineering: Theories, tools, and applications". In: *Metabolic Engineering* 63 (2021). Tools and Strategies of Metabolic Engineering, pp. 126–140. ISSN: 1096-7176. DOI: https://doi.org/10.1016/j.ymben.2020.08.015. URL: https://www.sciencedirect.com/science/article/pii/S1096717620301440 (cit. on p. 23).

[139] G. Stephanopoulos, A. Aristidou, and J. Nielsen. *Metabolic Engineering: Principles and Methodologies*. Elsevier Science, 1998. ISBN: 9780080536286. URL: https://books.google.cz/books?id=9mGzkso4NVQC (cit. on p. 23).

[140] *Metabolic Pathway - an overview | ScienceDirect Topics*. URL: https://www.sciencedirect.com/topics/biochemistry-genetics-and-molecular-biology/metabolic-pathway (cit. on p. 23).

[141] *Glycolysis 10 Steps with Diagram and ATP Formation*. 2023-09. URL: https://microbenotes.com/glycolysis-10-steps/ (cit. on p. 24).

[142] *Metabolic Network - an overview | ScienceDirect Topics*. 2023-09. URL: https://www.sciencedirect.com/topics/agricultural-and-biological-sciences/metabolic-network (cit. on pp. 24, 25).

[143] *EcoCyc: Encyclopedia of E. coli Genes and Metabolism*. 2023-09. URL: https://ecocyc.org/ (cit. on p. 24).

[144] P. Romero and P. Karp. "PseudoCyc, A Pathway-Genome Database for Pseudomonas aeruginosa". In: *Journal of Molecular Microbiology and Biotechnology* 5.4 (2003-07), pp. 230–239. ISSN: 1464-1801. DOI: 10.1159/000071075. URL: https://doi.org/10.1159/000071075 (cit. on p. 24).

[145] *KEGG: Kyoto Encyclopedia of Genes and Genomes*. 2023-09. URL: https://www.genome.jp/kegg/ (cit. on p. 24).

[146] URL: http://bigg.ucsd.edu/ (cit. on p. 24).

[147] W. Dubitzky, O. Wolkenhauer, H. Yokota, and K.-H. Cho. *Encyclopedia of Systems Biology*. 2013-01, pp. 2367–1154. ISBN: 9781441998644. DOI: 10.1007/978-1-4419-9863-7_708 (cit. on p. 26).

[148] S. Lee, J. Nielsen, and G. Stephanopoulos. *Metabolic Engineering: Concepts and Applications*. Advanced Biotechnology. Wiley, 2021. ISBN: 9783527823451. URL: https://books.google.cz/books?id=FoMxEAAAQBAJ (cit. on p. 26).

[149] K. Raman and N. Chandra. "Flux balance analysis of biological systems: applications and challenges". In: *Briefings in Bioinformatics* 10.4 (2009-03), pp. 435–449. DOI: 10.1093/bib/bbp011. eprint: https://academic.oup.com/bib/article-pdf/10/4/435/841894/bbp011.pdf. URL: https://doi.org/10.1093/bib/bbp011 (cit. on p. 26).

[150] O. Resendis-Antonio, C. González-Torres, G. Jaime-Muñoz, C. E. Hernandez-Patiño, and C. F. Salgado-Muñoz. "Modeling metabolism: A window toward a comprehensive interpretation of networks in cancer". In: *Seminars in Cancer Biology* 30 (2015). Cancer modeling and network biology, pp. 79–87. ISSN: 1044-579X. DOI: https://doi.org/10.1016/j.semcancer.2014.04.003. URL: https://www.sciencedirect.com/science/article/pii/S1044579X14000510 (cit. on p. 26).

[151] B. Palsson. "Systems Biology: Simulation of Dynamic Network States". In: *Systems Biology: Simulation of Dynamic Network States* (2011-01). DOI: 10.1017/CBO9780511736179 (cit. on p. 27).

[152] J. D. Orth, I. Thiele, and B. Ø. Palsson. "What is flux balance analysis?" In: *Nature Biotechnology* 28.3 (2010-03), pp. 245–248 (cit. on p. 27).

[153] *Microcon*. URL: http://www.microcon.cz/ (cit. on p. 30).

[154] *PID regulátor Ascon Tecnologic KR1 HCOR-D se třemi výstupy*. 2023-09. URL: https://www.logitron.cz/pid-regulator-ascon-tecnologic-kr1-hcor-d-se-tremi-vystupy-p5240/ (cit. on p. 30).

[155] *FUNDAMIX® Vibromixer – DrM, Dr. Mueller AG*. URL: https://drm-filters.com/portfolio-item/fundamix-vibromixer (cit. on p. 31).

[156] *17HS3401 Datasheet | MotionKing - Datasheetspdf.com*. 2023-09. URL: https://datasheetspdf.com/datasheet/17HS3401.html (cit. on p. 33).

[157] C. Myers. "Screw Propeller Patent". In: (1892). URL: https://patentimages.storage.googleapis.com/5d/b2/5e/f983b16c98b284/US467322.pdf (cit. on p. 34).

[158] T. Sebastian and C. Strem. "Toroidal propeller patent". In: (2018). URL: https://patents.google.com/patent/US10836466B2/en?q=(Toroidal+Propeller)\&oq=Toroidal+Propeller (cit. on p. 34).

[159] *Biostat® B - Controlador de biorreator de bancada*. 2023-09. URL: https://www.sartorius.com/en/products-pt/fermentation-bioreactors-pt/benchtop-bioreactors-pt/biostat-b-pt (cit. on p. 35).

[160] *CORIO CD-200F Refrigerated / heating circulator JULABO GmbH*. 2023-09. URL: https://www.julabo.com/en/products/refrigerated-circulators/refrigerated-heating-circulators/corio-cd-200f (cit. on p. 35).

[161] 2023-09. URL: https://www.theta90.cz/ (cit. on p. 35).

[162] *Product: OXY-1 SMA*. 2023-08. URL: https://www.presens.de/products/detail/oxy-1-sma (cit. on p. 35).

[163] *Product: Oxygen Sensor Spot SP-PSt3-NAU - contactless O2 measurements*. 2023-07. URL: https://www.presens.de/products/detail/oxygen-sensor-spot-sp-pst3-nau (cit. on p. 35).

[164] *EHEIM air200*. URL: https://eheim.com/en_GB/aquatics/technology/air-pumps/air/air200 (cit. on p. 35).

[165] *Digital Peristaltic Pump*. URL: https://datasheets.globalspec.com/ds/thermo-fisher-scientific/go-78001-78/95d954d8-0dae-46b2-9d0c-fe74f7177131 (cit. on p. 35).

[166] *Kamoer Peristaltic pumps & Diaphragm pumps*. URL: https://www.google.com/search?q=kamoer&rlz=1C1GCEA_enPT965PT965&oq=kamo&aqs=chrome.0.69i59j69i57j69i64j35i39j46i199i465i512j69i60l3.683j0j7&sourceid=chrome&ie=UTF-8 (cit. on p. 35).

[167] *Porous Sparger and Gas Sparger Manufacturer | HENGKO*. 2023-09. URL: https://www.hengko.com/sintered-porous-spargers/ (cit. on p. 36).

[168] 2023-07. URL: https://bodybybtl.com/ (cit. on p. 36).

[169] *HyClone Dulbecco's Modified Eagle Medium (DMEM)/ F12 1:1: Liquid*. 2023-09. URL: https://www.cytivalifesciences.com/en/us/shop/cell-culture-and-fermentation/media-and-feeds/classical-media/hyclone-dulbecco's-modified-eagle-medium-dmem-f12-1-1-liquid-p-06358 (cit. on p. 36).

[170] *Phenol Red Merck*. URL: https://www.sigmaaldrich.com/CZ/en/product/sial/p0290?cm_sp=Insite-_-caSrpResults_srpRecs_srpModel_phenol%20red-_-srpRecs3-2 (cit. on p. 36).

[171] *Merk - Sigma Aldrich - PEG*. URL: https://www.sigmaaldrich.com/CZ/en/product/sigma/81255?context=product (cit. on p. 36).

[172] *Merck - Sigma Aldrich - CMC*. URL: https://www.sigmaaldrich.com/CZ/en/product/aldrich/419281 (cit. on p. 36).

[173] *ThermoFisher PenStrep*. URL: https://www.thermofisher.com/order/catalog/product/15140122#/15140122 (cit. on p. 36).

[174] J. Vanags and A. Suleiko. "What is kLa in bioreactors?" In: (2020) (cit. on p. 37).

[175] A. Karimi, F. Golbabaei, M. MEHRNIA, M. Neghab, K. Mohammad, A. Nikpey, and M. Pourmand. "Oxygen Mass Transfer in a Sstirred Tank Bioreactor Using Different impeller Configurations for Environmental Purposes". In: *Iranian journal of environmental health science & engineering* 10 (2013-01), p. 6. DOI: 10.1186/1735-2746-10-6 (cit. on p. 39).

[176] P. Stanbury, A. Whitaker, and S. Hall. *Principles of Fermentation Technology*. Elsevier Science, 2013. ISBN: 9781483292915. URL: https://books.google.cz/books?id=CW8vBQAAQBAJ (cit. on p. 39).

[177] *Power Number calculator*. 2023-06. URL: https://cercell.com/bioreactor-support/power-number-details/power-number-calculator/ (cit. on p. 40).

[178] S. C. Sorenson. *Power Number*. URL: https://cercell.com/media/13383/power-number-from-spencer.pdf (cit. on p. 40).

[179] P. Baboo. *Power number calculation*. 2022-01 (cit. on p. 40).

[180] H. Zhang. "The Permeability Characteristics of Silicone Rubber". In: *SAMPE Fall Technical Conference* (2006-01) (cit. on p. 42).

[181] *The importance of baffles in a reactor vessels*. 2023-09. URL: https://www.spinchem.com/application/the-importance-of-baffles-in-a-reactor-vessels/ (cit. on p. 43).

[182] S.-P. Wang, Q. Wang, A.-M. Zhang, and E. Stride. "Experimental observations of the behaviour of a bubble inside a circular rigid tube". In: *International Journal of Multiphase Flow* 121 (2019), p. 103096. ISSN: 0301-9322. DOI: https://doi.org/10.1016/j.ijmultiphaseflow.2019.103096. URL: https://www.sciencedirect.com/science/article/pii/S0301932218305135 (cit. on p. 43).

[183] H.-S. Pei, C.-L. Guo, G.-F. Zhang, Q.-Y. Tang, and F.-Q. Guo. "Dynamic behavior of bubble forming at capillary orifice in methane oxidizing bacteria suspension". In: *International Journal of Heat and Mass Transfer* 110 (2017), pp. 873–879. ISSN: 0017-9310. DOI: https://doi.org/10.1016/j.ijheatmasstransfer.2017.03.094. URL: https://www.sciencedirect.com/science/article/pii/S0017931016321809 (cit. on p. 43).

[184] M. Islam. "A SINGLE AIR BUBBLE RISE IN WATER: A CFD STUDY". In: (2015-03) (cit. on p. 43).

[185] R. L. Davidson, K. A. O'Malley, and T. B. Wheeler. "Polyethylene glycol-induced mammalian cell hybridization: Effect of polyethylene glycol molecular weight and concentration". In: *Somatic Cell Genetics* 2.3 (1976-05), pp. 271–280. DOI: 10.1007/BF01538965. URL: https://doi.org/10.1007/BF01538965 (cit. on p. 44).

[186] *Carboxymethyl Cellulose - an overview | ScienceDirect Topics*. 2023-06. URL: https://www.sciencedirect.com/topics/medicine-and-dentistry/carboxymethyl-cellulose (cit. on p. 44).

[187] *Reynolds Shear Stress - an overview | ScienceDirect Topics*. 2023-04. URL: https://www.sciencedirect.com/topics/engineering/reynolds-shear-stress (cit. on p. 45).

[188] J. Robitaille, J. Chen, and M. Jolicoeur. "A Single Dynamic Metabolic Model Can Describe mAb Producing CHO Cell Batch and Fed-Batch Cultures on Different Culture Media". In: *PLOS ONE* 10 (2015-09). DOI: 10.1371/journal.pone.0136815. URL: https://doi.org/10.1371/journal.pone.0136815 (cit. on pp. 47, 48).

[189] *Nexera series*. 2023-09. URL: https://www.shimadzu.com/an/products/liquid-chromatography/hplcuhplc/nexera-series/index.html (cit. on p. 49).

[190] *Flow Cytometer - BriCyte E6*. 2023-09. URL: https://www.mindray.com/en/products/laboratory-diagnostics/flow-cytometry/bricyte-e6 (cit. on p. 49).

[191] *Merck - SigmaAldrich - Propidium Iodide*. URL: https://www.sigmaaldrich.com/CZ/en/product/sigma/p4170?cm_sp=Insite-_-caSrpResults_srpRecs_srpModel_propidium%20iode-_-srpRecs3-1 (cit. on p. 49).

[192] K. M. McKinnon. "Flow Cytometry: An Overview". In: *Current Protocols in Immunology* 120.1 (2018), pp. 5.1.1–5.1.11. DOI: https://doi.org/10.1002/cpim.40. URL: https://currentprotocols.onlinelibrary.wiley.com/doi/abs/10.1002/cpim.40 (cit. on p. 49).

[193] *ThermoFisher - GIBCO - Trypsin-EDTA*. URL: https://www.thermofisher.com/order/catalog/product/25200072?SID=srch-srp-25200072#/25200072?SID=srch-srp-25200072 (cit. on p. 50).

[194] A. Karimi, F. Golbabaei, M. MEHRNIA, M. Neghab, K. Mohammad, A. Nikpey, and M. Pourmand. "Oxygen Mass Transfer in a Sstirred Tank Bioreactor Using Different impeller Configurations for Environmental Purposes". In: *Iranian journal of environmental health science & engineering* 10 (2013-01), p. 6. DOI: 10.1186/1735-2746-10-6 (cit. on p. 55).

[195] W. Klöckner, R. Gacem, T. Anderlei, N. Raven, S. Schillberg, C. Lattermann, and J. Büchs. "Correlation between mass transfer coefficient kLa and relevant operating parameters in cylindrical disposable shaken bioreactors on a bench-to-pilot scale". In: *Journal of Biological Engineering* 7.1 (2013-12). ISSN: 1754-1611. DOI: 10.1186/1754-1611-7-28. URL: https://doi.org/10.1186/1754-1611-7-28 (cit. on p. 55).

[196] W.-S. Shin, D. Lee, S. Kim, Y.-S. Jeong, and G.-T. Chun. "Application of Scale-Up Criterion of Constant Oxygen Mass Transfer Coefficient (k(L)a) for Production of Itaconic Acid in a 50 L Pilot-Scale Fermentor by Fungal Cells of Aspergillus terreus". In: *Journal of microbiology and biotechnology* 23 (2013-08). DOI: 10.4014/jmb.1307.07084 (cit. on p. 55).

[197] S. Sundaramurthy, V. Srivastava, and I. Mishra. "Oxygen Mass Transfer in Bioreactors". In: vol. 2. 2011-08, pp. 947–956. ISBN: 978-0-08-088504-9. DOI: 10.1016/B978-0-08-088504-9.00409-8 (cit. on p. 55).

[198] *Axial Flow - an overview | ScienceDirect Topics*. 2023-09. URL: https://www.sciencedirect.com/topics/chemical-engineering/axial-flow (cit. on p. 62).

[199] M. C. Keller, J. Witzel, B. Tscheschke, M. Jurgait, M. Baas, M. Poggel, and M. Gottfried. "CFD-Aided and Experimental Characterization of Bioreactors under Low Power Input Conditions". In: *Chemie Ingenieur Technik* 94.12 (2022), pp. 2012–2017. DOI: https://doi.org/10.1002/cite.202200143. URL: https://onlinelibrary.wiley.com/doi/abs/10.1002/cite.202200143 (cit. on p. 63).

[200] *Rushton Turbine – 6 Blade (RT6)*. 2023-09. URL: https://fusionfluid.com/products/mixing-impellers/rushton-turbine-6-blade-rt6#:~:text=POWER%20NUMBER%20(NP)%20%3D%205.75 (cit. on p. 63).

[201] A. Abbaszadeh Mayvan, B. Ghobadian, and G. Najafi. "Analytical and FEM Design of Mixing System in STR Biodiesel Production". In: *Advances in Environmental Biology* 8 (2014-01), pp. 325–334 (cit. on p. 63).

[202] R. Wójtowicz. "Flow pattern and power consumption in a vibromixer". In: *Chemical Engineering Science* 172 (2017), pp. 622–635. ISSN: 0009-2509. DOI: https://doi.org/10.1016/j.ces.2017.07.010. URL: https://www.sciencedirect.com/science/article/pii/S0009250917304505 (cit. on p. 65).

[203] *FUNDAMIX® Vibromixer*. 2023-09. URL: https://drm-lifescience.com/fundamix-vibromixer/ (cit. on p. 65).

[204] *Bernoulli Effect - an overview | ScienceDirect Topics*. 2023-09. URL: https://www.sciencedirect.com/topics/engineering/bernoulli-effect (cit. on p. 65).

[205] A. Prikhodko and A. Smelyagin. "Development and research of vibromixing reactor with rotationally reciprocating motion of impeller". In: *Vibroengineering PROCEDIA* 8 (2016-10), pp. 102–107. ISSN: 2345-0533. URL: https://www.extrica.com/article/17635 (cit. on p. 65).

[206] I. de Arcos González-Turmo. "FUNDAMIX® Vibromixer Characterization". PhD thesis. 2014-07 (cit. on p. 66).

[207] S. Xueming, L. Xiaoling, and L. Yulin. "Experimental Study of Influence of the Impeller Spacing on Flow Behaviour of Double-Impeller Stirred Tank". In: *Canadian Journal of Chemical Engineering - CAN J CHEM ENG* 81 (2008-12), pp. 1239–1245. DOI: 10.1002/cjce.5450810613 (cit. on p. 68).

[208] J. Fitschen, M. Maly, A. Rosseburg, J. Wutz, T. Wucherpfennig, and M. Schlüter. "Influence of Spacing of Multiple Impellers on Power Input in an Industrial-Scale Aerated Stirred Tank Reactor". In: *Chemie Ingenieur Technik* 91.12 (2019), pp. 1794–1801. DOI: https://doi.org/10.1002/cite.201900121. URL: https://onlinelibrary.wiley.com/doi/abs/10.1002/cite.201900121 (cit. on p. 69).

[209] Z. Lu, C. Li, L. Fei, H. Zhang, and Y. Pan. "Effect of baffle structure on flow field characteristics of orbitally shaken bioreactor". In: *Bioprocess and Biosystems Engineering* 44.3 (2021-03), pp. 563–573. DOI: 10.1007/s00449-020-02469-4. URL: https://doi.org/10.1007/s00449-020-02469-4 (cit. on p. 78).

[210] Z. Chen, X. Zhang, and B. Su. "Influence of arc baffle configuration on gas–liquid mass transfer in flat-plate bubble column". In: *Chemical Engineering Research and Design* 165 (2021-01), pp. 129–136. DOI: 10.1016/j.cherd.2020.10.024 (cit. on p. 79).

[211] A. Sharma. "Effect of Different Impellers and Baffles on Aerobic Stirred Tank Fermenter using Computational Fluid Dynamics". In: *Journal of Bioprocessing & Biotechniques* 04 (2014-01). DOI: 10.4172/2155-9821.1000184 (cit. on p. 79).

[212] K. Phuakpunk, B. Chalermsinsuwan, and S. Assabumrungrat. "Reduction of bubble coalescence by louver baffles in fluidized bed gasifier". In: *Energy Reports* 8 (2022-11), pp. 96–106. DOI: 10.1016/j.egyr.2022.06.098 (cit. on p. 79).

[213] A. A. T. Alkhalidi and R. S. Amano. "Factors affecting fine bubble creation and bubble size for activated sludge". In: *Water and Environment Journal* 29.1 (2015), pp. 105–113. DOI: https://doi.org/10.1111/wej.12083. URL: https://onlinelibrary.wiley.com/doi/abs/10.1111/wej.12083 (cit. on p. 79).

[214] M. Wild, Y. Mast, and R. Takors. "Revisiting Basics of kLa Dependency on Aeration in Bubble Columns: a Is Surprisingly Stable". In: *Chemie Ingenieur Technik* 95.4 (2023), pp. 511–517. DOI: https://doi.org/10.1002/cite.202200165. URL: https://onlinelibrary.wiley.com/doi/abs/10.1002/cite.202200165 (cit. on p. 81).

[215] V. Cappello, C. Plais, C. Vial, and F. Augier. "Bubble size and liquid-side mass transfer coefficient measurements in aerated stirred tank reactors with non-Newtonian liquids". In: *Chemical Engineering Science* 211 (2020), p. 115280. ISSN: 0009-2509. DOI: https://doi.org/10.1016/j.ces.2019.115280. URL: https://www.sciencedirect.com/science/article/pii/S0009250919307705 (cit. on p. 81).

[216] A. Song, S. Zhao, Y. Cao, and C. Li. "Effect of Sparger Characteristics on Bubble-Formation Dynamics under Oscillatory Air Pattern". In: *Processes* 10.5 (2022). ISSN: 2227-9717. DOI: 10.3390/pr10050997. URL: https://www.mdpi.com/2227-9717/10/5/997 (cit. on p. 82).

[217] J. Vogelaar, A. Klapwijk, J. van Lier, and W. Rulkens. "Temperature effects on the oxygen transfer rate between 20 and 55°C". In: *Water Research* 34.3 (2000), pp. 1037–1041. ISSN: 0043-1354. DOI: https://doi.org/10.1016/S0043-1354(99)00217-1. URL: https://www.sciencedirect.com/science/article/pii/S0043135499002171 (cit. on p. 84).

[218] *4 things you need to know about oxygen transfer*. 2023-09. URL: https://pharsol.com/knowledge-hub/blog/oxygen-transfer (cit. on p. 84).

[219] *Oxygen Solubility - an overview | ScienceDirect Topics*. 2023-05. URL: https://www.sciencedirect.com/topics/engineering/oxygen-solubility (cit. on p. 84).

[220] M. Anabtawi, N. Hilal, and A. Al-Muftah. "Volumetric Mass Transfer Coefficient in non-Newtonian Fluids in Spout Fluid Beds". In: *Chemical Engineering & Technology* 26 (2003-07), pp. 759 –764. DOI: 10.1002/ceat.200301718 (cit. on p. 84).

[221] *SigmaAldrich Sodium carboxymethyl cellulose Datasheet*. URL: https://www.sigmaaldrich.com/specification-sheets/160/380/419273-BULK_____ALDRICH__.pdf (cit. on p. 84).

[222] *SigmaAldrich PPoly(ethylene glycol) BioUltra, 6,000 datasheet*. URL: https://www.sigmaaldrich.com/specification-sheets/386/518/81255-BULK.pdf (cit. on p. 84).

[223] G. Campolongo. "Biopharma PAT - Quality Attributes, Critical Process Parameters & Key Performance Indicators at the Bioreactor". In: (2018-05) (cit. on p. 85).

[224] H. J. G. Lindström and R. Friedman. "Inferring time-dependent population growth rates in cell cultures undergoing adaptation". In: *BMC Bioinformatics* 21.1 (2020-12), p. 583. ISSN: 1471-2105. DOI: 10.1186/s12859-020-03887-7. URL: https://doi.org/10.1186/s12859-020-03887-7 (cit. on p. 85).

[225] R. Pörtner. "Bioreactors for Mammalian Cells". In: *Animal Cell Culture*. Ed. by M. Al-Rubeai. Cham: Springer International Publishing, 2015, pp. 89–135. DOI: 10.1007/978-3-319-10320-4_4. URL: https://doi.org/10.1007/978-3-319-10320-4_4 (cit. on p. 85).

[226] B. Neunstoecklin, M. Stettler, T. Solacroup, H. Broly, M. Morbidelli, and M. Soos. "Determination of the maximum operating range of hydrodynamic stress in mammalian cell culture". In: *Journal of Biotechnology* 194 (2015), pp. 100–109. ISSN: 0168-1656. DOI: https://doi.org/10.1016/j.jbiotec.2014.12.003. URL: https://www.sciencedirect.com/science/article/pii/S0168165614010396 (cit. on p. 85).

[227] J. B. Sieck, T. Cordes, W. E. Budach, M. H. Rhiel, Z. Suemeghy, C. Leist, T. K. Villiger, M. Morbidelli, and M. Soos. "Development of a Scale-Down Model of hydrodynamic stress to study the performance of an industrial CHO cell line under simulated production scale bioreactor conditions". In: *Journal of Biotechnology* 164.1 (2013), pp. 41–49. ISSN: 0168-1656. DOI: https://doi.org/10.1016/j.jbiotec.2012.11.012. URL: https://www.sciencedirect.com/science/article/pii/S0168165612007286 (cit. on p. 85).

[228] T. Tanzeglock, M. Soos, G. Stephanopoulos, and M. Morbidelli. "Induction of Mammalian Cell Death by Simple Shear and Extensional Flows". In: *Biotechnology and bioengineering* 104 (2009-10), pp. 360–70. DOI: 10.1002/bit.22405 (cit. on p. 89).

[229] L. van der Pol, I. Beeksma, and J. Tramper. "Polyethylene glycol as protectant against damage caused by sparging for hybridoma suspension cells in a bubble column". In: *Enzyme and Microbial Technology* 17.5 (1995), pp. 401–407. ISSN: 0141-0229. DOI: https://doi.org/10.1016/0141-0229(94)00063-W. URL: https://www.sciencedirect.com/science/article/pii/014102299400063W (cit. on p. 90).

[230] S. S. Ozturk and B. O. Palsson. "Effect of medium osmolarity on hybridoma growth, metabolism, and antibody production". In: *Biotechnology and Bioengineering* 37.10 (1991), pp. 989–993. DOI: https://doi.org/10.1002/bit.260371015. eprint: https://onlinelibrary.wiley.com/doi/pdf/10.1002/bit.260371015. URL: https://onlinelibrary.wiley.com/doi/abs/10.1002/bit.260371015 (cit. on p. 94).

[231] B. Traustason. "Amino Acid Requirements of the Chinese Hamster Ovary Cell Metabolism during Recombinant Protein Production". In: *bioRxiv* (2019). DOI: 10.1101/796490. URL: https://www.biorxiv.org/content/early/2019/10/07/796490 (cit. on p. 94).

[232] T. M. Duarte, N. Carinhas, L. C. Barreiro, M. J. T. Carrondo, P. M. Alves, and A. P. Teixeira. "Metabolic responses of CHO cells to limitation of key amino acids". In: *Biotechnology and Bioengineering* 111.10 (2014), pp. 2095–2106. DOI: https://doi.org/10.1002/bit.25266. URL: https://onlinelibrary.wiley.com/doi/abs/10.1002/bit.25266 (cit. on p. 94).

[233] M. Coulet, O. Kepp, G. Kroemer, and S. Basmaciogullari. "Metabolic Profiling of CHO Cells during the Production of Biotherapeutics". In: *Cells* 11.12 (2022). ISSN: 2073-4409. DOI: 10.3390/cells11121929. URL: https://www.mdpi.com/2073-4409/11/12/1929 (cit. on p. 94).

[234] *scipy.optimize.minimize — SciPy v1.11.3 Manual*. URL: https://docs.scipy.org/doc/scipy/reference/generated/scipy.optimize.minimize.html (cit. on p. 107).

[235] *cma*. URL: https://cma-es.github.io/apidocs-pycma/ (cit. on p. 107).

[236] *How to use the cma.fmin function in cma | Snyk*. 2023-08. URL: https://snyk.io/advisor (cit. on p. 107).

[237] *CMA-ES*. 2023-09. URL: https://en.wikipedia.org/w/index.php?title=CMA-ES&oldid=1170980342 (cit. on p. 107).

[238] URL: https://cma-es.github.io/ (cit. on p. 108).

[239] *cmaes: Lightweight Covariance Matrix Adaptation Evolution Strategy (CMA-ES) implementation for Python 3*. 2023-09. URL: https://github.com/CyberAgentAILab/cmaes (cit. on p. 108).

[240] *GECCO2021 - tut104 - Advanced Tutorials - CMA-ES and Advanced Adaptation Mechanisms*. 2023-06. URL: https://www.youtube.com/watch?v=7VBKLH3oDuw (cit. on p. 108).